



**NTNU – Trondheim**  
Norwegian University of  
Science and Technology

# Catalytic conversion of oxygenates to fuels

**Astri Karin Torvik Jenssen**

Chemical Engineering and Biotechnology

Submission date: June 2015

Supervisor: De Chen, IKP

Co-supervisor: van der Wijst Cornelis Gerardus, IKP

Norwegian University of Science and Technology  
Department of Chemical Engineering



## Abstract

A catalytic study of copper coated on silica  $CuSiO_2$ , titanium dioxide,  $TiO_2$ , with and without carbon nanotubes, CNT, as support material and zeolite, HZSM 5, has been performed for conversion of n-propanol into C9+ alkanes and alkenes for jet fuel production. A copper catalyst converts n-propanol to its corresponding aldehyde, propanal, and propanal reacts by aldol condensation over  $TiO_2$  to produce long chained alkanes alkenes, aldehydes and ketones. Carboxylic acid in the product was removed by ketonization over  $TiO_2$ . Since n-propanol contains oxygen, zeolite was applied for removal of oxygen.

Various characterization methods were used to examine the different catalysts. Some of these methods were performed in the specialization project in fall 2014, and these are included in the report when necessary. The X-ray diffraction, XRD, spectra of  $TiO_2$  before and after calcination illustrates that the crystallite size of the  $TiO_2$  peaks are smaller after calcination and bigger peaks occur before calcination. Temperature programmed desorption, TPD, was used to examine the basic and acid sites of the four different loadings of  $TiO_2$  supported on CNT, synthesized in the specialization project, and for CNT and  $TiO_2$ . Both acid and basic sites were found for all tested catalysts and support, and the basic sites were stronger when  $TiO_2$  was coated on CNT than for pure  $TiO_2$ , except for the 30 wt. %  $TiO_2/CNT$ . Strength increased when the loading decreased for all  $TiO_2/CNT$  catalysts, except for the 40 wt. %  $TiO_2$  catalyst.

A reduction temperature of 230°C is not high enough for full reduction of the copper catalyst, and a reduction temperature of 300°C gives a higher conversion of reactants to products. Reduction conditions of 1.2 bar and 300°C and reaction conditions of 5 bar and 300°C resulted in the highest selectivity towards C9 hydrocarbons for the tested reduction and reaction conditions. The applied zeolite removed oxygen, and the selectivity towards C9 hydrocarbons was the same for  $TiO_2$  with and without CNT as support.



---

## Sammendrag

En katalytisk studie med silisiumdioksid som bærer for kobber,  $CuSiO_2$ , titaniumdioksid,  $TiO_2$ , med og uten karbon nanorør som bærer, og zeolitt, HZM 5, har blitt utført for konvertering av n-propanol til C9+ alkaner og alkener for produksjon av jetdrivstoff. En kobber katalysator er brukt for å konvertere n-propanol til dens korresponderende aldehyd, propanal, og propanal reagerer videre via aldol kondensasjon over  $TiO_2$  for å produsere langkjedede alkaner, alkener, aldehyder og ketoner. Produktene inneholder også karboksylsyrer som fjernes via ketonisering over  $TiO_2$  katalysatoren. Siden n-propanol inneholder oksygen er zeolitt nødvendig for å fjerne oksygenet.

Forskjellige karakteriseringsmetoder ble brukt for å undersøke de forskjellige katalysatorene. Noen av disse metodene ble utført i spesialiseringsprosjektet fra høsten 2014, og disse er inkludert i rapporten ved behov. Røntgenstrålediffraksjon, XRD, spekter av  $TiO_2$  før og etter kalsinering viser at krystallitt størrelsen er mindre etter kalsinering, og toppene er større før kalsinering. Temperaturprogrammert desorpsjon ble brukt for å undersøke de basiske og syrlige setene for fire forskjellige mengder med  $TiO_2$  med CNT som bærer som ble syntetisert i spesialiseringsprosjektet. Både basiske og syrlige seter ble funnet for alle testede katalysatorer og de basiske setene var sterkere når karbon nanorør var bærer for  $TiO_2$ , med unntak av 30 vekt %  $TiO_2/CNT$ . Styrken av syrlige seter øker med minkende mengde  $TiO_2$  for  $TiO_2/CNT$  katalysatorene, med unntak av 40 vekt %  $TiO_2/CNT$  katalysatoren.

En reduksjonstemperatur på  $230^\circ C$  er ikke høy nok for full redusering av kobber katalysatoren, og en reduksjonstemperatur på  $300^\circ C$  gir høyere konvertering av reaktanter til produkter. Reduksjonsbetingelser på 1.2 bar og  $300^\circ C$  og reaksjonsbetingelser på 1.2 bar og  $300^\circ C$  resulterte i den høyeste selektiviteten mot C9 hydrokarboner. Zeolitten som ble brukt fjernet oksygen, og når CNT ble brukt som bæremateriale for  $TiO_2$  resulterte det i en høyere selektivitet mot C9 hydrokarboner enn uten CNT. Reaksjon med 20 vekt %  $TiO_2$  med et partialtrykk for n-propanol på 0.32, et partialtrykk for hydrogen på 0.63 og et partialtrykk for nitrogen på 4.06 resulterte i høyest selektivitet for C9 hydrokarboner.



## Preface

I would like to express my gratitude to Professor De Chen for the opportunity to investigate the reaction of copper, titanium dioxide and zeolite for production of jet fuels. I have appreciated his guidance and help, and his excitement towards the obtained results.


I would also like to thank Karin Dragsten for training for the common instruments in fall 2014, and for help when needed. I would also like to thank the men working at the workshop for help with improvement of the reactor setup and Arne Fossum and Kine Skjærbusdal for providing of equipment and gloves.

Additionally I would like to thank Cornelis van der Wijst for help performing the laboratory work, and discussions about the results. I would also like to thank Siri Foss Morken for the cooperation in our project related to one-pot conversion of biomass to jet fuels. It has been a pleasure working with you, and it has been nice to have someone to discuss results with.

Finally yet importantly, I would like to give a big thank you to my mom, Karin Torvik, for her support through my years as a master student.

I declare that this is an independent work according to the exam regulations of the Norwegian University of Science and Technology (NTNU).

Trondheim, Thursday 18<sup>th</sup> June, 2015



---

Astri Karin Torvik Jenssen





## Contents

<b>1</b>	<b>Introduction</b>	<b>1</b>
<b>2</b>	<b>Theory</b>	<b>3</b>
2.1	Biomass . . . . .	3
2.1.1	Biomass to fuels . . . . .	4
2.2	Catalysts . . . . .	6
2.2.1	Catalyst synthesis . . . . .	6
2.2.2	Carbon nanotubes . . . . .	8
2.2.3	Titanium dioxide . . . . .	9
2.2.4	Zeolite . . . . .	10
2.2.5	Copper coated on silica . . . . .	11
2.3	Characterization methods . . . . .	12
2.3.1	Thermogravimetric analysis and temperature programmed desorption . . . . .	12
2.3.2	Nitrogen adsorption . . . . .	12
2.3.3	X-Ray diffraction . . . . .	13
2.3.4	Gas chromatography . . . . .	13
2.4	Reactions . . . . .	15
2.4.1	Reaction of n-propanol to propanal . . . . .	15
2.4.2	Aldol condensation . . . . .	16
2.4.3	Ketonization reaction . . . . .	18
<b>3</b>	<b>Experimental procedure</b>	<b>19</b>
3.1	Carbon nanotube pretreatment . . . . .	19
3.2	Preparation of titanium dioxide on carbon nanotubes . . . . .	19
3.3	Preparation of copper coated on silica . . . . .	20
3.4	Preparation of titanium dioxide and zeolite . . . . .	20
3.5	Reaction . . . . .	20
3.6	Characterization . . . . .	24
3.6.1	Temperature programmed desorption . . . . .	24
3.6.2	X-ray diffraction . . . . .	25
3.6.3	Gas chromatography . . . . .	25
<b>4</b>	<b>Results and discussion</b>	<b>27</b>
4.1	X-ray diffraction . . . . .	27
4.2	Temperature programmed desorption . . . . .	29

---

4.2.1	Basic sites . . . . .	29
4.2.2	Acid sites . . . . .	35
4.3	Reaction . . . . .	41
4.3.1	Reaction with 10 wt. % titanium dioxide coated on carbon nanotubes .	44
4.3.2	Effect of reduction pressure . . . . .	46
4.3.3	Effect of reduction temperature and reaction pressure . . . . .	47
4.3.4	Reaction with different catalysts . . . . .	58
4.3.5	Reaction with different zeolites . . . . .	64
<b>5</b>	<b>Further work</b>	<b>71</b>
<b>6</b>	<b>Conclusion</b>	<b>73</b>
<b>A</b>	<b>Calculations</b>	<b>A.1</b>
<b>B</b>	<b>Risk evaluation</b>	<b>B.1</b>
<b>C</b>	<b>Calibration of mass flow controllers</b>	<b>C.1</b>
<b>D</b>	<b>Percents and mass for basic and acid sites</b>	<b>D.1</b>
<b>E</b>	<b>Tables for product conversion and selectivity for oxygenates and hydrocarbons</b>	<b>E.1</b>
<b>F</b>	<b>Response factors for the products</b>	<b>F.1</b>
<b>G</b>	<b>Areas obtained for the different products on the GC-FID</b>	<b>G.2</b>

## List of Figures

1	The cycle of $CO_2$ in biomass. . . . .	4
2	Utilization methods for cellulosic biomass. . . . .	6
3	Three different structures of CNT . . . . .	8
4	Rutiles fundamental structure.[19] . . . . .	9
5	Anatases fundamental structure . . . . .	10
6	Brookites fundamental structure.[19] . . . . .	10
7	Reaction mechanism of n-propanol and propanal over a copper catalyst. . . . .	16
8	The proposed reaction mechanism for n-propanol over a copper catalyst and a titanium dioxide catalyst. . . . .	17
9	Proposed reaction mechanism for n-propanol over a copper catalyst and a titanium dioxide catalyst. . . . .	18
10	The reactor setup with flow controllers, valves, reactor, gas tanks, lines, vaporizer and condenser . . . . .	22
11	X-ray diffraction scans of the $TiO_2$ powder before and after calcination at $600^\circ C$ . 28	
12	Ion current, A, and temperature, $^\circ C$ , over time, min, for basic sites of 10 wt. % $TiO_2$ , CNT and $TiO_2$ . . . . .	30
13	Mass, %, lost and temperature, $^\circ C$ , over time, min, for basic sites of 10 wt. % $TiO_2$ , CNT and $TiO_2$ . . . . .	31
14	Ion current, A, and temperature, $^\circ C$ , over time, min, for basic sites of 20 wt. % $TiO_2$ , CNT and $TiO_2$ . . . . .	31
15	Mass, %, lost and temperature, $^\circ C$ , over time, min, for basic sites of 20 wt. % $TiO_2$ , CNT and $TiO_2$ . . . . .	32
16	Ion current, A, and temperature, $^\circ C$ , over time, min, for basic sites of 30 wt. % $TiO_2$ , CNT and $TiO_2$ . . . . .	32
17	Mass, %, lost and temperature, $^\circ C$ , over time, min, for basic sites of 30 wt. % $TiO_2$ , CNT and $TiO_2$ . . . . .	33
18	Ion current, A, and temperature, $^\circ C$ , over time, min, for basic sites of 40 wt. % $TiO_2$ , CNT and $TiO_2$ . . . . .	33
19	Mass, %, lost and temperature, $^\circ C$ , over time, min, for basic sites of 40 wt. % $TiO_2$ , CNT and $TiO_2$ . . . . .	34
20	Ion current, A, and temperature, $^\circ C$ , over time, min, for CO desorption. . . . .	34
21	Ion current, A, and temperature, $^\circ C$ , over time, min, for acid sites of 10 wt. % $TiO_2$ , CNT and $TiO_2$ . . . . .	36

22	Mass, %, lost and temperature, °C, over time, min, for acid sites of 10 wt. % $TiO_2$ , CNT and $TiO_2$ . . . . .	36
23	Ion current, A, and temperature, °C, over time, min, for acid sites of 20 wt. % $TiO_2$ , CNT and $TiO_2$ . . . . .	37
24	Mass, %, lost and temperature, °C, over time, min, for acid sites of 20 wt. % $TiO_2$ , CNT and $TiO_2$ . . . . .	37
25	Ion current, A, and temperature, °C, over time, min, for acid sites of 30 wt. % $TiO_2$ , CNT and $TiO_2$ . . . . .	38
26	Mass, %, lost and temperature, °C, over time, min, for acid sites of 30 wt. % $TiO_2$ , CNT and $TiO_2$ . . . . .	38
27	Ion current, A, and temperature, °C, over time, min, for acid sites of 40 wt. % $TiO_2$ , CNT and $TiO_2$ . . . . .	39
28	Mass, %, lost and temperature, °C, over time, min, for acid sites of 40 wt. % $TiO_2$ , CNT and $TiO_2$ . . . . .	39
29	Ion current, A, and temperature, °C, over time, min, for CO desorption for acid sites. . . . .	40
30	Conversion of products from reaction with 10 wt. % $TiO_2/CNT$ . . . . .	45
31	Selectivity for C6 oxygenates, C9 hydrocarbons and C9 oxygenates for products from reaction with 10 wt. % $TiO_2/CNT$ . . . . .	46
32	Conversion for reaction with $TiO_2$ and zeolite at reduction conditions of 1.2 bar and 230°C and reaction conditions of 5, 10, 15 and 20 bar and 300°C. . . . .	47
33	Conversion for reaction with $TiO_2$ and zeolite at a reduction temperature of 300°C and 1.2 bar and reaction temperature of 300°C and 5, 10, 15 or 20 bar. . . . .	48
34	Selectivity for all hydrocarbons and oxygenates from reaction with $TiO_2$ and zeolite at reduction conditions of 1.2 bar and 230°C and reaction conditions of 5, 10, 15 and 20 bar and 300°C. . . . .	49
35	Selectivity for C6 hydrocarbons and oxygenates for reaction with $TiO_2$ and zeolite at reduction conditions of 1.2 bar and 230°C and reaction conditions of 5, 10, 15 and 20 bar and 300°C. . . . .	50
36	Selectivity for C6 ketones, aldehydes, alcohols, esters/ethers, alkanes and alkenes from reaction with $TiO_2$ and zeolite at reduction conditions of 1.2 bar and 230°C and reaction conditions of 5, 10, 15 and 20 bar and 300°C . . . . .	51
37	Selectivity for C9 hydrocarbons and oxygenates for reaction with $TiO_2$ and zeolite at reduction conditions of 1.2 bar and 230°C and reaction conditions of 5, 10, 15 and 20 bar and 300°C. . . . .	52

---

38	Selectivity for C9 aromatics and ketones for reaction with $TiO_2$ and zeolite at reduction conditions of 1.2 bar and 230°C and reaction conditions of 5, 10, 15 and 20 bar and 300°C. . . . .	52
39	Selectivity for all hydrocarbons and oxygenates for reaction with $TiO_2$ and zeolite at a reduction conditions of 1.2 bar and 300°C and reaction conditions of 5, 10, 15 and 20 bar and 300°C . . . . .	53
40	Selectivity for C6 hydrocarbons and oxygenates for reaction with $TiO_2$ and zeolite at a reduction temperature of 300°C and 1.2 bar and reaction temperature of 300°C and 1.2, 5, 10, 15 or 20 bar. . . . .	55
41	Selectivity for C9 ketones, aldehydes, alcohols, esters/ethers, alkanes and alkenes and conversion for reaction with $TiO_2$ and zeolite at reduction conditions of 1.2 bar and 300°C and reaction conditions of 1.2, 5, 10, 15 and 20 bar and 300°C. . . . .	55
42	Selectivity for C9 hydrocarbons and oxygenates for reaction with $TiO_2$ and zeolite at reduction conditions of 1.2 bar and 300°C and reaction conditions of 1.2, 5, 10, 15 and 20 bar and 300°C. . . . .	57
43	Selectivity for C9 ketones, alkanes and aromatics and conversion for reaction with $TiO_2$ and zeolite at reduction conditions of 1.2 bar and 300°C and reaction conditions of 1.2, 5, 10, 15 and 20 bar and 300°C. . . . .	57
44	Conversion of products from reaction of $TiO_2$ . . . . .	59
45	Selectivity for C6 hydrocarbons and oxygenates produced from reaction of $TiO_2$ . . . . .	60
46	Selectivity for C6 hydrocarbons and oxygenates produced from reaction with $TiO_2$ . . . . .	61
47	Selectivity for C6 ketones, aldehydes, alcohols, esters/ethers, alkanes and alkenes and the conversion produced with $TiO_2$ . . . . .	62
48	Selectivity for C9 hydrocarbons and oxygenates produced from reaction with $TiO_2$ . . . . .	63
49	Selectivity for C9 aromatics, ketones and alkenes and the conversion produced with different catalysts. . . . .	64
50	Conversion with different zeolite types and calcination temperatures . . . . .	65
51	Selectivity for hydrocarbons and oxygenates for different types of zeolite and calcination temperature . . . . .	66
52	Selectivity for C6 ketones, aldehydes and esters/ethers and conversion for reaction with different zeolite types and calcination temperature. . . . .	67
53	Selectivity for C9 hydrocarbons and oxygenates for reaction with different zeolites and different calcination temperature. . . . .	68

---

54	Selectivity for C9 ketones and aromatics and the conversion with different zeolite types and calcination temperature. . . . .	69
C.1	Calibration curve for the mass flow controller for nitrogen (100 ml), $NH_2$ . . . .	C.1
C.2	Calibration curve for the mass flow controller for nitrogen (250 ml), $N_2$ . . . .	C.4
C.3	Calibration curve for the mass flow controller for hydrogen, $H_2$ . . . . .	C.5
C.4	Calibration curve for the mass flow controller for n-propanol (7.42 ml/min, gas flow). . . . .	C.6
C.5	Calibration curve for the mass flow controller for n-propanol (3.71 ml/min, gas flow). . . . .	C.7
D.1	Ion current (A) and mass (%) for the adsorption of $CO_2$ on the 10 wt. % $TiO_2/CNT$ . . . . .	D.2
D.2	Ion current (A) and mass (%) for the adsorption of $CO_2$ on the 20 wt. % $TiO_2/CNT$ . . . . .	D.2
D.4	Ion current (A) and mass (%) for the adsorption of $CO_2$ on the 40 wt. % $TiO_2/CNT$ . . . . .	D.3
D.3	Ion current (A) and mass (%) for the adsorption of $CO_2$ on the 30 wt. % $TiO_2/CNT$ . . . . .	D.3
D.5	Ion current (A) and mass (%) for the adsorption of $CO_2$ on the $TiO_2$ . . . . .	D.4
D.6	Ion current (A) and mass (%) for the adsorption of $CO_2$ on the CNT. . . . .	D.4

## List of Tables

2	Percent used on the mass flow controllers under reduction and normal reaction conditions. . . . .	21
3	Partial pressure for n-propanol, $H_2$ and $N_2$ under reaction at 1.2 bar, 5 bar, 10 bar, 15 bar and 20 bar. . . . .	23
4	Flow for n-propanol, $H_2$ and $N_2$ under reaction with half of the original n-propanol flow and half of the partial pressure at 5 bar, the partial pressure and the percent used on the mass flow controller. . . . .	23
5	TGA loading, mass adsorbed of $CO_2$ and moles adsorbed of $CO_2$ for both catalysts and support . . . . .	30
6	$NH_3$ desorbed in the first peak for the different catalysts and CNT. . . . .	35
7	Amount of water and oil in different products from reaction with 10 wt. % $TiO_2/CNT$ . . . . .	41
8	Amount of water and oil in different products from reduction conditions of 1.2 bar and 230°C and reaction conditions of 5, 10, 15 and 20 bar and 300°C . . . .	41
9	Amount of water and oil in different products from reduction conditions of 1.2 bar and 300°C and reaction conditions of 1.2, 5, 10, 15 and 20 bar and 300°C. . .	42
10	Amount of water and oil in different products from reaction with different zeolite types. . . . .	42
11	Amount of water and oil in different products from reduction conditions of 1.2 bar and 300°C and reaction conditions of 5 bar and 300°C. . . . .	43
12	Reduction/reaction conditions, time of reaction, conversion, selectivity for C6 oxygenates, C9 hydrocarbon and C9 oxygenates for 10 wt. % $TiO_2/CNT$ from the specialization project in fall 2014. . . . .	45
A.1	Amount of CNT, precursor, ethanol and $TiO_2$ used to make the four different catalysts . . . . .	A.1
C.1	Values obtained during calibration of the mass flow controller for nitrogen (100 ml), $N_2$ . . . . .	C.2
C.2	Values obtained during calibration of the mass flow controller for nitrogen (250 ml), $N_2$ . . . . .	C.3
C.3	Values obtained during calibration of the mass flow controller for hydrogen, $H_2$ . . . . .	C.4
C.4	Values obtained during calibration of the mass flow controller for n-propanol, to get 7.42 ml/min (gas flow). . . . .	C.5
C.5	Values obtained during calibration of mass flow controller for n-propanol, to get 3.71 ml/min (gas flow). . . . .	C.6

D.1	Mass and percent for the basic sites. . . . .	D.1
D.2	Mass and percent for the acid sites. . . . .	D.1
E.1	Conversion and selectivity of all the oxygenates and hydrocarbons in the products from experiments with $TiO_2$ , Zeolite and $CuSiO_2$ at reduction conditions of 1.2 bar and 300°C and reaction conditions of 1.2, 5, 10, 15 and 20 bar and 300°C. . . . .	E.1
E.2	Conversion and selectivity of all the oxygenates and hydrocarbons in the products from experiments with $TiO_2$ , Zeolite and $CuSiO_2$ at reduction conditions of 1.2 bar and 230°C and reaction conditions of 5, 10, 15 and 20 bar and 300°C. . . . .	E.1
E.3	Conversion and selectivity with different catalysts. . . . .	E.2
E.4	Conversion and selectivity with different zeolite types . . . . .	E.2
F.1	Response factors for the different products. . . . .	F.2
F.2	Response factors for the different products. . . . .	F.3
F.3	Response factors for the different products. . . . .	G.1
G.1	Areas obtained for the different products on the GC-FID from reaction of 10 wt. % $TiO_2/CNT$ from the specialization project fall 2014. The reduction conditions where 230°C and 1.2 bar and 300°C and 1.2 bar and the reaction conditions where 230°C and 300°C and 1.2 bar. . . . .	G.2
G.2	Areas obtained for the different products on the GC-FID. The reduction conditions where 230°C and 1.2 bar and the reaction conditions where 300°C and 5, 10, 15 and 20 bar. . . . .	G.3
G.3	Areas obtained for the different products on the GC-FID. The reduction conditions where 300°C and 1.2 bar and the reaction conditions where 300°C and 1.2, 5, 10, 15 and 20 bar. . . . .	G.4
G.4	Areas obtained for the different products on the GC-FID from reaction with $TiO_2$ and $CuSiO_2$ without zeolite and 20 wt. % $TiO_2/CNT$ , $CuSiO_2$ with zeolite at normal partial pressure and half of the normal partial pressure. The reduction conditions where 300°C and 1.2 bar and the reaction conditions where 300°C and 5 bar. . . . .	G.6
G.5	Areas obtained for the different products on the GC-FID from reaction with different zeolite types. . . . .	G.8



## Abbreviations and Symbols

BET	Brauner-Emmet-Teller
BJH	Barrett-Joyner-Hanelda
C	Carbon
CNT	Carbon nanotubes
$C_{12}H_{28}TiO_4$	Precursor for titanium dioxide
$Cu(NO_2) \cdot 2.5H_2O$	Precursor for copper
$CuSiO_2$	Copper coated on silica
FID	Flame ionization detector
GC	Gas chromatography
m	Mass
MFC	Mass flow controller
MS	Mass spectrometer
MWCNT	Multi-walled carbon nanotubes
Mw	Molar mass
n	Moles
R80	Zeolite with an Al/Si ratio of 80
R30	Zeolite with an Al/Si ratio of 30
Si/Al	Silisium/Aluminium
SEM	Scanning electron microscopy
S(T)EM	Scanning electron microscopy with high resolution
SWCNT	Single-walled carbon nanotubes
TGA	Thermogravimetric analysis
$TiO_2$	Titanium dioxide
$TiO_2/CNT$	Titanium dioxide coated on carbon nanotubes
O	Oxygen
TPD	Temperature programmed desorption
V	Volume
wt. %	weight %
XRD	X-ray-diffraction
Z30(450)	Zeolite with an Si/Al ratio of 30 calcined at 450°C
Z30(550)	Zeolite with an Si/Al ratio of 30 calcined at 550°C
Z(80)	Zeolite with an Si/Al ratio of 80



# 1 Introduction

The biggest energy source in the world today is from petroleum resources. These resources are declining, so it is necessary to find new alternative sources for energy. Biomass from plants are also a carbon source, and biomass can be used to generate bio-fuels, with lower greenhouse gas emissions.[1] Biomass used for bio-fuels may compete with feedstocks used for animals and human food, since some bioenergy plants needs to be grown in agricultural areas.[2] The simplest biomass to use for chemicals and fuels are resources used for food like sugar, oils and starch. These starting materials are simple, and the conversion into products of value is easy. Lignocellulosic biomass are not used for food, but the composition makes it difficult to convert to fuels and products.[3] Lignocellulosic biomass consists of hemicellulose, cellulose and lignin which varies in amount depending on the biomass.[2]

Pyrolysis, hydrolysis and gasification are three different routes to convert cellulosic biomass into bio-fuels. Bio-fuels contains a significant amount of oxygen, which have to be removed by using dehydrogenation or zeolites before utilized as fuel.[1]

Ethanol generated from biomass, bio-ethanol, is already in use as a transportation fuel world-wide. Starch, sugar and lignocellulose are some of the utilized raw materials to produce bio-ethanol. The biomass feedstock is a renewable feedstock, and it has positive environmental properties. This is due to the low sulphur content and the low net carbon dioxide release. If the fossil fuel price increases in the future, using bio-ethanol will have a significant economic potential.[4]

In this report, a copper catalyst is used to convert n-propanol into propanal, and the propanal is reacted over a titanium dioxide,  $TiO_2$ , catalyst into C9 and higher carbon molecules for utilization as jet fuel. If diesel is the product, it would have to compete with cars running on electricity, but it is more difficult to use batteries in airplanes. Zeolite, HZSM 5, is used to remove oxygen from the products, and aldol condensation and ketonization are the two main reactions, and these reactions are catalysed by a basic catalyst like  $TiO_2$ .

This project is based on the work of a previous master student and a specialization project from fall 2014. This master student in association with Professor De Chen developed the precipitation method used.



## 2 Theory

This section contains theory about biomass, biomass to fuels, the main reactions, the catalysts and support materials, the different characterization methods used and how to calculate the response factors, conversion and selectivity. The theory section is divided into four different sections, biomass, reactions, catalysts and characterization methods, which also is divided into different subsections.

### 2.1 Biomass

Biomass is a renewable carbon neutral energy resource used to produce valuable chemicals and fuels. The amounts of greenhouse gases formed are lower than for fossil fuels, due to the consumption of carbon dioxide,  $CO_2$ , under regrowth of biomass as displayed in Figure 1. Industrial products were produced from wood-based resources at the beginning of the 20th century, but after World War II crude oil was used.[2, 5, 6]

It is important to use non-edible biomass for food production, to avoid competition from food production. This could be biomass from crop residues, residues from wood and forest residues or industrial and municipal waste. Lignocellulosic biomass is not edible, so when this biomass source is used for bio-fuel, it is no competition with food production.[7, 8] For the rest of this report, only lignocellulosic biomass is mentioned, since this is the biomass source that will be utilized for jet fuel production.

Lignocellulosic biomass consists of cellulose (40-50 %), hemicellulose (25-35 %), lignin (15-20 %) and some organic compounds which is extraneous (around 4 %), and the amount depends on biomass type. Cellulose is a glucose polymer which is crystalline and contains linear polysaccharides. Bindings between these molecules of d-glucose are  $\beta$ -1,4-glycosidic linkages. Cellulose is surrounded by hemicellulose, which is heterogeneous and amorphous and contains branched polysaccharides. Hemicellulose is also the component that links cellulose and lignin together. Lignin is an aromatic mononuclear polymer, substituted and highly branched. Lignin contains units of phenyl propane with carbon-carbon bonds and ether bonds. Lignin holds the polysaccharide layers together and gives structural rigidity. [1, 2, 9]

Lignocellulosic biomass has to be pre-treated prior to utilization. Pre-treatment includes both chemical methods, base or acid hydrolysis, and physical methods, milling or steaming. Pre-treatment depolymerizes and penetrates the lignin seal and preserves and extracts the fraction

of pentose, and the crystalline cellulose is increased for further hydrolysis.[9]

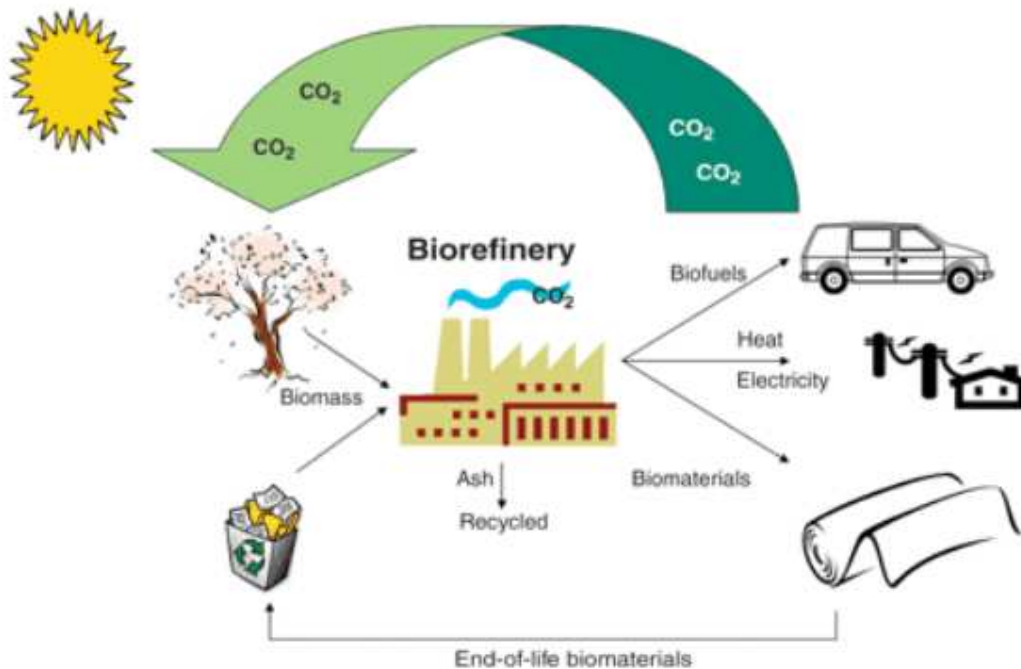


Figure 1: The cycle of  $CO_2$  in biomass. Plants use  $CO_2$  produced from fuel in cars in the photo synthesis.[6]

### 2.1.1 Biomass to fuels

Bioethanol and biodiesel are first-generation biofuels produced from carbohydrate rich plants. The second-generation biofuels will be developed in an integrated bio refinery and the products will be heat, materials, electricity and biofuels. First-generation biofuels are already in application, but the second generation is on the stage of research and development. [2]

Biomass feedstocks used for fuel production is starch, sugars, triglycerides and lignocellulose. Feedstock of starch are polysaccharides of glucose with  $\alpha$  glycosidic linkages like amylopectin and amylose. Hydrolysis of this feedstock to monomers of sugar is easy, and this feedstock is processed in first generation biofuels. Glycerol and fatty acids from plants are triglyceride feedstock. For biodiesel production, the triglyceride sources are products from waste oil, trap grease, vegetable oils and algae. Lignocellulose is always present in plants, while triglycerides and starch only exists in some plants. Lignocellulose contains hemicellulose, lignin and cellulose as explained in section 2.1.[9]

There are three primary routes for converting lignocellulose materials into fuels, gasification, pyrolysis and hydrolysis, as illustrated in Figure 2. Gasification is based on reacting liquid or solid carbonaceous materials, biomass, with oxygen, air and/or steam for syngas production. Syngas contains hydrogen,  $H_2$ , carbon monoxide, CO, carbon dioxide,  $CO_2$ , methane,  $CH_4$  and nitrogen,  $N_2$ . Syngas is converted to liquid fuels by Fisher-Tropsch Synthesis to alkanes or fermentation to ethanol. Pyrolysis is based on heating the biomass feedstock without air, and form a gas product. High yields of bio-oils are produced when fast pyrolysis is used, and can be 80 wt % of the dry feed, and coke is produced when slow pyrolysis is applied. Hydrolysis is a process where the biomass is utilized to produce sugar monomer units in an aqueous solution, which can be further converted to bio-fuels. Biomass also contains oxygen, which has to be removed before the product can be used as liquid fuel.[1] In thermal conversion of lignocellulose, the removal of oxygen is non-selective, and it is selective in the liquid phase reaction through hydrogenolysis, decarbonylation, dehydration or decarboxylation.[10]

An advantage with hydrolysis is that the temperature applied is lower than for gasification reaction and pyrolysis. Another important aspect is the mild processing conditions compared to the thermal methods. Since the operating conditions are more flexible, it is possible to adjust these conditions according to desired products. Thermal processing of lignocellulosic biomass is simpler and no pre-treatment is necessary. In liquid phase catalytic reaction, the lignocellulose needs pre-treatment before utilization. This is expensive, and removal of hemicellulose and some lignin from the biomass occur. Furfural is a produced from hemicellulose, while the lignin is burned for heat or used to create solvents or aromatics. [10] One pot conversion of lignocellulosic biomass to oxygenates or chemicals is a new option for utilization of lignocellulosic biomass. A nickel/zinc, Ni/Zn catalyst is applied for hydrolysis of lignocellulosic biomass in this method. No pre-treatment of the biomass is necessary, and the temperature applied is lower than for thermal treatment of the lignocellulosic biomass.

This project has two steps, and the first step is one pot conversion of cellulose or lignocellulosic biomass to produce polyalcohol hydrocarbons with C2 and C3 length or valuable chemicals. Siri Foss Morken, also a master student, is working on this step, while the second step is to upgrade these polyalcohols to C9-C20 hydrocarbons with low branching to produce jet fuel. For removal of oxygen in the jet fuel, a zeolite catalyst, HZSM 5, is used and both the upgrading of the polyalcohols and the production of bio-oil occur in the same reaction. Only the second step was performed in this master thesis. Instead of using polyalcohols from the first step, n-propanol is the reactant in the reaction. Next step will be to use a feedstock mixture of ethanol and water, before the reactant will be the feedstock from one pot conversion in the end.

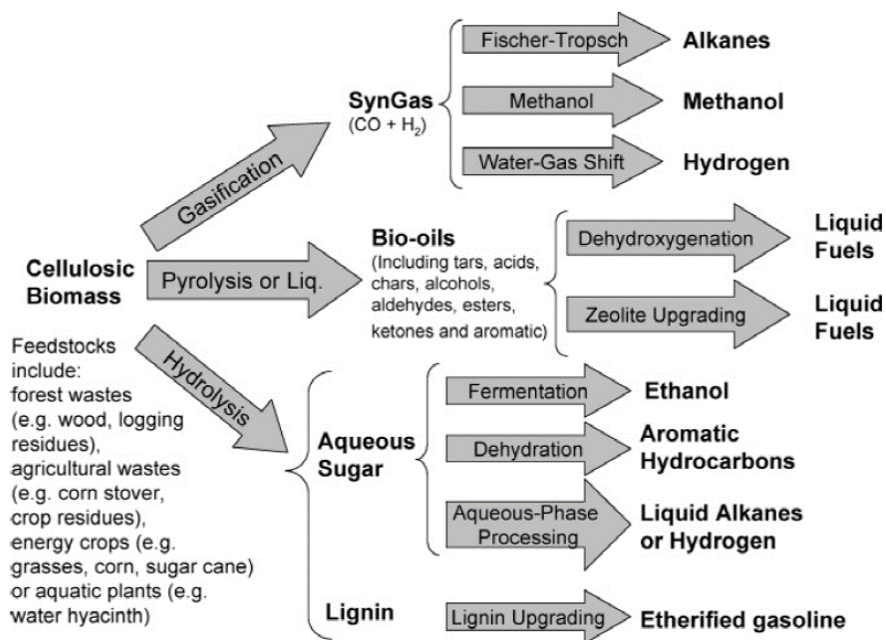


Figure 2: Utilization methods for cellulosic biomass. Biomass is feedstock in gasification to produce alkanes, methanol or hydrogen from syngas, in liquid pyrolysis to produce bio-oils as liquid fuels and in hydrolysis to produce aqueous sugars and lignin. Sugars can be fermented to ethanol, dehydrated to aromatic hydrocarbons or the aqueous phase can be processed to liquid alkanes or hydrogen, while the lignin can be upgraded to etherified gasoline.[1]

## 2.2 Catalysts

There is different catalysts used for reaction of n-propanol to jet fuel compounds, and this section describes the impregnation method for the different catalysts. In this section, there is also found a description of the different catalysts.

### 2.2.1 Catalyst synthesis

Four different catalysts are used for reaction, and these are titanium dioxide,  $TiO_2$ , catalysts coated on carbon nanotubes, CNT, a 5 wt. % copper catalyst coated on silica,  $CuSiO_2$ ,  $TiO_2$  powder and zeolite, HZM 5. Different preparation methods exists for catalysts, like incipient wetness impregnation, wet impregnation, dry pore volume impregnation and ion exchange. Wet impregnation and incipient wetness impregnation are the two methods applied in this report.[11]



Wetness impregnation uses a desired amount of liquid mixed with the metal precursor, and added to a support material. Ethanol was used in the wetness impregnation method, and the amount was three times the volume of CNT as shown in equation 2.1. In this method, the surface may be restructured, surface area loss etc., but the species distribution is well controlled. However it might be obtained a high dispersion, and if interactions of ion/solid are involved this method works good.[11]

Incipient wetness impregnation coats the copper catalyst on silica support in this report. In this method, the support is added to a liquid, here water, until the pores are filled and the support starts to look wet. Then a precursor is added to the corresponding amount of liquid, and mixed until complete dissolution of the precursor. This solution is then drop wise added to the support under continuous stirring. [12, 11]

For both impregnation methods the mass of the support multiplied by the loading is equal to the mass of the metal as shown in equation 2.2. This equation is used to find the mass of the metal precursor or support. Number of moles of the metal precursor is equal to the number of moles of the metal, as illustrated in equation 2.3 and 2.4 and this is used to calculate the amount of precursor needed.[12, 11]

After impregnation, the samples have to dry before calcination to transform the precursor to its active phase. A detailed description of the impregnation methods, and calcination temperatures are found in section 3.2, 3.3 and 3.4.[12, 11]

$$V_{ethanol} = 3 \cdot V_{CNT} \quad (2.1)$$

$$m_{metal/support} = m_{total} \cdot loading \quad (2.2)$$

$$n_{precursor} = n_{metal} \quad (2.3)$$

$$m_{precursor} = \frac{m_{metal}}{M_{w,metal}} \cdot M_{w,precursor} \quad (2.4)$$

Where:

$m_{metal/support}$  = mass of metal or support in gram

$n_{precursor}$  = number of moles of precursor

$n_{metal}$  = number of moles of metal

$m_{precursor}$  = mass of precursor in gram

$M_{w,metal}$  = molar mass of metal in gram/moles

$M_{w,precursor}$  = molar mass of precursor in gram/moles

$V_{ethanol}$  = volume of ethanol in millilitre

$V_{support}$  = volume of support in millilitre

### 2.2.2 Carbon nanotubes

Temperatures used for reactions with catalysts can lead to sintering of small particles, so the particles has to be stabilized either by applying an inert support or by adding structural promoters. Carbon nanotubes, CNT, is a support material with a large internal surface area and pores. This support offers thermal stability, porosity, controlled surface area and makes the catalyst strong against attrition and crushing.[13]

Iijimm discovered CNT in 1991, and today there is several methods to produce CNT. [14, 15, 16] Carbon nanotubes are fullerenes with graphitic carbon needles and is produced by the standard arc-discharge technique with an atmosphere containing helium.[14, 15] The graphitic carbon needles has a diameter of 4-10 nm and a length of up to 1 mm.[14, 17]

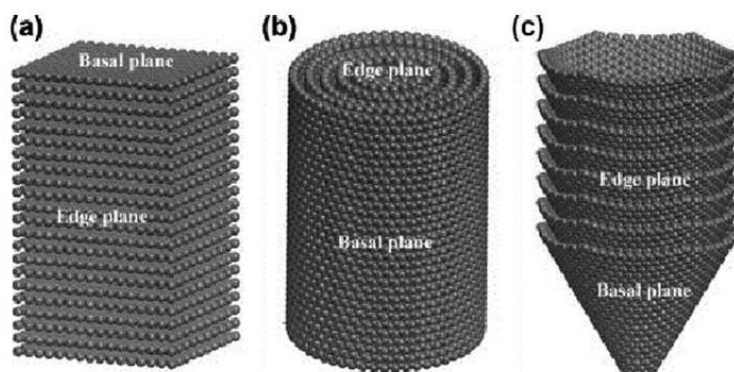


Figure 3: Three different structures of CNT, (a) platelet structure, (b) ribbon structure and (c) fishbone structure.[18]

CNT and carbon nanofibers, CNF, contains carbon atoms of curved  $sp^2$ -hybridization, but the properties and nanostructure is different. The carbon atoms alignment in the underlying planes are the main distinction between CNT and CNF. The cylindrical planes of the CNT are concentric and the alignment is axial with mainly hexagonal structures. CNT is classified into two

subgroups according to the alignment of the cylindrical tubes of axial alignment, single-walled carbon nanotubes, SWCNTs, and multiwalled carbon nanotubes, MWCNTs. CNFs classification are based on the orientation of the graphene sheet, and the angle,  $\alpha$ , between the graphene sheet and fibre axis.[18]

CNT has physico-chemical properties, fibrous or tubular structure, high electric conductivity, surface area of  $80 - 200m^2/g$ , mesoporous properties which is easily tuned, the resistance to strong bases and acids are high and the mechanical strength is high. CNT is a good support material due to its many edges for catalyst precursor anchoring, and the surface properties are easy to adjust. It is also a conductor for heat electrical and heat crystallite, which could form strong interaction between CNT and metal atoms. For high-speed reactions in gas and liquid phase, it is a superior support material due to the large external surfaces and mesopores. [18]

### 2.2.3 Titanium dioxide

Titanium dioxide  $TiO_2$  has two different forms, a crystalline and an amorphous form.  $TiO_2$  has three crystalline forms, brookite, anatase and rutile. The structure of the brookite form is orthorhombic, while the structure of the rutile and anatase form is tetragonal. All three has  $TiO_6^{2-}$  octahedral molecules, but the bonds between these octahedral molecules are different. In the rutile structure it is formed a linear chain, due to sharing of two of twelve edges. These chains are then connected to oxygen atoms in the corners, as illustrated in Figure 4. Four edges per octahedron are shared for the anatase form, and no corners, as depicted in Figure 5 [19, 20] while three edges per octahedral are shared in the brookite form as illustrated in Figure 6.[19, 21]

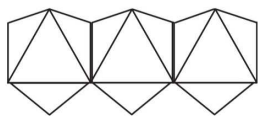


Figure 4: Rutiles fundamental structure.[19]

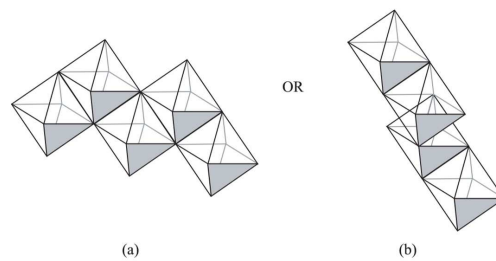


Figure 5: Anatases fundamental structural units, (a) a configuration which is right angled is formed due to the sharing of two edges per octahedron and (b) sharing of the fourth and third edges and out of the adjacent layers.[19]

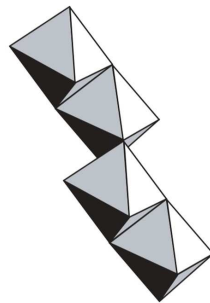


Figure 6: Brookites fundamental structure.[19]

$TiO_2$  can be used as a support material, or as a catalyst. It is active in processes with hydrocarbon selectivity oxidation and formaldehyde dimerization.[19]  $TiO_2$  in crystalline phase, anatase and rutile, is used in waste water treatment as a photo catalyst.[22, 23] It contains both acid sites as  $Ti^{4+}$  and basic sites as  $O^{2-}$ . [19]

#### 2.2.4 Zeolite

Zeolites have pore structures of 5-12 Å, and the material is microporous and crystalline. Active sites of zeolites are mostly acid sites, and both the capacity of adsorption and the surface area are very high. [1] Zeolites are in the ammonium form when bought commercially, so calcination has to be applied to get the acid form.[24]

The stability of the catalyst depends on temperature and time of calcination and the ratio of Si/Al. Benito et al. found that the stability of the catalyst increased when the Si/Al ration was increased or the temperature was increased.[25]

Reactions like hydrolysis, esterification and hydration has water as product or reactant, which can poison the catalyst. Zeolites are solid acids with water tolerance, and the hydrophobicity increases with increasing Si/Al ratios. Under calcination, ammonia is removed, and Brønsted acid sites appear.[26] Gayubo et al. upgraded oxygen components from pyrolysis of biomass over a zeolite catalyst, HZSM 5. The oxygen compounds were 1-propanol, 2-propanol, phenol, 2-methoxyphenol, 1-butanol and 2-butanol. Dehydration of alcohols to olefins occurs rapidly, and begins around 200°C. Above 250°C the olefins are transformed to C5+ olefins. At higher temperatures than 350°C it is produced paraffins of C4+ length formed from 1-butanol, 2-butanol and aromatics. Aromatic cracking and C5+ paraffins cracking creates butene, ethene and propene. The reactivity of phenol was low, due to blocking of the catalytic bed by coke generated in the reaction. When feeds water content increase, the coke deposition deactivation rate decrease.[27]

Zeolites are applied in upgrading of bio-oils to remove oxygen and increase thermal stability of the product. Atmospheric pressure and 350 – 500°C is the temperature range used for bio oil upgrading. Reactions included in bio oil upgrading are cracking, deoxygenation, polymerization, dehydration and aromatization. [1]

### 2.2.5 Copper coated on silica

Silica is used as a support material for catalysts at temperatures below 300°C for polymerization, some oxidation reactions and hydrogenation. Pore size, surface area and particle size is easy to adjust, and silica is made by flame hydrolysis or sol-gel precipitation. [13].

Toxic heavy metal salts in stoichiometric amounts or catalysts containing transition metals like rhodium, ruthenium and palladium was required to convert alcohols into aldehydes. Today copper catalysts are used for this, and these are less expensive.[28, 29]

The copper catalyst has to be reduced prior to application, in a mixture of hydrogen and nitrogen. If the temperature is too high, sintering of the catalyst may occur due to a rapid reduction reaction. This can happen at temperatures above 232°C.[30] Dominique et al. investigated the reduction temperature for copper coated on zinc oxide,  $Cu/ZnO$ , with temperature programmed reduction and the reduction of copper started at 150°C. Above 275°C there is not observed any peaks of hydrogen consumption, indicating that for reduction of copper to its metallic species it is enough to use a temperature of 300°C.[31] Copper coated on silica,  $CuSiO_2$ , has also been investigated, and Vasiliadou et al. found that the reduction temperature should be above 250°C.[32]

## 2.3 Characterization methods

Different characterization methods was applied to find the urface area, pore volume, catalyst loading, crystalline structure, crystallite size and acid and basic sites of the catalyst. A description of the characterization methods is found in this chapter.

### 2.3.1 Thermogravimetric analysis and temperature programmed desorption

Thermogravimetric analysis, TGA, is a characterization method for catalysts, which measures the weight change of a catalyst when temperature is increased. [33] It is used to find the loading of the titanium dioxide,  $TiO_2$ , on the carbon nanotubes, CNT.

Temperature programmed desorption, TPD, is used to examine the way species react, adsorbs and decomposes on the surface of a catalyst.[13] Basic and acidic sites can be measure by using carbon dioxide,  $CO_2$ , and ammonia,  $NH_3$ , respectively, both with an adsorption temperature of  $30^\circ C$ .[34]

Watanabe et al. used TPD to investigate the basic and acid sites of anatase and rutile  $TiO_2$ . One peak was observed for both the acid and basic TPD of anatase  $TiO_2$ , and the acid sites where weak, while the basic sites had middle strength. Rutile  $TiO_2$  had three peaks on both acid and basic TPD, and both the acid and basic sites where strong.[35]

A STA 449C Jupiter Netch is the machine used for both TGA and TPD. It contains a vacuum chamber, and inside there is a manipulator with a crystal mounted to it. When heating the crystal, it is a linear increase of the temperature over time. A thermocouple is used to measure the temperature of the sample carrier. When species are desorbing from the sample, the concentration is monitored with either a pressure gauge or a mass spectrometer.[13] Three different ways of desorption is possible, zero order, first order and second order. Zero order adsorption are rare, and occur when desorption rate is independent of the adsorption coverage. When the maximum peak of an adsorbed species is at the same temperature even when the coverage varies, it is a first order adsorption. Second order adsorption is rate on coverage dependent, so an increase in coverage shifts the peak to lower temperature.[13]

### 2.3.2 Nitrogen adsorption

Nitrogen adsorption measures the surface area and pore size of the catalyst. Nitrogen is an inert gas and is physically adsorbed to the sample and the amount of molecules necessary to form a

monolayer is determined. A formation of a multilayer may occur, if the molecules continues to adsorb on the monolayer. If the sample has small pores, condensation into these small pores may happen, which is described by the Kelvin equation. A catalysts pore size distribution and pore types are determined by the Kelvin equation. The total surface area of the catalyst or support can be found by using the Brunauer Emmet Teller, BET, isotherm.[13] Barrett-Joyner-Halenda, BJH, is a method used for calculating the pore size distribution.[36]

The t-plot is a measurement of the pore structure. A straight line describes the formation of multi molecular formed on the surface, and the adsorption isotherm is equal to the t-plot. When there is a curve upwards at a certain pressure, capillary condensation occur in different pores at a given pressure. This leads to more adsorption on the catalyst than the amount of the multi molecular layer, and the adsorption isotherm is above the t-plot. If the line is curved down at a certain pressure, adsorption will not occur on the whole surface, and the adsorption isotherm is below the t-plot.[37]

### 2.3.3 X-Ray diffraction

X-ray Diffraction, XRD, is a catalyst characterization method used to identify a catalysts crystalline phases. This is done by using parameters of lattice structure and the particle size is also indicated.[13] Byrappa et al prepared titanium dioxide coated on carbon nanotubes,  $TiO_2/CNT$ , composites and the only  $TiO_2$  crystalline form discovered was the anatase form.[38] The same result was obtained by Xia et al, even though a different coating methods was used.[39]

Equation 2.5 shows the Scherrer equation which is used to calculate L, the average crystallite size. The X-ray wavelength,  $\lambda$ , is in nanometre, nm, the constant K is related to the shape of the crystallite and is normally set to 0.9 and  $\beta$  is the diffraction of the peak profiles peak width at half maximum height due to radians of small crystallite size.[40, 41]

$$L = \frac{K\lambda}{\beta \cdot \cos\phi} \quad (2.5)$$

### 2.3.4 Gas chromatography

In gas chromatography, GC, the carrier gas, mobile-phase, is an inert gas, in this case helium. A GC consists of a system for sample injection, syringe, a column and a detector. The column used is a HP-5MS 5 % PMS and the detector is a mass spectrometer, MS. The sample produces ions and the MS detects the mass to charge ratio. A mass spectrum is obtained for the different

peaks in the GC spectrum. This mass spectrum is then analyzed in a mass specter analyzer to find out which compound the different peaks in the GC spectrum belongs to.[42]

A GC with a flame ionization detector, FID, was also used to analyse the products, and to calculate the conversion and selectivity. Response factors for the hydrocarbons are calculated by using equation 2.6, while the other response factors used where found by Ondrej.[12]. Molecular weight and response factors for the different products are listed in table F.1, in Appendix F, and the areas are listed in table G.1, G.2, G.3, G.4 , G and G.5 in Appendix G. Conversion and selectivity where then calculated by using equation 2.7, 2.8, 2.9, 2.10, 2.11 and 2.12 as illustrated in Appendix A.

$$FID \text{ response factor} = \frac{M_{w,C} \cdot \# \text{ of } C}{((M_{w,C} \cdot \# \text{ of } C) + \# \text{ of } H) \cdot 0.7487} \quad (2.6)$$

$$\text{weight rate} = \frac{\text{peak area}}{\text{response factor}} \quad (2.7)$$

$$\text{weight \%} = \frac{\text{weight rate}}{\sum \text{weight rates}} \quad (2.8)$$

$$\text{mol rate} = \frac{\text{weight \%}}{\text{Molecular weight}} \quad (2.9)$$

$$\text{mol \%} = \frac{\text{mol rate}}{\sum \text{mol rates}} \quad (2.10)$$

$$\text{number of } C_6(C_9, C_{12}) = \text{mol \%} \cdot \text{number of carbons in hydrocarbon structure} \quad (2.11)$$

$$\text{selectivity} = \frac{\sum \text{number of } C_6(C_9, C_{12}) \text{ (rate)}}{\sum \text{number of } C_{6+} \text{ (rate)}} \quad (2.12)$$

Where:

$M_{w,C}$  = molecular weight of carbon



## 2.4 Reactions

Four different catalysts are used, a copper catalyst coated on silica,  $CuSiO_2$ , a titanium dioxide catalyst,  $TiO_2$ , a titanium dioxide catalyst coated on carbon nanotubes,  $TiO_2/CNT$ , and a zeolite catalyst, HZSM 5. The copper catalyst transforms n-propanol into propanal, and propanal is further reacted to jet fuel compounds on the basic titanium dioxide catalysts.[43, 12] Zeolite removes oxygen from the products before application as fuel. All reactions happens simultaneously in one reactor, and reaction of n-propanol and propanal, aldol condensation reaction and ketonization reaction is described in this chapter.

### 2.4.1 Reaction of n-propanol to propanal

The reaction of 1,3-propanediol over a copper catalyst consisting of 5 wt. % copper on silica support,  $CuSiO_2$ , was investigated by Sad et. al. Copper surfaces has high reactivity, and the rate and selectivity are not influenced by addition of silica as support material. Acid sites is required to form propene and propane, and this is formed through hydrogenation and dehydrogenation reactions. Under hydrogen pressure, it is obtained a rapid equilibrium of propanol and propanal and the ratio of propanol and propanal is proportional to the pressure of hydrogen,  $H_2$ . Oxidation of propanol, a primary alcohol, to propanal, its corresponding aldehyde is performed at 300 K and 5 bar. Mixtures of  $H_2$ , propanal and propanol in equilibrium, reacts through esterification and condensation to form molecules with five and six carbons and less oxygen atoms and some molecules with three carbons. [43, 44] Figure 7 illustrates the products obtained from reaction of 1,3-propanediol over a copper catalyst. [43]

Different reactions illustrated in Figure 7 are:

1. Aldol condensation reaction, described in section 2.4.2
2. C6 linear alkanone and alkanal formation due to activation of the  $\beta$ -position of the C-H bonds
3. Propyl propionate formed by esterification reaction
4. Propanol is dehydrated to propene and hydrogenation[43]

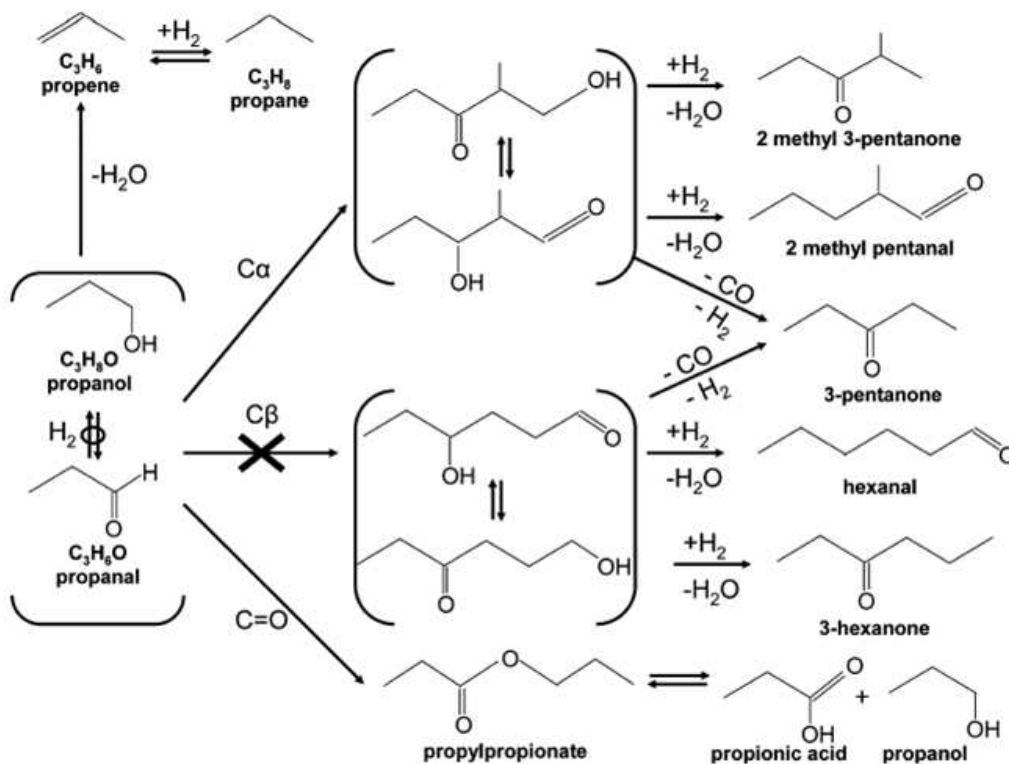


Figure 7: Reaction mechanism of n-propanol and propanal over a copper catalyst. Propanal and n-propanol is in equilibrium, and different ketones and aldehydes were produced. Propyl propionate is also a product which further reacts to propionic acid and propanol.[43]

### 2.4.2 Aldol condensation

One of the main reactions is aldol condensation, which occurs readily with aldehydes and is a reaction used to form carbon bonds. A carbon-carbon double bond is formed between two aldehyde molecules or ketone molecules containing atoms with  $\alpha$ -hydrogen. If the reaction is added hydrogen, a single bond can be produced instead. The bond is formed between the carbonyl group of one molecule and the  $\alpha$  carbon of a second molecule. Products formed over elevated temperature is water and an aldehyde which is  $\alpha$ ,  $\beta$ -unsaturated.[45, 46] If a base is present, the molecules may condense or combine, and form either a  $\beta$ -hydroxy keton or aldehyde, aldol, combination of an alcoholic group and an aldehyde, which will be converted to a conjugated enone by dehydration.[47]

There is two steps involved, a nucleophilic reaction and an elimination reaction. Nucleophiles

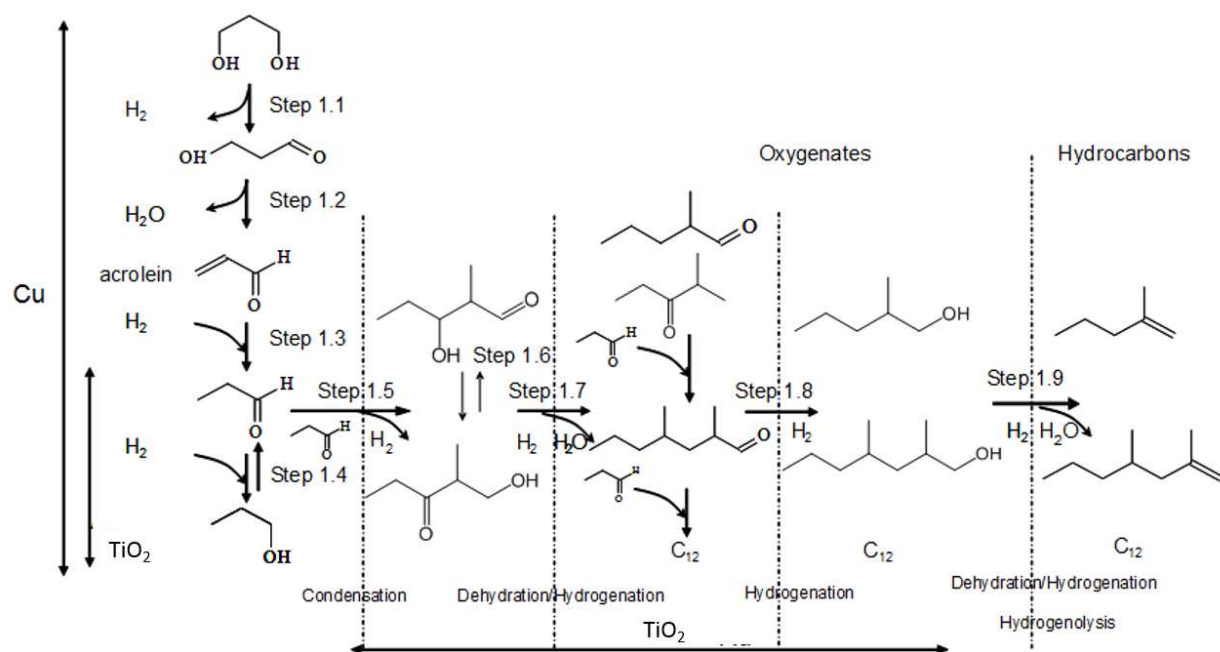


Figure 8: The proposed reaction mechanism for n-propanol over a copper catalyst and a titanium dioxide catalyst. Reactions involved are condensation, oxygenation, hydrogenation and dehydrogenation, and the products are oxygenates and hydrocarbons with different carbon lengths.[12, 48]

used in aldol reaction is enolates, enols and enol ethers of aldehydes, ketones and other compounds containing carboxyl. The electrophilic partner is an aldehyde and two different mechanisms can occur which is enol mechanism and enolate mechanism. The enol mechanism is catalysed by acid, while the enolate mechanism is catalysed by a base.[47]

### 2.4.3 Ketonization reaction

Bio-oil contains a significantly large amount of carboxylic acid, 30 %, formed from esters as illustrated in Figure 9. Carboxylic acid is corrosive and has high reactivity leading to bio-oil instability. One way of removing carboxylic acids from the bio-oil is by ketonization.[49]

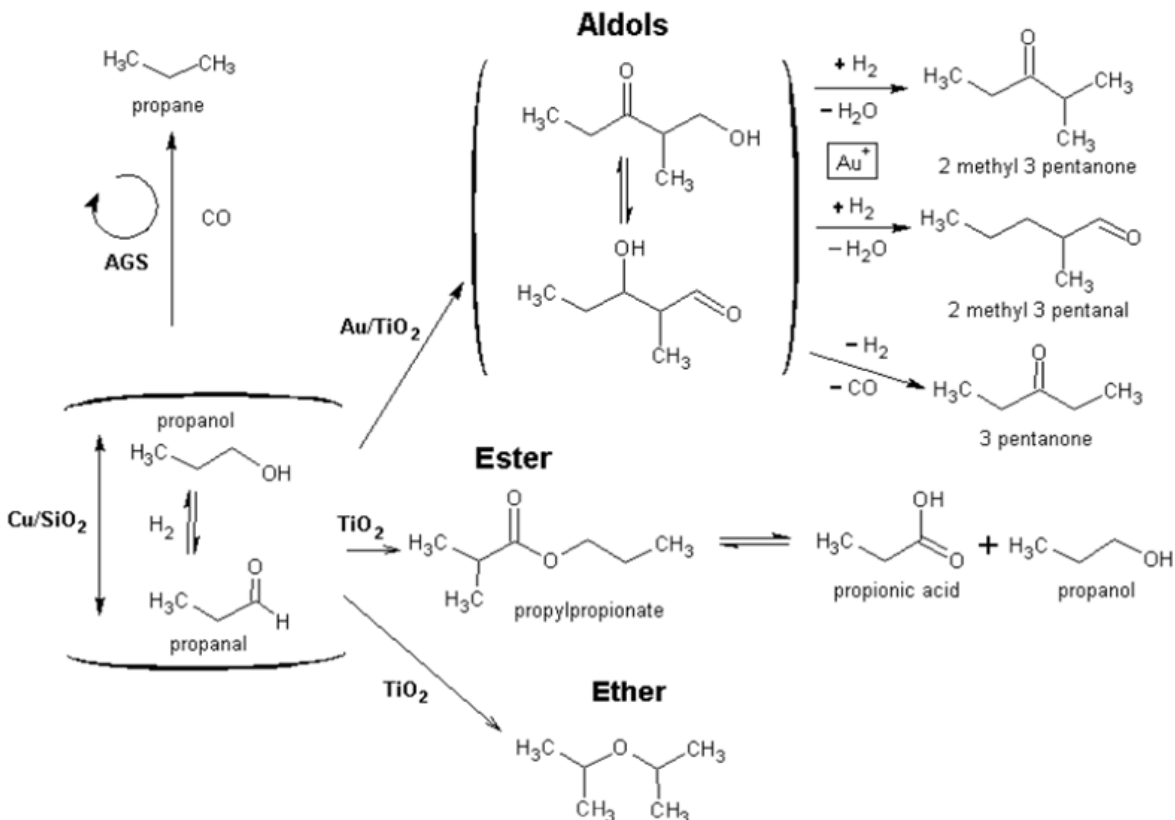


Figure 9: Proposed reaction mechanism for n-propanol over a copper catalyst and a titanium dioxide catalyst. The products are esters, ethers, propionic acid, ketones and aldehydes with different carbon lengths.[12, 48]

Carboxylic acids undergo ketonization in the presence of a heterogeneous oxide catalyst. Products from ketonization is ketone, water and carbon dioxide,  $CO_2$ , and zirconia and titanium surfaces are the most active catalysts for this kind of reaction. The oxide form is zirconium dioxide,  $ZrO_2$ , and titanium dioxide,  $TiO_2$ . Catalysts used in this report is  $TiO_2$  and  $TiO_2/CNT$ . [50] Reaction conditions are atmospheric pressure and temperatures between 300 – 500°C.[49]

### 3 Experimental procedure

Before performance of the experiments, a risk evaluation was performed. Possible problems and dangers that could occur during the experiments was identified on this risk evaluation, and is displayed in Appendix B.

#### 3.1 Carbon nanotube pretreatment

Commercial carbon nanotubes, CNT, bought from Chengdu Organic Chemicals Co. Ltd, where pre-treated in order to remove impurities and remaining growth catalyst. The pre-treatment is described in a previous work by Liland, which work was about Ni-ZnO/CNT catalyst.[51] This was done by mixing CNT, 10 g, with nitric acid, 65 %, 250 mL, for one hour at 100°C. After cooling to room temperature, the solution was filtrated and deionized water was used to wash off the nitric acid. This step was carried out three times, and after the third time, the CNT was washed with deionized water until the pH on the washing water was around five. Then the CNT was dried in a drying cabinet for 12 hours.

#### 3.2 Preparation of titanium dioxide on carbon nanotubes

Carbon nanotubes, CNT, where measured and put into a graded cylinder to find the volume of the CNT. This volume was then multiplied by three to find the amount of ethanol and coating solution to add to the CNT. A titanium precursor,  $C_{12}H_{28}TiO_4$ , was mixed with ethanol before it was added to the CNT. Then sonication of the mixture was sonicated for 15 minutes before stored in a fume hood for 10 hours. After 10 hours, the mixture was filtrated and drying of the fibres happend in drying cabinet for 12 hours. Since the catalyst powder was fluctuate, a pellet press was used to pelletize the powder. The pellets where then calcinated in a high temperature furnace, and heated to 350°C with a heating rate of 5°C/min, and then kept at 350°C for four hours. After calcination, the pellets where crushed to powder before characterization. Before reaction, the catalysts where pelletized again and then crushed and sieved to get particles in the size range of 50-100 mesh.

### 3.3 Preparation of copper coated on silica

The catalyst of copper coated on silica,  $CuSiO_2$ , was prepared by using the wet insipient method. Calculations was done by using equations 2.2, 2.3 and 2.4 in section 2.2.1, and the precursor used was  $Cu(NO_3) \cdot 2.5H_2O$ . The precursor was dissolved in water, and this mixture was added to the support drop wise under continuous stirring. The mixture was placed in the fume hood for 10 hour, before it was left in the drying cabinet for 12 hours to dry. Calcination was performed in a high temperature calcination furnace where it was heated to  $350^\circ C$  with a heating rate of  $5^\circ C/min$ , and then kept at  $350^\circ C$  for four hours. After calcination, the catalyst was pelletized before it was crushed and sieved to get particles in the size range of 50-100 mesh.

### 3.4 Preparation of titanium dioxide and zeolite

Titanium dioxide,  $TiO_2$ , was calcinated in a high temperature furnace at  $600^\circ C$  for three hours. Then the powder was pelletized, before it was crushed and sieved to get particles in the size range of 50-100 mesh.

Zeolite, ZSM5, with a Si/Al ratio of 30 was calcinated at  $450^\circ C$  and  $550^\circ C$  for four hours in a high temperature furnace. Then the powder was pelletized, before it was crushed and sieved to get particles in the size range of 50-100 mesh.

Another type of zeolite with a Si/Al ratio of 80 was calcinated in a calcination reactor under an airflow of 330 ml/min. The calcination temperature was set to  $550^\circ C$  for four hours with a heating rate of  $4^\circ C$ . After calcination, the catalyst was pelletized before it was crushed and sieved to get particles in the size range of 50-100 mesh.

### 3.5 Reaction

The mass flow controllers where calibrated as shown in table C.1, C.2, C.3, C.4 and C.5 and figure C.1, C.2, C.3, C.4 and C.5 as shown in Appendix C. The flow controllers where controlled by setting the desired percent calculated as shown in Appendix A. Table 2 shows the percent used for the different mass flow controllers.

Table 2: Percent used on the mass flow controllers under reduction and normal reaction conditions.

Flow controller	Reduction (%)	Reaction (%)
1 MFC (propanol)	-	58
2 MFC (nitrogen, 100 ml)	18	12.6
3 MFC (nitrogen, 250 ml)	1.6	10.8
5 MFC (hydrogen)	5	2

The reaction was carried out in a fixed bed reactor system with mass flow controllers and pressure modules as shown in Figure 10. Two thermocouples were used to control the temperature, one in the reactor and the other one in the evaporator. The thermocouple for the reactor was attached to the top of the reactor, and located right above the catalyst bed. The reactor used was a 15 mm ID reactor, and quartz wool was positioned on top of the catalyst bed with zeolite, 0.5 g on top. Then two catalysts were mixed together, which was either  $TiO_2$ , 2 g or 1.5 g, or 20 wt % titanium dioxide coated on carbon nanotubes,  $TiO_2/CNT$ , mixed with a  $CuSiO_2$  catalyst, 0.5 g, and this catalyst was placed on top of the zeolite. Reduction of the catalyst was performed in situ before reaction, with a mixture of 70 mol% nitrogen and 30 mol% hydrogen at a total flow of 50 ml/min in 1.2 bar and 300°C and 1.2 bar or 20 bar and 230°C. The feed was liquid n-propanol, which was evaporated in the evaporator at 180 °C prior to the reactor. The gas mixture for the reaction consisted of n-propanol, 7.49 ml/min, hydrogen, 7.42 ml/min, nitrogen (100 ml), 22.27 ml/min, and nitrogen (250 ml), 22.27 ml/min. The reaction was performed in gas phase at 1.2 bar, 5 bar, 10 bar, 15 bar or 20 bar and 300 °C and 5 bar, 10 bar, 15 bar or 20 bar and 230°C. The percents used are illustrated in table 2 and the partial pressures for the gas flows are shown in table 3

One reaction was also performed with n-propanol, 3.75 ml/min, hydrogen, 7.2 ml/min, nitrogen (100 ml), 11.14 ml/min, and nitrogen (250 ml), 11.14 ml/min. The reduction conditions were 1.2 bar and 300°C while the reaction conditions were 5 bar and 300°C. The partial pressures and percents used are shown in table 4. The catalyst used was 20 wt. %  $TiO_2/CNT$ , 1.5 g, Zeolite, 0.5 g and  $CuSiO_2$ , 0.5 g.

After reaction, condensation of the gas mixture occurred in a condenser before collection of the liquid product after 4 and 20 hours. The product was collected in a boiler shell before the gas was bypassed through the stationary condenser and into the ventilation in the roof. The bypass was to ensure that all of the products would condense, so some of the product appeared in the stationary condenser. Reactions performed at higher pressure than 1.2 bar were

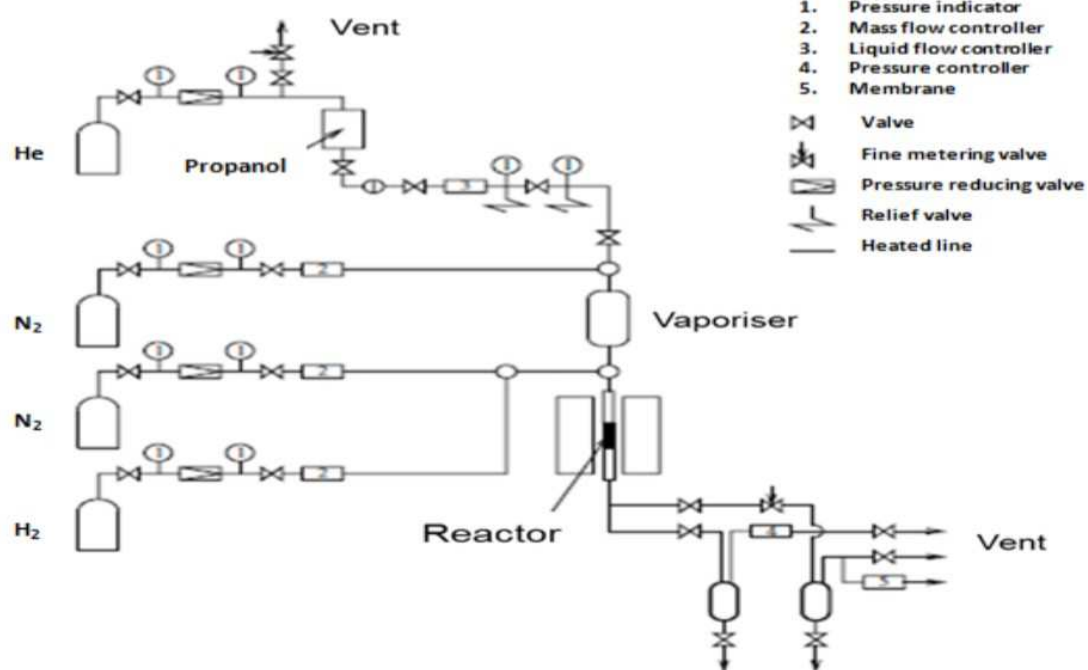


Figure 10: The reactor setup with flow controllers, valves, reactor, gas tanks, lines, vaporizer and condenser



collected only in the stationary condenser. The collected products were analysed with two gas chromatographs, one with a flame ionization detector, FID, and one with a mass spectrometer detector, MS detector, before the conversion and selectivity was calculated by using equation 2.7, 2.8, 2.9, 2.10, 2.11 and 2.12 in Section 2.3.4. A calculation example is found in Appendix A

Table 3: Partial pressure for n-propanol,  $H_2$  and  $N_2$  under reaction at 1.2 bar, 5 bar, 10 bar, 15 bar and 20 bar.

Gas	Flow (ml/min)	Partial pressure at 1.2 bar (bar)	Partial pressure at 5 bar (bar)	Partial pressure at 10 bar (bar)	Partial pressure at 15 bar (bar)	Partial pressure at 20 bar (bar)
n-propanol	7.49	0.15	0.63	1.26	1.89	2.52
$N_2$	44.54	0.90	3.745	7.49	11.24	14.98
$H_2$	7.42	0.15	0.625	1.25	1.88	2.50

Table 4: Flow for n-propanol,  $H_2$  and  $N_2$  under reaction with half of the original n-propanol flow and half of the partial pressure at 5 bar, the partial pressure and the percent used on the mass flow controller.

Gas	Flow (ml/min)	Partial pressure (bar)	Percent
n-propanol	3.75	0.315	27
$N_2$ (100 ml)	11.14	3.03	5.4
$N_2$ (250 ml)	11.14	3.03	4.6
$H_2$	3.71	0.625	2

## 3.6 Characterization

Different characterization methods were used to find pore volume, surface area, size distribution, active sites, basic sites and loading of titanium dioxide,  $TiO_2$  on the carbon nanotube, CNT, support. Some of these characterization methods were performed in the specialization project in fall 2014, and these were the nitrogen adsorption to find the pore volume, the S(T)EM imaging to see the structure of the carbon nanotubes (CNT) and the size of the tubes and the thermogravimetric analysis to find the loading of  $TiO_2$  on the CNT. These results are only included in this report when needed.

### 3.6.1 Temperature programmed desorption

Temperature programmed desorption, TPD, was performed on a thermogravimetric analyser, Netzch STA-429-instrument, connected to a mass spectrometer, MS, detector. TPD was performed on both the basic and the acid sites to find the strength of the sites and if these sites have any influence on the reaction.

The TPD analysis of the basic sites was performed by heating the catalyst to 350°C with a heating rate of 10°C/min in argon flow, 50 ml/min. Then the temperature was set to 350°C for 1 hour in argon flow, 50 ml/min. The catalyst was then cooled down to 30°C with a cooling rate of 20°C/min in argon flow, 50 ml/min, before it was kept at this temperature and flow for one hour. It was then kept at 30°C for one hour in argon and carbon dioxide flow, both at 25 ml/min. After one hour, the flow of  $CO_2$  was turned off, and an argon flow of 25 ml/min was used for one hour. After one hour, the temperature was set to 900°C with a heating rate of 10°C/min in argon flow, 25 ml/min. Then the temperature was kept at 1000°C for 10 minutes.

The TPD analysis of the acid sites was performed by heating the catalyst to 350°C with a heating rate of 10°C/min in argon flow, 50 ml/min. Then the temperature was set to 350°C for 1 hour in argon flow, 50 ml/min. The catalyst was then cooled down to 30°C with a cooling rate of 20°C/min in argon flow, 50 ml/min, before it was kept at this temperature and flow for one hour. It was then kept at 30°C for one hour in argon and  $NH_3$  flow, both at 25 ml/min. After one hour, the flow of  $NH_3$  was turned off, and an argon flow of 25 ml/min was used for one hour. After one hour, the temperature was set to 900°C with a heating rate of 10°C/min in argon flow, 25 ml/min. Then the temperature was kept at 1000°C for 10 minutes.

### 3.6.2 X-ray diffraction

X-ray diffraction was performed with  $TiO_2$  anatase powder before calcination and after calcination at  $600^\circ\text{C}$ . Then the EVA program on the computer on the XRD laboratory was used to find the structure of the  $TiO_2$  and to calculate the crystallite size of the peaks from the Scherrer equation as shown in Section 2.3.3, equation 2.5.

### 3.6.3 Gas chromatography

Two different machines were used, a gas chromatograph with a mass spectrometer as a detector, GC-MS, and a gas chromatograph with a flame ionization detector, GC-FID. GC-MS was used to find the product for each peak, while the GC-FID was used to find the areas to calculate conversion and selectivity as described in Section 2.3.4, and a calculation example is found in Appendix A. The GC-MS had an automatic injection mechanism, while in the GC-FID, the products had to be injected manually. A syringe was used for injection, and the injection volume was two  $\mu\text{L}$ .



## 4 Results and discussion

This section is divided into results from X-ray diffraction, results from temperature programmed desorption and results from different reactions. The reaction chapter is further divided into reaction of titanium dioxide coated on carbon nanotubes, effect of reaction pressure, effect of reduction temperature and reaction pressure, reaction with different catalysts and reaction with different zeolites.

### 4.1 X-ray diffraction

From the specialization report from fall 2014, it was observed from X-ray diffraction, XRD, that titanium dioxide coated on carbon nanotubes  $TiO_2/CNT$  was anatase  $TiO_2$ , so  $TiO_2$  anatase powder was analysed on the XRD both before and after calcination. Peaks from XRD is displayed in Figure 11. This illustrates that the  $TiO_2$  powder was in anatase form, same as for the  $TiO_2/CNT$  catalysts. The crystallite size of the biggest peak was calculated before and after calcination. The size was 564 Å before calcination and 513 Å after calcination. Figure 11 depicts that the peaks are larger and sharper before calcination than after calcination. Also the  $TiO_2$  crystallite size is reduced after calcination, which may be due to the pelletizing and crushing/sieving of the catalyst, since the non-calcinated  $TiO_2$  was not pelletized and crushed.

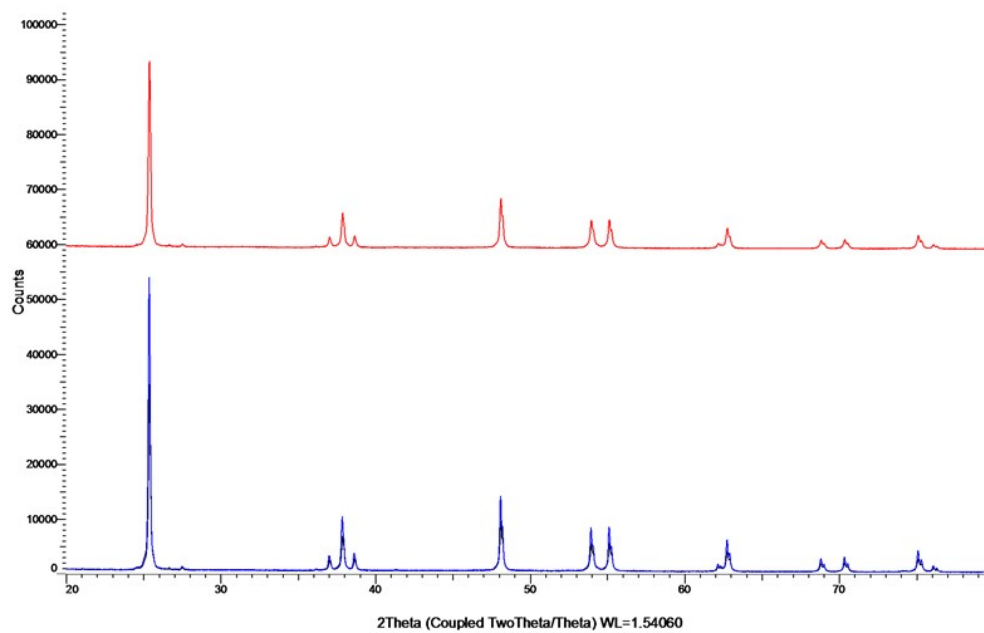


Figure 11: X-ray diffraction scans of  $TiO_2$  powder before and after calcination at  $600^\circ C$ . The red line is for  $TiO_2$  after calcination and the blue line is for  $TiO_2$  before calcination. Peaks are larger for  $TiO_2$  before calcination.

## 4.2 Temperature programmed desorption

Temperature programmed desorption was performed to investigate basic and acid sites of carbon nanotubes, CNT, titanium dioxide,  $TiO_2$ , calcinated at  $600^\circ C$ , 10 wt.%  $TiO_2/CNT$ , 20 wt. %  $TiO_2/CNT$ , 30 wt. %  $TiO_2/CNT$  and 40 wt. %  $TiO_2/CNT$ . Basic sites was measured with carbon dioxide,  $CO_2$ , while the acid sites where measured with ammonia,  $NH_3$ , and results are illustrated and discussed in Section 4.2.1 and 4.2.2.

### 4.2.1 Basic sites

Large peaks where observed at high temperature for the temperature programmed desorption of  $CO_2$ , for all  $TiO_2/CNT$  catalysts, as illustrated in Figure 12, 14, 16 and 18. Only  $TiO_2$  had small peaks around  $350 - 400^\circ C$ , and no peaks where found for  $TiO_2/CNT$  in this area.  $TiO_2$  anatase is known to have strong or medium strong basic sites, which was observed by Watanabe et al.[35] Peaks in the high temperature area appeared only for CNT and  $TiO_2/CNT$  and not for  $TiO_2$ . This was due to both cracking of C-O bonds, measured as CO desorbed and  $CO_2$  desorbed as illustrated when comparing the peaks in Figure 12, 14, 16, 18 and 20, and no CO is desorbed when only  $TiO_2$  is used. As illustrated in Figure 13, 15,17 and 19 there was a large mass loss in this area, which resulted from both CO and  $CO_2$  desorption. The ion current for CO was higher than for  $CO_2$ , indicating that most of the mass lost was from CO, but it was not possible to separate the mass lost due to CO and  $CO_2$ . Due to this, the adsorption of  $CO_2$  was calculated after purging of  $CO_2$  for one hour and then argon until the mass was stable, as illustrated in Appendix D, Figure D.1, D.2, D.3, D.4, D.5 and D.6. This was to ensure that the  $CO_2$  left had been adsorption strongly, and the values are found in table 5. Calculation examples are found in Appendix A with values from table D.1 in Appendix D. The mass of  $CO_2$  adsorbed increased with increasing loading for the 10 wt. %  $TiO_2/CNT$  and the 20 wt. %  $TiO_2/CNT$ . Loading from thermogravimetric analysis, TGA, from the specialization report was also included in this table, and a higher loading than 17 % of  $TiO_2$  makes the basic sites of the catalyst weaker. This may be due to clustering of  $TiO_2$  when coated on CNT, which leads to less available basic sites on the catalyst. Small amounts of  $CO_2$  was adsorb on only CNT, but the amount was lower than for  $TiO_2$  and the four different  $TiO_2/CNT$  catalysts.  $TiO_2$  has weaker basic sites than 10 and 20 wt. %  $TiO_2/CNT$ . A reason for this may be due to a larger surface area of the catalyst when CNT is applied as support.[13]

Table 5: Loading from TGA and amount of  $CO_2$  adsorbed by the basic sites of 10 wt. %  $TiO_2/CNT$ , 20 wt. %  $TiO_2/CNT$ , 30 wt. %  $TiO_2/CNT$ , 40 wt. %  $TiO_2/CNT$ , CNT and  $TiO_2$  in  $g/g_{catalyst}$  and  $mmol/g_{catalyst}$ .

Catalyst	Loading from TGA (%)	Mass adsorbed ( $mg/mg_{catalyst}$ )	Moles adsorbed ( $mmol/mg_{catalyst}$ )
10 wt. % $TiO_2/CNT$	14	$3.18 \cdot 10^{-2}$	$7.23 \cdot 10^{-4}$
20 wt. % $TiO_2/CNT$	17	$4.37 \cdot 10^{-2}$	$9.94 \cdot 10^{-4}$
30 wt. % $TiO_2/CNT$	28	$1.29 \cdot 10^{-2}$	$4.96 \cdot 10^{-4}$
40 wt. % $TiO_2/CNT$	24	$2.67 \cdot 10^{-2}$	$6.04 \cdot 10^{-4}$
CNT	-	$2.29 \cdot 10^{-3}$	$5.20 \cdot 10^{-5}$
$TiO_2$	-	$1.33 \cdot 10^{-2}$	$5.84 \cdot 10^{-3}$

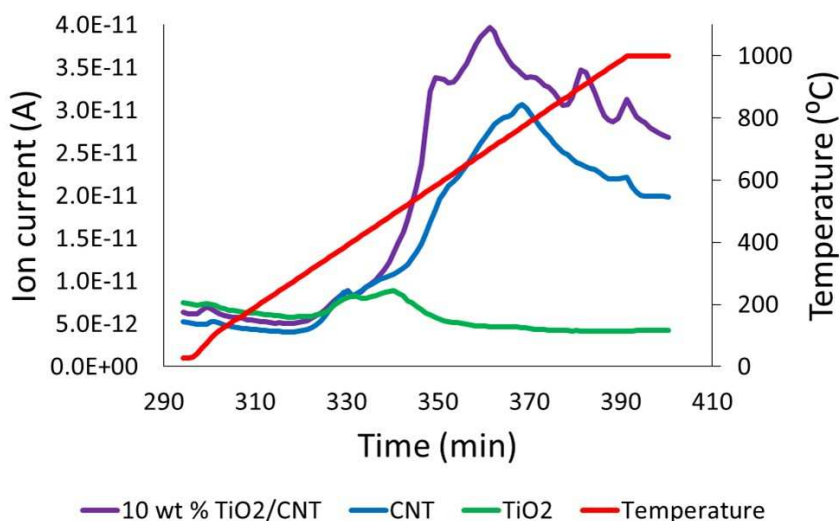


Figure 12: Ion current, A, and temperature, °C, over time, min, for basic sites of 10 wt. %  $TiO_2$ , CNT and  $TiO_2$ . The purple line is ion current of  $CO_2$  for the 10 wt. %  $TiO_2/CNT$ , blue line is ion current of  $CO_2$  for CNT, the green line is ion current of  $CO_2$  for  $TiO_2$  and the red line is the temperature.



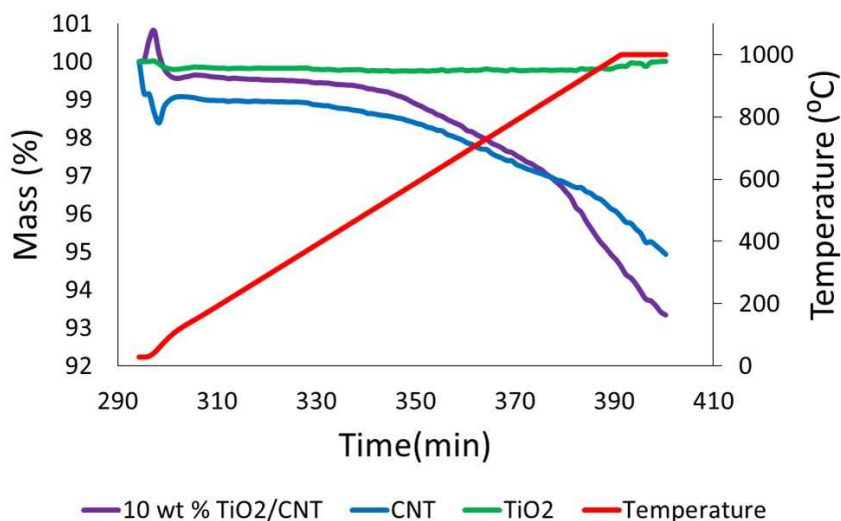


Figure 13: Mass, %, lost and temperature over time, min, for basic sites for 10 wt. %  $TiO_2$ , CNT and  $TiO_2$ . The purple line is the mass lost over time for 10 wt. %  $TiO_2/CNT$ , the blue line is the mass lost over time for CNT, the green line is the mass lost over time for  $TiO_2$  and the red line is the temperature.

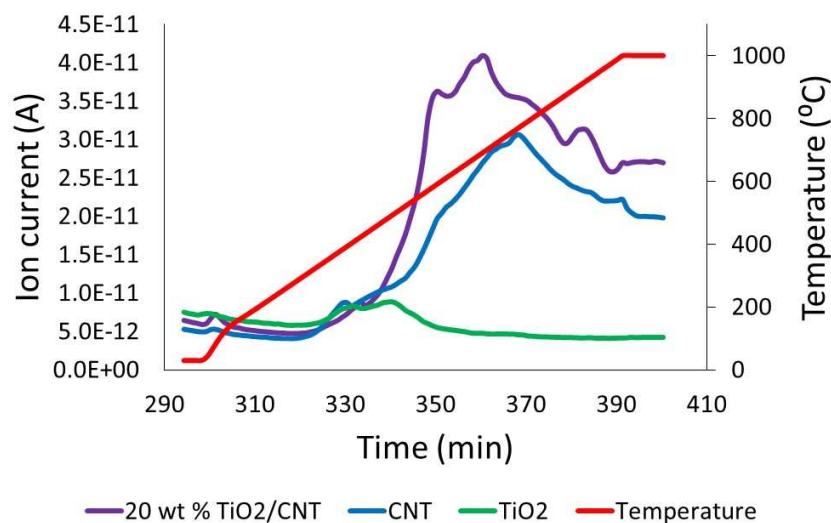


Figure 14: Ion current, A, and temperature, °C, over time, min, for basic sites of 20 wt. %  $TiO_2$ , CNT and  $TiO_2$ . The purple line is ion current of  $CO_2$  for the 20 wt. %  $TiO_2/CNT$ , blue line is ion current of  $CO_2$  for CNT, the green line is ion current of  $CO_2$  for  $TiO_2$  and the red line is the temperature.

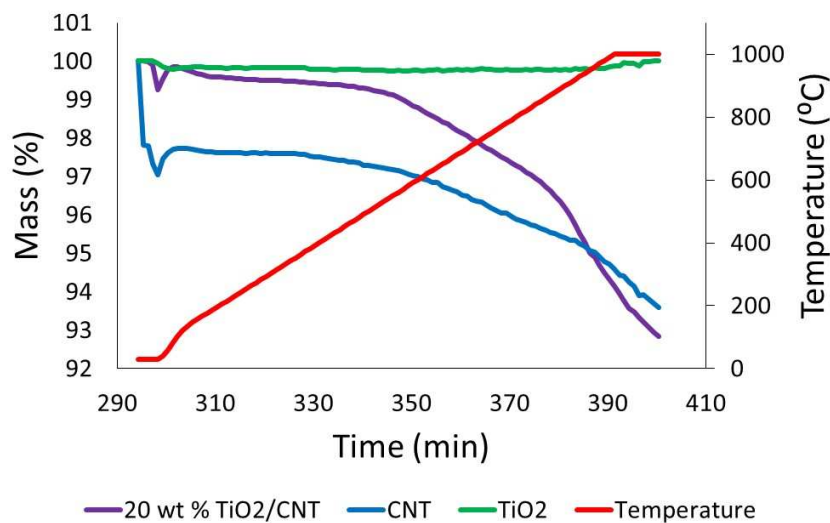


Figure 15: Mass, %, lost and temperature over time, min, for basic sites for 20 wt. %  $TiO_2$ , CNT and  $TiO_2$ . The purple line is the mass lost over time for 20 wt. %  $TiO_2/CNT$ , the blue line is the mass lost over time for CNT, the green line is the mass lost over time for  $TiO_2$  and the red line is the temperature.

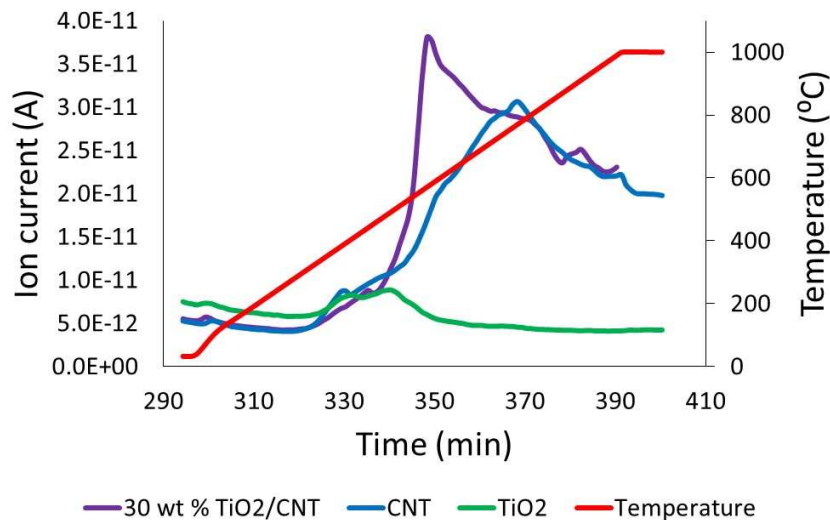


Figure 16: Ion current, A, and temperature, °C, over time, min, for basic sites of 30 wt. %  $TiO_2$ , CNT and  $TiO_2$ . The purple line is ion current of  $CO_2$  for the 30 wt. %  $TiO_2/CNT$ , blue line is ion current of  $CO_2$  for CNT, the green line is ion current of  $CO_2$  for  $TiO_2$  and the red line is the temperature.

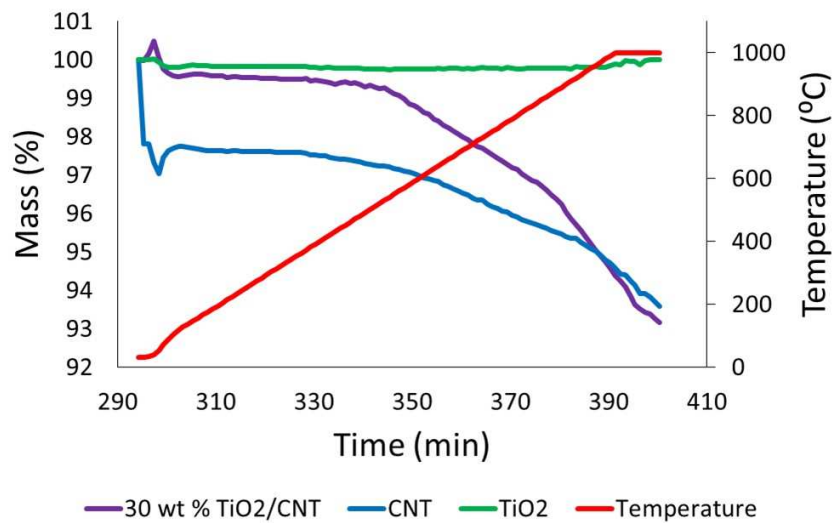


Figure 17: Mass, %, lost and temperature over time, min, for basic sites for 30 wt. %  $TiO_2$ , CNT and  $TiO_2$ . The purple line is the mass lost over time for 30 wt. %  $TiO_2/CNT$ , the blue line is the mass lost over time for CNT, the green line is the mass lost over time for  $TiO_2$  and the red line is the temperature.

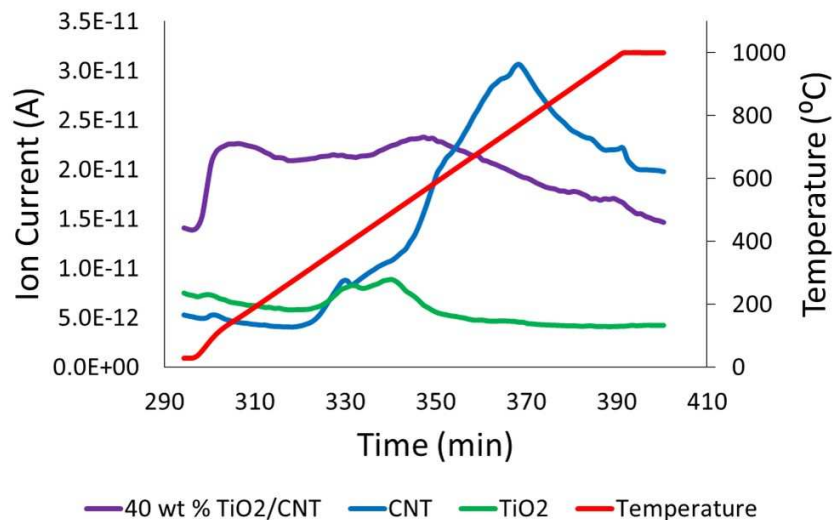


Figure 18: Ion current, A, and temperature, °C, over time, min, for basic sites of 40 wt. %  $TiO_2$ , CNT and  $TiO_2$ . The purple line is ion current of  $CO_2$  for the 40 wt. %  $TiO_2/CNT$ , blue line is ion current of  $CO_2$  for CNT, the green line is ion current of  $CO_2$  for  $TiO_2$  and the red line is the temperature.

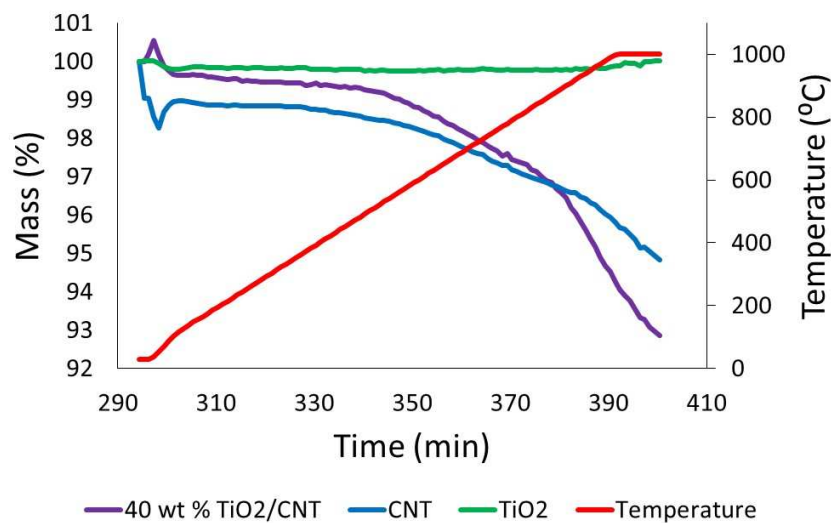


Figure 19: Mass, %, lost and temperature over time, min, for basic sites for 40 wt. %  $TiO_2$ , CNT and  $TiO_2$ . The purple line is the mass lost over time for 40 wt. %  $TiO_2/CNT$ , the blue line is the mass lost over time for CNT, the green line is the mass lost over time for  $TiO_2$  and the red line is the temperature.

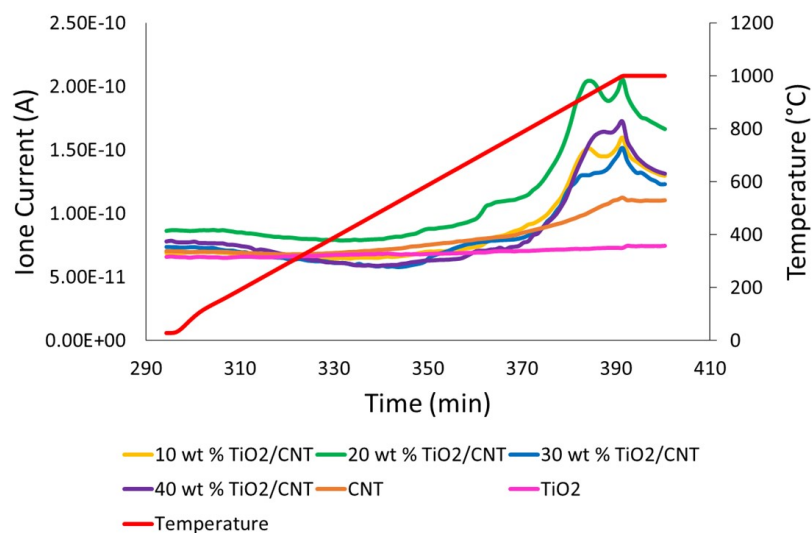


Figure 20: Ion current, A, and temperature, °C, over time, min, for CO desorption. The yellow line is 10 wt. %  $TiO_2/CNT$ , the green line is 20 wt. %  $TiO_2/CNT$ , the blue line is 30 wt. %  $TiO_2/CNT$ , the purple line is 40 wt. %  $TiO_2/CNT$ , the orange line is CNT, the pink line is  $TiO_2$  and the red line is the temperature.

### 4.2.2 Acid sites

Two acidic sites were observed for all four  $TiO_2/CNT$  catalysts, as illustrated in Figure 21, 23, 25 and 27 which was in accordance with the findings of Watanabe et al for anatase  $TiO_2$ .<sup>[35]</sup> Results from adsorbed  $NH_3$  for the first peak is displayed in table 6, without results from only  $TiO_2$ . When looking at Figure 22, 24, 26 and 28 it was observed that the mass of only  $TiO_2$  increased instead of decreasing. This may be due to production of gases, which may have been adsorbed by  $TiO_2$ . The amount of  $NH_3$  desorbed decreased with increasing loading of  $TiO_2$ , except for with a loading of 40 %, which had the largest amount of  $NH_3$  adsorbed. A reason for this may be that the coating of  $TiO_2$  on CNT may be different from the three others.

At higher temperature, there was also observed some peaks, as depicted in Figure 21, 23, 26 and 28. This is due to both cracking of C-O bonds, as illustrated in Figure 29 for CO desorption, and desorption of  $NH_3$ . Since the molecular weight of CO was not measured on the MS for  $TiO_2$ ,  $TiO_2$  was not included in this figure. It was not possible to find the mass of each of the CO desorbed and  $NH_3$  desorbed so this peak has not been calculated.

Table 6:  $NH_3$  desorbed in the first peak for the different catalysts and CNT.

Catalyst	Peak at time (min)	NH3 desorbed	
		Mass ( $mg/mg_{catalyst}$ )	Moles ( $mmol/mg_{catalyst}$ )
10 wt. % $TiO_2/CNT$	302	0.14	$3.26 \cdot 10^{-6}$
20 wt. % $TiO_2/CNT$	303	$8.48 \cdot 10^{-2}$	$4.99 \cdot 10^{-3}$
30 wt. % $TiO_2/CNT$	303	$5.31 \cdot 10^{-2}$	$3.12 \cdot 10^{-3}$
40 wt. % $TiO_2/CNT$	301	0.15	$1.47 \cdot 10^{-6}$
CNT	301	0.16	$9.22 \cdot 10^{-3}$

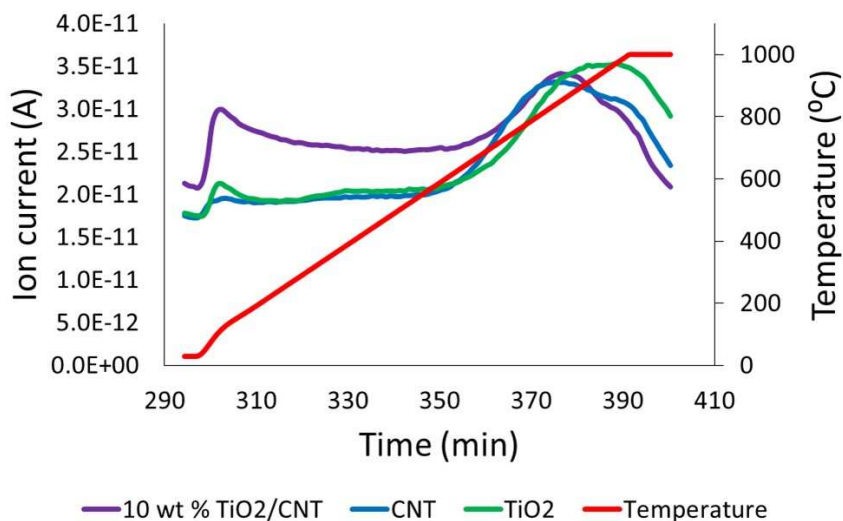


Figure 21: Ion current, A, and temperature, °C, over time, min, for acid sites of 10 wt. %  $TiO_2$ , CNT and  $TiO_2$ . The purple line is ion current of  $CO_2$  for the 10 wt. %  $TiO_2/CNT$ , blue line is ion current of  $CO_2$  for CNT, the green line is ion current of  $CO_2$  for  $TiO_2$  and the red line is the temperature.

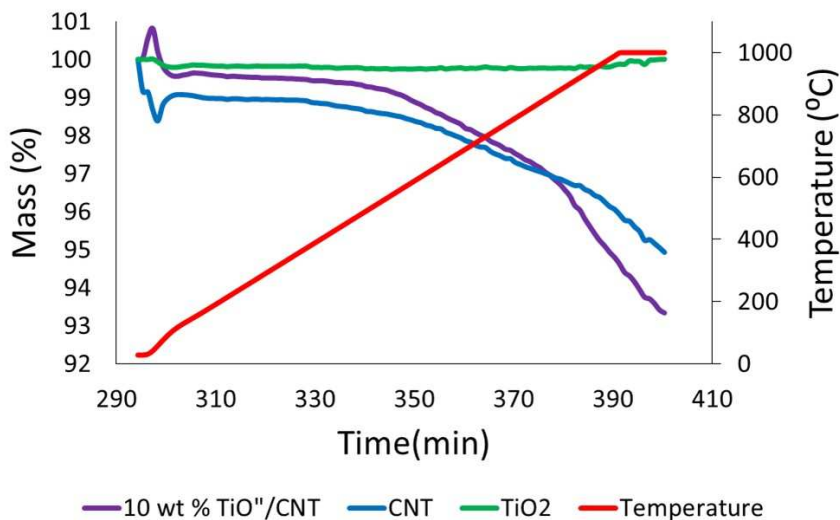


Figure 22: Mass, %, lost and temperature over time, min, for acid sites for 10 wt. %  $TiO_2$ , CNT and  $TiO_2$ . The purple line is the mass lost over time for 10 wt. %  $TiO_2/CNT$ , the blue line is the mass lost over time for CNT, the green line is the mass lost over time for  $TiO_2$  and the red line is the temperature.

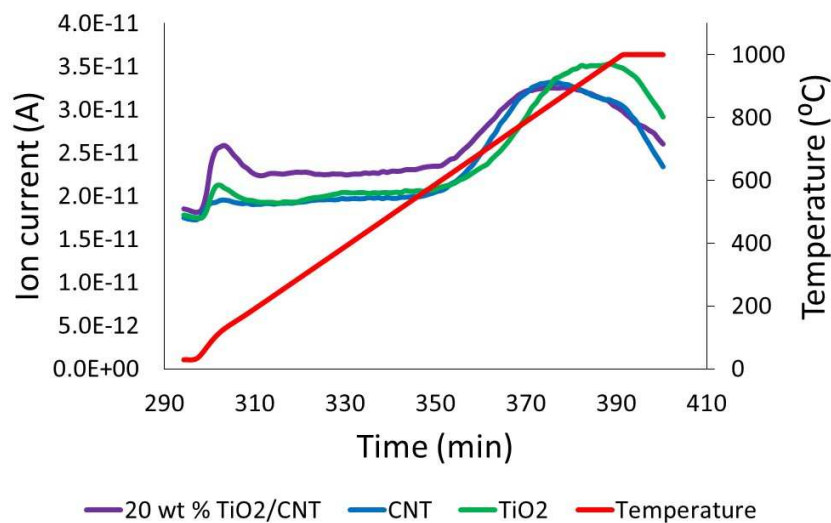


Figure 23: Ion current, A, and temperature, °C, over time, min, for acid sites of 20 wt. %  $TiO_2$ , CNT and  $TiO_2$ . The purple line is ion current of  $CO_2$  for the 20 wt. %  $TiO_2/CNT$ , blue line is ion current of  $CO_2$  for CNT, the green line is ion current of  $CO_2$  for  $TiO_2$  and the red line is the temperature.

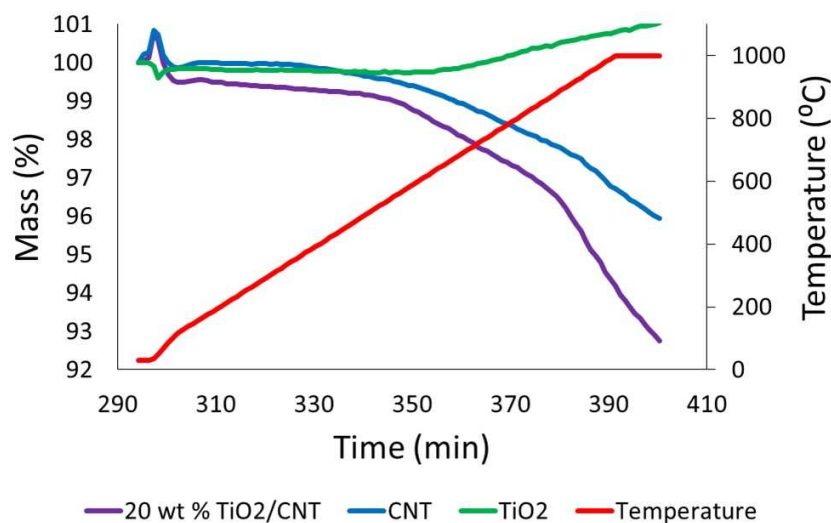


Figure 24: Mass, %, lost and temperature over time, min, for acid sites for 20 wt. %  $TiO_2$ , CNT and  $TiO_2$ . The purple line is the mass lost over time for 20 wt. %  $TiO_2/CNT$ , the blue line is the mass lost over time for CNT, the green line is the mass lost over time for  $TiO_2$  and the red line is the temperature.

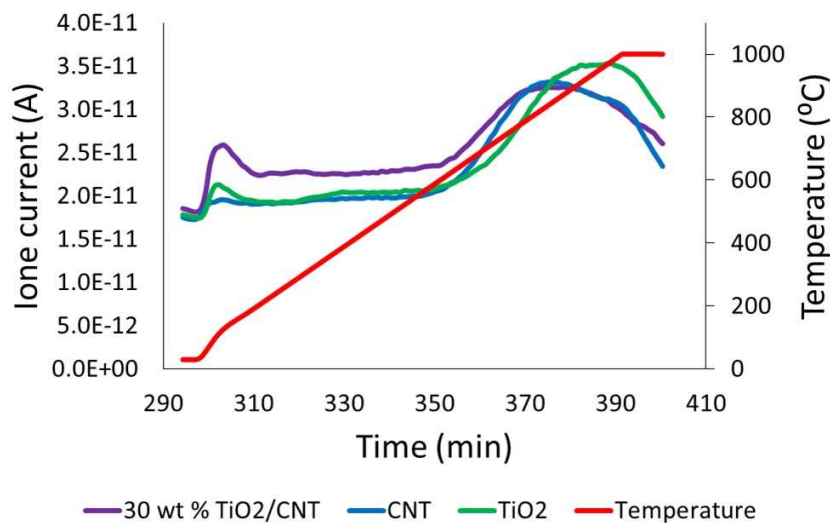


Figure 25: Ion current, A, and temperature, °C, over time, min, for acid sites of 30 wt. %  $TiO_2$ , CNT and  $TiO_2$ . The purple line is ion current of  $CO_2$  for the 30 wt. %  $TiO_2/CNT$ , blue line is ion current of  $CO_2$  for CNT, the green line is ion current of  $CO_2$  for  $TiO_2$  and the red line is the temperature.

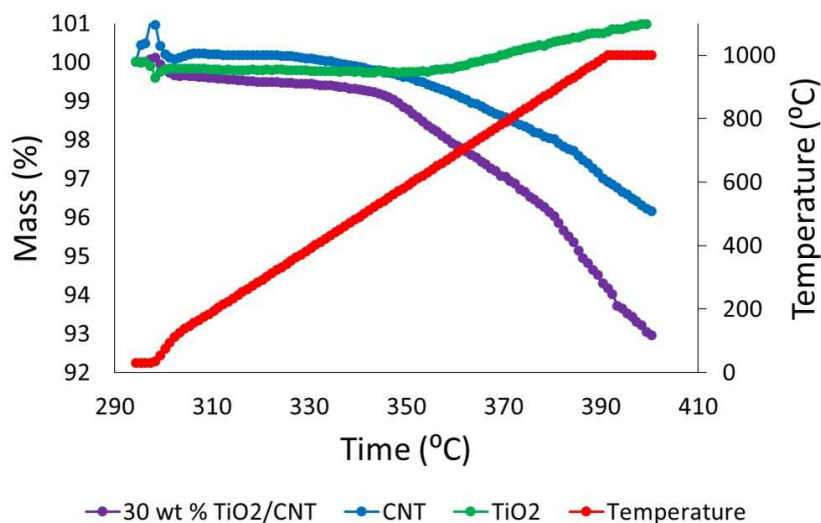


Figure 26: Mass, %, lost and temperature over time, min, for acid sites for 30 wt. %  $TiO_2$ , CNT and  $TiO_2$ . The purple line is the mass lost over time for 30 wt. %  $TiO_2/CNT$ , the blue line is the mass lost over time for CNT, the green line is the mass lost over time for  $TiO_2$  and the red line is the temperature.



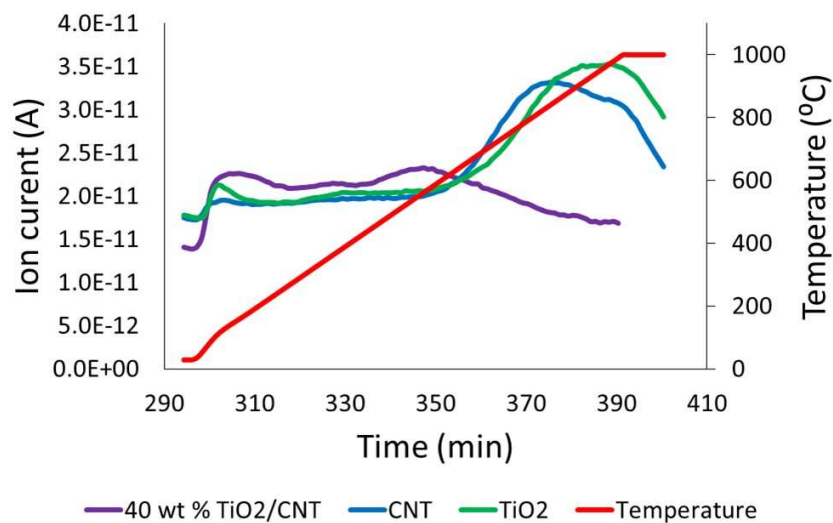


Figure 27: Ion current, A, and temperature, °C, over time, min, for acid sites of 40 wt. %  $TiO_2$ , CNT and  $TiO_2$ . The purple line is ion current of  $CO_2$  for the 40 wt. %  $TiO_2/CNT$ , blue line is ion current of  $CO_2$  for CNT, the green line is ion current of  $CO_2$  for  $TiO_2$  and the red line is the temperature.

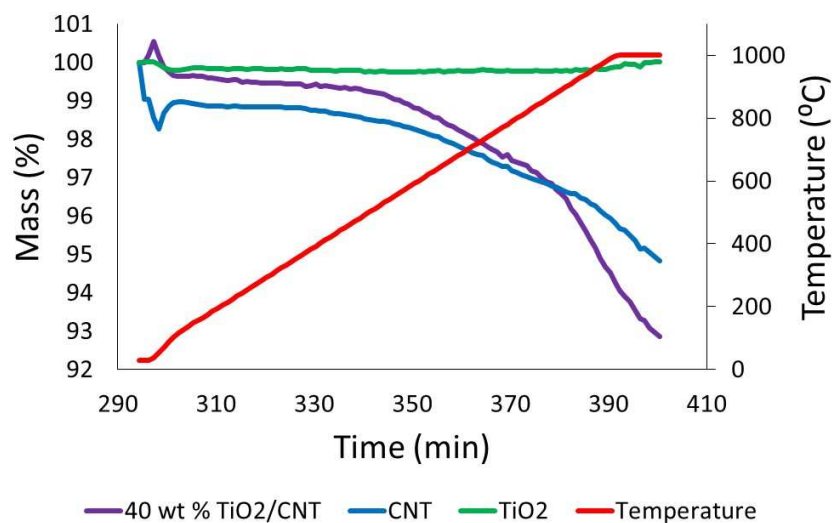


Figure 28: Mass, %, lost and temperature over time, min, for acid sites for 40 wt. %  $TiO_2$ , CNT and  $TiO_2$ . The purple line is the mass lost over time for 40 wt. %  $TiO_2/CNT$ , the blue line is the mass lost over time for CNT, the green line is the mass lost over time for  $TiO_2$  and the red line is the temperature.

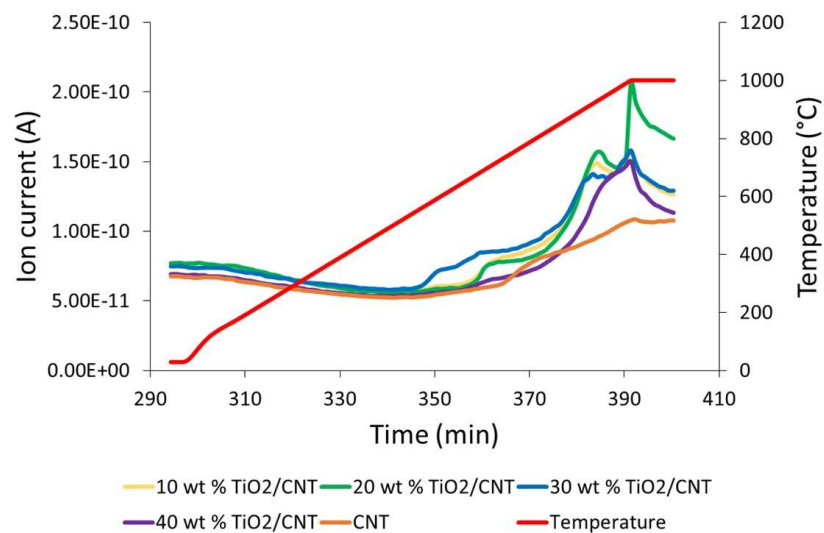


Figure 29: Ion current, A, and temperature, °C, over time, min, for CO desorption for acid sites. The yellow line is 10 wt. %  $TiO_2/CNT$ , the green line is 20 wt. %  $TiO_2/CNT$ , the blue line is 30 wt. %  $TiO_2/CNT$ , the purple line is 40 wt. %  $TiO_2/CNT$ , the orange line is CNT and the red line is temperature.

### 4.3 Reaction

Reactions were performed with different reduction conditions, different reaction pressures, different catalysts and different zeolite types. All products were collected after 20 hours, and in some reactions products were also collected after four hours. Collected products had either an oil phase, water phase or an oil phase and a water phase, and only the oil phase has been studied for the products with both an oil phase and a water phase in this report. Due to this, the conversion is actually lower than what has been reported, so the conversion should be calculated again with the water phase included, which requires different standard curves. The amount of oil and water phase was different for all products, and this was listed in table 7, 8, 9, 11 and 10. These tables illustrate both the amount of the two phases in mL and in %. All calculated conversions were for conversion of both n-propanol and propanal, and n-propanol and propanal was not included in the selectivity. Only products from C6, C9 and C12 were illustrated and discussed, since these were the desired products from reaction with propanal.

Table 7: Amount of water and oil in different products from reaction of 10 wt. %  $TiO_2/CNT$  with reduction/reaction conditions of 300°C and 1.2 bar and reduction/reaction conditions of 300°C and 1.2 bar.

Reduction/reaction temperature	Time (h)	Oil phase (ml)	Water phase (ml)	Oil phase (%)	Water phase (%)
230°C	4	0	1.32	0	100
230°C	20	0	12.40	0	100
300°C	4	0.34	0	100	0
300°C	20	8.20	0.45	94.8	5.2

Table 8: Amount of water and oil in different products from reduction conditions of 1.2 bar and 230°C and reaction conditions of 5, 10, 15 and 20 bar and 300°C

Reaction pressure (bar)	Oil phase (ml)	Water phase (ml)	Oil phase (%)	Water phase (%)
5	10.99	5	68.7	31.3
10	12.5	4.4	74.0	26.0
15	11.33	4	73.9	26.1
20	14.6	4	78.5	21.5

Table 9: Amount of water and oil in different products from reduction conditions of 1.2 bar and 300°C and reaction conditions of 1.2, 5, 10, 15 and 20 bar and 300°C.

Reaction pressure (bar)	Oil phase (ml)	Water phase (ml)	Oil phase (%)	Water phase (%)
1.2	7.5	2.1	78.1	21.9
5	6.8	5.5	55.3	44.7
10	8.8	5.5	61.5	38.5
15	10.7	4.57	70.1	29.9
20	8.4	4.5	65.1	34.9

Table 10: Amount of water and oil in different products from reaction with different zeolite types.

Zeolite	Time (h)	Oil phase (ml)	Water phase (ml)	Oil phase (%)	Water phase (%)
Z80	20	7.5	2.1	78.1	21.9
Z30(450)	4	0.001	0.00	100	0.00
Z30(450)	20	1.17	3.12	27.3	72.7
Z30(550)	4	2.55	0.55	82.3	17.7

Table 11: Amount of water and oil in different products from reduction conditions of 1.2 bar and 300°C and reaction conditions of 5 bar and 300°C.

Catalysts	Oil phase (ml)	Water phase (ml)	Oil phase (%)	Water phase (%)
<i>TiO<sub>2</sub></i>	15.17	1.44	91.3	8.7
<i>TiO<sub>2</sub>/CNT</i> and zeolite	4.8	7.0	61.9	38.1
<i>TiO<sub>2</sub>/CNT</i> and zeolite at half of normal partial pressure and flow	2.8	3.2	46.7	53.3

### 4.3.1 Reaction with 10 wt. % titanium dioxide coated on carbon nanotubes

Products from reaction with 10 wt. % titanium dioxide coated on carbon nanotubes,  $TiO_2/CNT$ , from the specialization project in fall 2014, collected after four hours and 20 hours was not analysed on the GC-FID, and the conversion and selectivity was not calculated. This has been done, and the conversion is illustrated in Figure 30 and the selectivity is illustrated in Figure 31 with values from table 12. Conversion was highest when reduction and reaction conditions were 1.2 bar and 300°C. A reason for this may be because the copper catalyst needs temperatures above 250°C for complete reduction.[32]. Two phases were present in all products, but the oil phase had a brighter colour when the reduction temperature was 300°C, which indicated that a higher conversion was achieved. This leads to more n-propanol transformed to propanal, and propanal was further reacted to desired products via aldol condensation reaction as described in Section 2.4.2. The selectivity for both C6 oxygenates and C9 hydrocarbons and oxygenates was highest at reduction and reaction temperature of 1.2 bar and 300°C. Selectivity towards C9 hydrocarbons was low, so a higher pressure and/or a higher or lower temperature should be applied to increase the selectivity towards C9 and higher hydrocarbons. Removal of oxygen molecules are necessary, since the selectivity towards hydrocarbons are zero for C6 molecules and low for C9 molecules, so zeolite, HZSM 5, R80, will be used for oxygen removal.

These results illustrates that aldol condensation of propanal to create carbon bonds over a  $TiO_2$  catalyst has worked, since C6 oxygenates and C9 hydrocarbons and oxygenates are produced.[45, 46] The C6 oxygenates are alcohols, aldehydes and small quantities of carboxylic acids, which is in agreement with the proposed reaction mechanism in Section 2.4.2, Figure 7 and 8.[12, 48] Production of C9 oxygenates where ketones and esters and for C9 hydrocarbons some small quantities of C9 alkenes was produced. The C6 carboxylic acid produced was produced from C9 esters, illustrated in Figure 9. Ketones and aldehydes readily undergo aldol condensation [45, 46], and propanal can also form esters as shown in Figure 9. Carboxylic acids are usually removed by ketonization[49], but some small quantities was still present, so ketonization had not fully occurred. The reason for this may be due to the applied reduction and reaction conditions.

Table 12: Reduction/reaction conditions, time of reaction, conversion, selectivity for C6 oxygenates, C9 hydrocarbon and C9 oxygenates for 10 wt. %  $TiO_2/CNT$  from the specialization project in fall 2014.

Reduction/ reaction conditions	Time (h)	$C_3$ based conversion	Selectivity		
			C6		C9
			Oxygenates	Hydrocarbons	Oxygenates
1.2 bar and 230°C	4	0.24	1.00	0.00	0.00
	20	0.22	1.00	0.00	0.00
1.2 bar and 300°C	4	0.48	0.62	0.44	0.00
	20	0.36	0.60	0.35	0.04

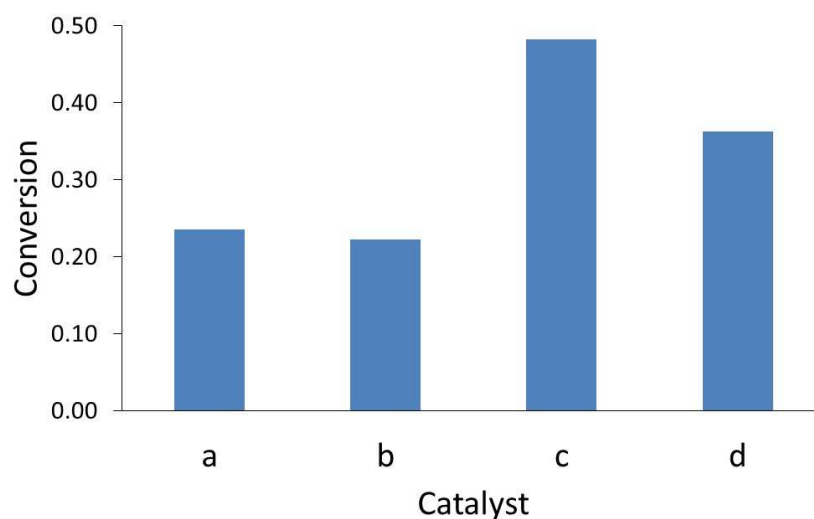


Figure 30: Conversion of products from reaction with 10 wt. %  $TiO_2/CNT$ . Reduction/reaction conditions of 1.2 bar and 230°C for (a), after four hours, and (b), after 20 hours. Reduction/reaction conditions at 1.2 bar and 300°C for (c), after four hours, and (d), after 20 hours.

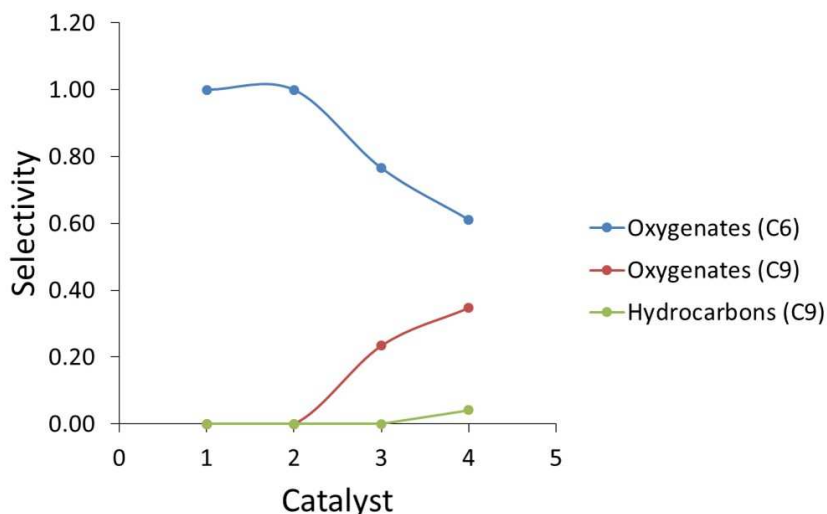


Figure 31: Selectivity for C6 oxygenates, C9 oxygenates and C9 hydrocarbons for products from reaction with 10 wt. %  $TiO_2/CNT$ . Catalyst 1 and 2 with reduction and reaction at 1.2 bar and  $230^\circ C$ , (1) collected after 4 hours and (2) collected after 20 hours. Catalyst 3 and 4 with reduction and reaction at 1.2 bar  $300^\circ C$ , (3) collected after 4 hours and (4) collected after 20 hours.

### 4.3.2 Effect of reduction pressure

Different reduction pressures were tested, and the first reduction and reaction conditions were  $230^\circ C$  and 20 bar. Products from this reaction were analysed on the gas chromatograph with a mass spectrometer as detector, GC-MS, and the results illustrated that it contained different olefins, aromatics and oxygenates with six and higher carbons in the chain. No n-propanol was found, so the conversion was 100 %. When the same reaction was performed with same reduction and reaction conditions, the conversion was low, and much n-propanol was left in the product. This reaction was performed multiple times to get the same results as first obtained, but it seemed like there were some parameters in the reaction that were different the first time. It may be that 20 bar was too high a reduction pressure for copper coated on silica,  $CuSiO_2$ , since much n-propanol was left, and almost no propanal was produced. A reason for this may be because the reduction occurred too fast at 20 bar, and the catalyst became less active, due to production of water. Due to this, these results are not included in this report, and the reduction pressure was decreased to 1.2 bar for the rest of the experiments.



### 4.3.3 Effect of reduction temperature and reaction pressure

Three different catalysts were used, 5 wt. % copper coated on silica,  $CuSiO_2$ , titanium dioxide,  $TiO_2$  and zeolite with a Si/Al ratio of 80, HZSM 5, Z80. Reduction was performed at 1.2 bar and 230°C and 1.2 bar and 300°C, and the reaction was performed at 1.2, 5, 10, 15 and 20 bar and 300°C. The effect of reduction temperature and reaction pressure are presented and discussed in this section. Values for conversion and selectivity towards all oxygenates and hydrocarbons is found in table E.2 and E.1 in Appendix E.

Figure 32 illustrates the conversion when reaction was performed with  $TiO_2$ ,  $CuSiO_2$ , and zeolite, at reduction conditions of 1.2 bar and 230°C and reaction conditions of 5, 10, 15 and 20 bar and 300°C. Highest conversion was obtained with a reaction pressure of 5 bar, at 0.57. For reaction pressures of 10, 15 and 20 bar, the conversion was 0.44, 0.44 and 0.40 respectively. Since the conversion was low for all different pressures applied, it may be that the  $CuSiO_2$  catalyst was not fully reduced when a reduction temperature of 230°C was applied. According to Vasiliadou et al. a copper catalyst is fully reduced when a temperature of above 250°C is applied for reduction.[32] This indicates that since the reduction temperature used was below this value, only some of the copper has been reduced.

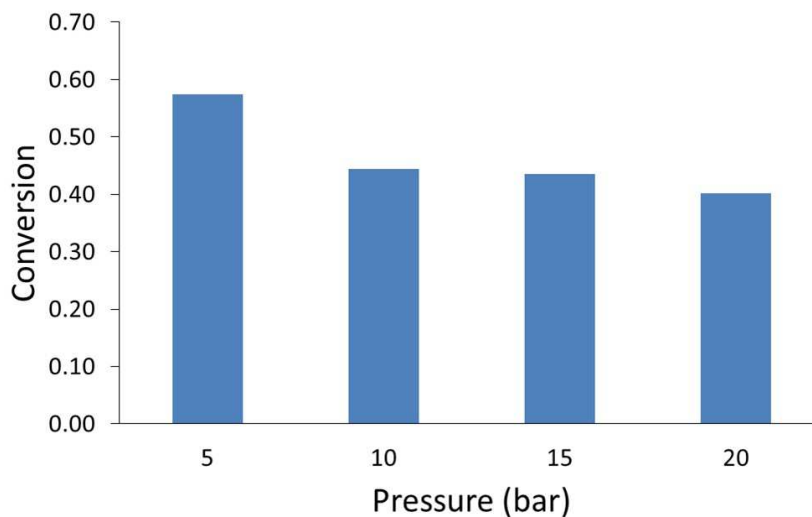


Figure 32: Conversion for reaction with  $TiO_2$  and zeolite at reduction conditions of 1.2 bar and 230°C and reaction conditions of 5, 10, 15 and 20 bar and 300°C.

Conversion for reactions performed with reduction conditions of 1.2 bar and 300°C and reaction conditions of 1.2, 5, 10, 15 and 20 bar and 300°C is depicted in Figure 33. Highest conversion

was achieved with a reaction pressure of 5 and 10 bar at 0.96 and 0.98 respectively. With a reaction pressure of 1.2 bar, 15 bar and 20 bar, the conversion was 0.73, 0.73 and 0.72 respectively. This indicated that at a reaction temperature of 300°C and reduction conditions of 1.2 bar and 300°C, a pressure of 5 or 10 bar is necessary for high conversion.

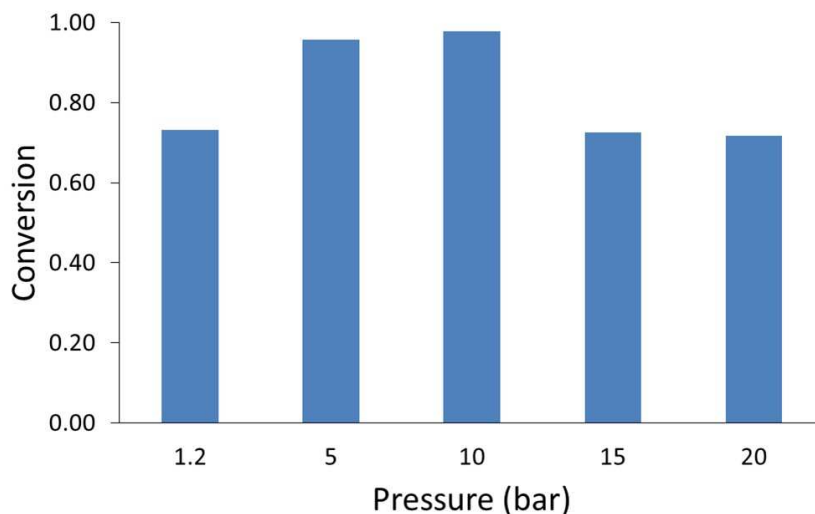


Figure 33: Conversion for reaction with  $TiO_2$  and zeolite at a reduction temperature of 300°C and 1.2 bar and reaction temperature of 300°C and 5, 10, 15 or 20 bar.

When the results from reduction at 230°C and 300°C was compared, the conversion was higher at a reduction temperature of 300°C. A reason for this may be because the copper catalyst needs a temperatures above 250°C to become fully reduced, as mentioned above.[32]

Figure 34 depicts the selectivity of all oxygenates and hydrocarbons at reduction conditions of 1.2 bar and 230°C and reaction conditions of 5, 10, 15 and 20 bar and 300°C. The selectivity to hydrocarbons was 0.46 with a reaction pressure of 5 bar, before decreasing to 0.24 with a reaction pressure of 10 bar. Then it increased to 0.41 at 15 bar before it decreased to 0.30 for 20 bar. With a reaction pressure of 5 and 10 bar, the selectivity of oxygenated was 0.54 and 0.76 respectively. When the pressure was increased to 15 and 20 bar, the selectivity of oxygenates was at 0.59 and 0.70 respectively. This indicated that the zeolite was not working properly at the applied reduction and reaction conditions, since there was much oxygen left in the products.[1]

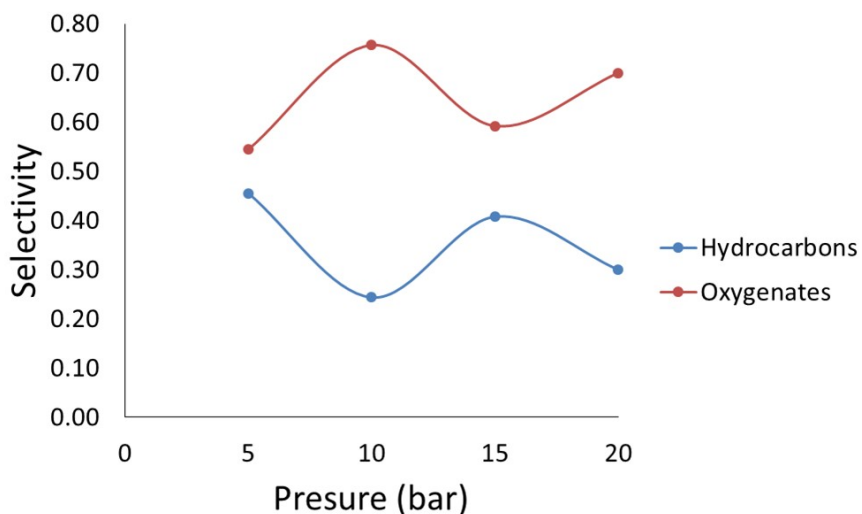


Figure 34: Selectivity for all hydrocarbons and oxygenates from reaction with  $TiO_2$  and zeolite at reduction conditions of 1.2 bar and  $230^\circ\text{C}$  and reaction conditions of 5, 10, 15 and 20 bar and  $300^\circ\text{C}$ .

Selectivity of C6 hydrocarbons and oxygenates with reduction conditions of 1.2 bar and  $230^\circ\text{C}$  and reaction conditions of 5, 10, 15 and 20 bar and  $300^\circ\text{C}$  are displayed in Figure 35. Conversion and selectivity of ketones, aldehydes, alcohols, esters/ethers, alkanes and alkenes are illustrated in Figure 36. When a reaction pressure of 5 bar and 15 bar was applied the selectivity towards C6 hydrocarbons was 0.22 and 0.23 respectively, while the selectivity towards oxygenates was 0.38 and 0.30. The selectivity towards C6 oxygenates was 0.54 and 0.50 at a reaction pressure of 5 and 10 bar respectively, while the selectivity towards oxygenates was 0.38 and 0.70 when a reaction pressure of 15 and 20 bar was applied, respectively. It was clear that the zeolite removed more oxygen from C6 oxygenates at a pressure of 15 bar.

Aldehydes were present when the reaction pressure was 5 bar and 20 bar, while ketones were present in small amounts at 10, 15 and 20 bar. This may be due to a more favourable formation of C6 aldols to aldehyde at pressures of 1.2 and 20 bar, while the formation of ketones or aldehydes and then dehydration to alcohols was favoured at 5 and 10 bar. Alcohols were present in highest amount with a reaction pressure of 10 and 15 bar. When two propanal molecules are combined through aldol condensation and a C-C bond is formed between the molecules, to produce an aldol. Further hydrogenation of this aldol to ketone or an aldehyde then occurs. This ketone or aldehyde is then hydrogenated to form an alcohol, as illustrated in Figure 8.[12, 48] This indicates that further hydrogenation of ketones and aldehydes formed to alcohols have oc-

curred, but the last dehydrogenation step from alcohols to alkenes has not fully occurred. Since most alkenes are formed with a reaction pressure of 20 bar, it may be that high pressures was necessary for the zeolite dehydrogenation step to occur for C6 alcohols at the applied reduction and reaction conditions. Esters/ethers where formed at all the applied reaction pressures, but the highest selectivity was obtained when the pressure was 20 bar. A reason for this may be that 20 bar favours both C-O coupling between n-propanol and propanal and C-C coupling over aldol condensation reaction. Since the selectivity towards aldehydes are higher than ketones, aldehydes where most likely formed more readily than ketones after aldol condensation reaction at 20 bar.

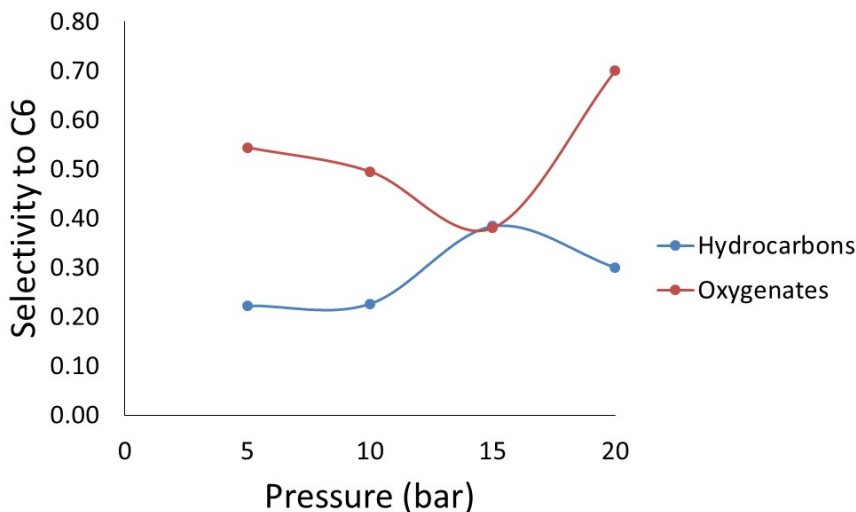


Figure 35: Selectivity for C6 hydrocarbons and oxygenates for reaction with  $TiO_2$  and zeolite at reduction conditions of 1.2 bar and 230°C and reaction conditions of 5, 10, 15 and 20 bar and 300°C.

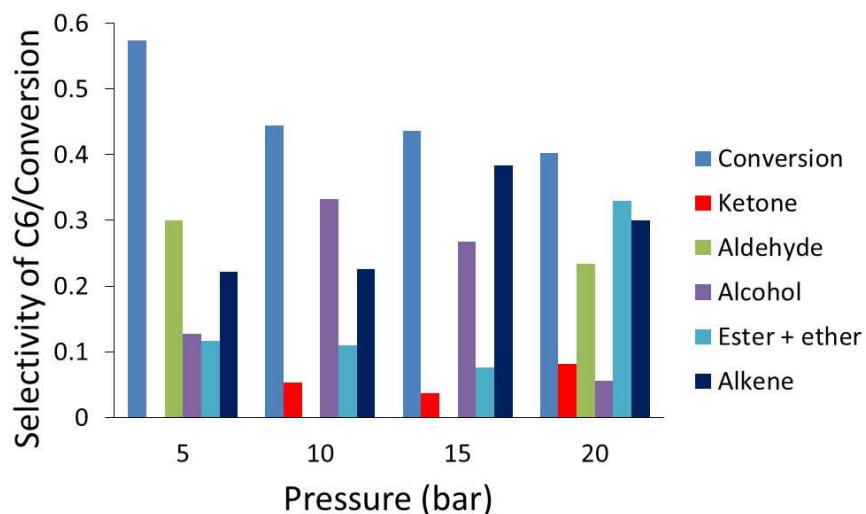


Figure 36: Selectivity for C6 ketones, aldehydes, alcohols, esters/ethers, alkanes and alkenes from reaction with  $TiO_2$  and zeolite at reduction conditions of 1.2 bar and 230°C and reaction conditions of 5, 10, 15 and 20 bar and 300°C

Figure 37 illustrates the selectivity towards C9 hydrocarbons and oxygenates. Selectivity towards C9 hydrocarbons was highest with a reaction pressure of 5 bar, and it was 0.14, before decreasing to zero for the rest of the applied pressures. The oxygenate selectivity started at zero for 5 bar, before it increased to 0.17 and 0.14 with a reaction pressure of 10 and 15 bar respectively, and then decreased to zero at a pressure of 20 bar. Aromatics were the only hydrocarbons produced at 5 bar, while the oxygenates produced at 10 and 15 bar were ketones as displayed in Figure 38. This indicated that zeolite only could remove oxygen at low pressures at the applied reduction and reaction conditions. Aromatization reaction was due to the zeolite, which made the larger molecules form ring structures of benzene.[1] Since the only C9 oxygenates produced were ketones, it may be that the zeolite more easily removes oxygen from C-OH bonds as illustrated in Figure 9,[12, 48] but not carbons double bonded to oxygen. The products produced under aldol condensation reaction were C9 ketones and these ketones did not undergo hydrogenation to alcohols and then dehydration to hydrocarbons. Since there were not produced any molecules in the C9 range when the reaction pressure was 20 bar, it looks like this pressure was too high for aldol condensation to C9 oxygenates for the applied reduction and reaction conditions.

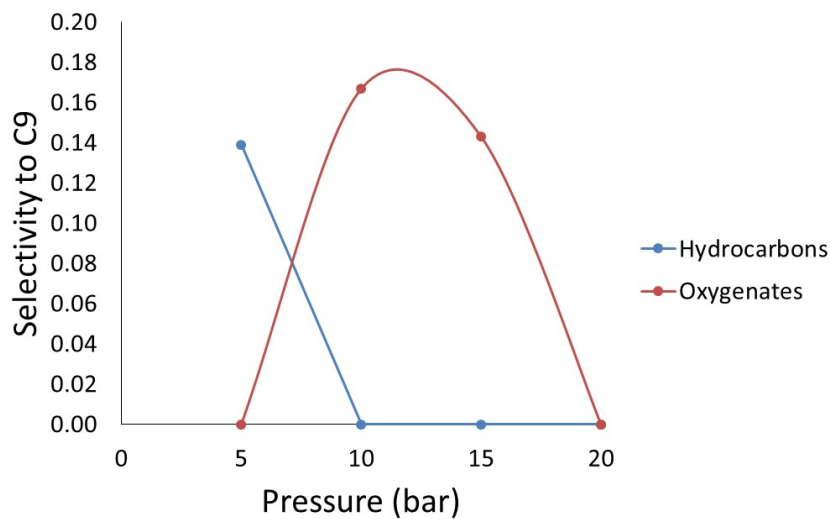


Figure 37: Selectivity for C9 hydrocarbons and oxygenates for reaction with  $TiO_2$  and zeolite at reduction conditions of 1.2 bar and 230°C and reaction conditions of 5, 10, 15 and 20 bar and 300°C.

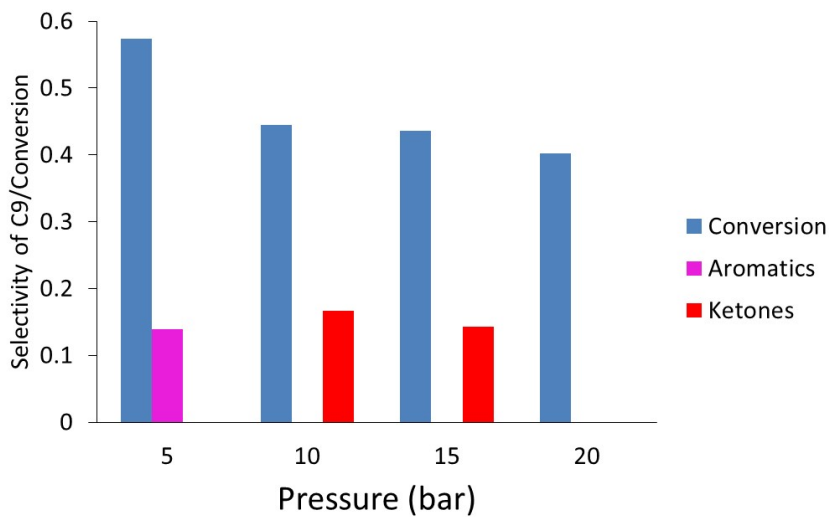


Figure 38: Selectivity for C9 aromatics and ketones for reaction with  $TiO_2$  and zeolite at reduction conditions of 1.2 bar and 230°C and reaction conditions of 5, 10, 15 and 20 bar and 300°C.

Selectivity for all hydrocarbons and oxygenates at reduction conditions of 1.2 bar and 300°C and reaction conditions of 1.2, 5, 10, 15 and 20 bar and 300°C is illustrated in Figure 39. At a

pressure of 1.2 bar, the selectivity towards hydrocarbons was 0.02, before increasing to 0.78 and 0.84 at reaction pressures of 5 and 10 bar respectively. Then the selectivity decreased to 0.36 and 0.44 for reaction pressures of 15 and 20 bar respectively. For oxygenates, an opposite trend was found, since the selectivity begun at 0.98 before decreasing to 0.22 and 0.16 at reaction pressure of 1.2, 5 and 10 bar respectively. Then the selectivity increased to 0.64 and 0.56 at reaction pressures of 15 and 20 bar respectively. Based on this it was clear that most removal of oxygen occurred with a reaction pressure of 5 and 10 bar. A lower pressure than 1.2 bar or higher pressure than 10 bar was not suitable reaction pressures for Z80 when a reaction temperature of 300°C was applied.

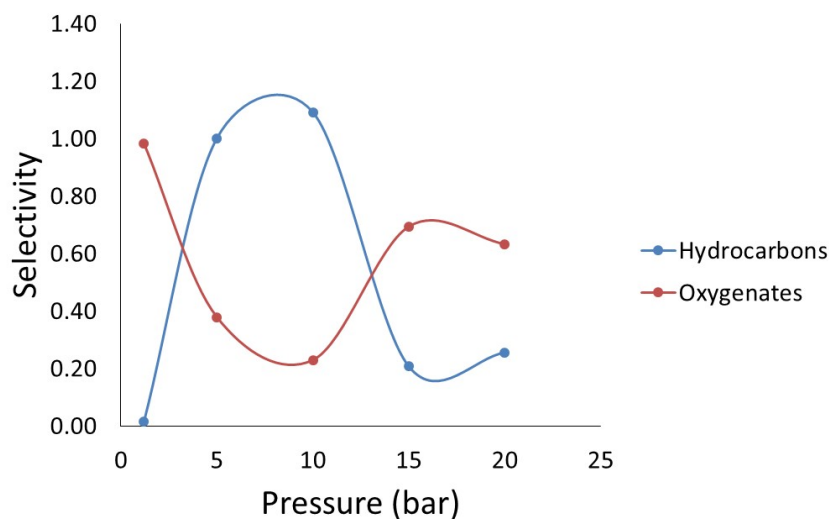


Figure 39: Selectivity for all hydrocarbons and oxygenates for reaction with  $TiO_2$  and zeolite at a reduction conditions of 1.2 bar and 300°C and reaction conditions of 5, 10, 15 and 20 bar and 300°C

Figure 40 depict that the C6 selectivity of hydrocarbons, increased from zero at a reaction pressure of 1.2 bar to 0.06 and 0.32 at reaction pressures of 5 and 10 bar respectively. Then the selectivity increased to 0.36 and 0.42 reaction pressures of 15 and 20 bar, respectively. Selectivity towards oxygenates followed an opposite trend, and decreased from 0.66 at a reaction pressure of 1.2 bar to 0.14 at a reaction pressure of 5 bar. Then it decreased to 0.10 for a reaction pressure of 10 bar before increasing to 0.45 at a reaction pressure of 15 bar. At a reaction pressure of 20 bar, the selectivity decreased to 0.36. Selectivity towards the different C6 oxygenates and hydrocarbons and the conversion are illustrated in Figure 41, and the different products are ketones, aldehydes, alcohols, esters/ethers, alkanes and alkenes. It was difficult to compare

the three reactions performed with a reaction pressure of 1.2, 15 and 20 bar with the reactions performed with a reaction pressure of 5 and 10 bar, since the conversion was different. Due to this, the selectivity towards the different products were compared first for a reaction pressure of 5 and 10 bar, and then for the three remaining pressures.

Aldehyde selectivity decreased from a reaction pressure of 5 to 10 bar, while the selectivity towards alkenes and alkanes increased. This was possibly due to hydrogenation of aldehyde to alcohol before it reacted further to an alkene by dehydration of alcohol as illustrated in Figure 8. It looks like this reaction sequence is favoured by a high pressure at a reaction temperature of 300°C. Some selectivity towards ketones occurred when the reaction pressure was 10 bar. This might be due to the formation of C6 ketones, which does not undergo further hydrogenation to alcohols and then dehydration to hydrocarbons. Esters/ethers are only produced at a reaction pressure of 10 bar, which is also a product produced when  $TiO_2$  is used as a catalyst as illustrated in Figure 9.

A similar trend was observed when the reaction pressure was increased from 1.2 bar to 15 and 20 bar, where the selectivity of aldehydes decreased with increasing pressure. Aldehydes have possibly reacted further to alcohols, but not all the alcohols have dehydrated to alkenes at a reaction pressures of 15 and 20 bar. This may explain the selectivity for alcohols and alkenes at reaction pressures of 15 and 20 bar. The selectivity towards alkenes increased with increasing pressure, and this indicated that a higher pressure favours alkene production. At a reaction pressure of 1.2 bar, there was no alkenes produced, but the selectivity towards aldehydes were large. Since aldehydes are favoured at this low pressure and no alcohols are present, it was likely that the hydrogenation of aldehydes and ketones did not occur. For all three applied reaction pressures there was some selectivity towards esters/ethers, and some ketones was present.



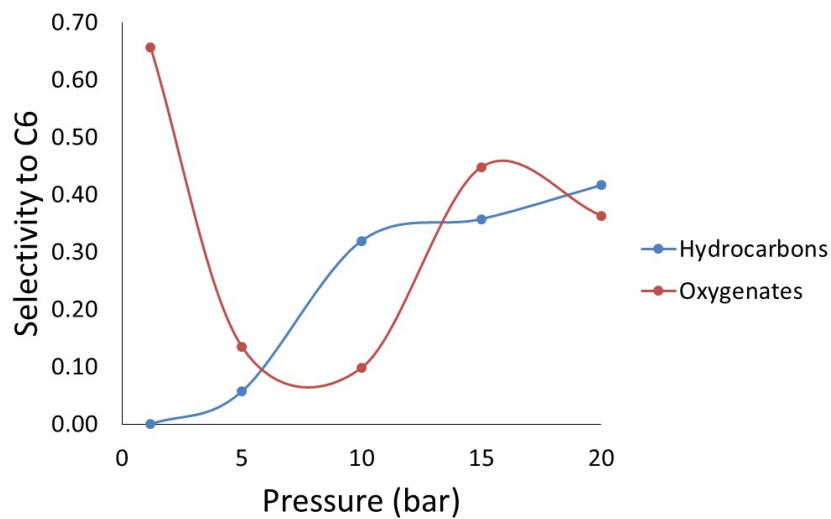


Figure 40: Selectivity for C6 hydrocarbons and oxygenates for reaction with  $TiO_2$  and zeolite at a reduction temperature of  $300^\circ\text{C}$  and 1.2 bar and reaction temperature of  $300^\circ\text{C}$  and 1.2, 5, 10, 15 or 20 bar.

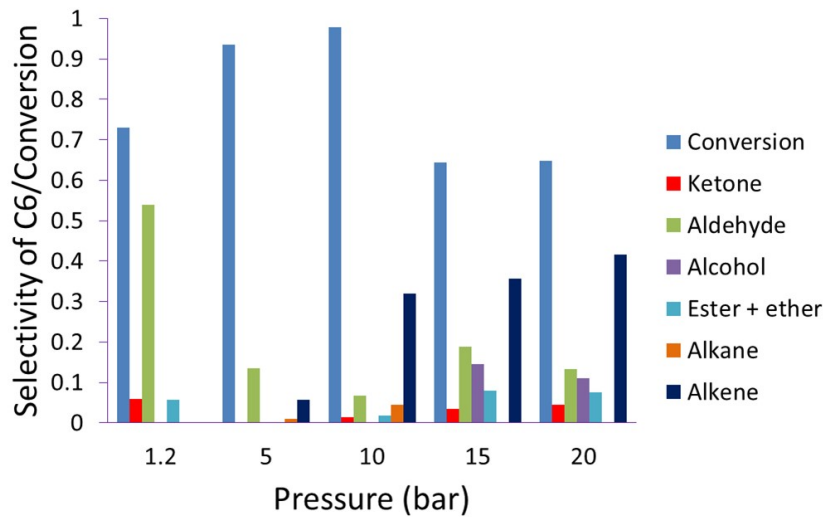


Figure 41: Selectivity for C9 ketones, aldehydes, alcohols, esters/ethers, alkanes and alkenes and conversion for reaction with  $TiO_2$  and zeolite at reduction conditions of 1.2 bar and  $300^\circ\text{C}$  and reaction conditions of 1.2, 5, 10, 15 and 20 bar and  $300^\circ\text{C}$ .

Figure 42 illustrates the selectivity of C9 hydrocarbons and oxygenates with reduction conditions of 1.2 bar and 300°C and reaction conditions of 1.2, 5, 10, 15 and 20 bar and 300°C. The selectivity of hydrocarbons increased from zero at a reaction pressure of 1.2 bar to 0.22 and 0.13 at reaction pressures of 5 and 10 bar respectively. Then the selectivity decreased to zero for reaction pressures of 15 and 20 bar. The oxygenates decreased from 0.28 at a reaction pressure of 1.2 bar to 0.09 at a reaction pressure of 5 bar. Then the selectivity decreased to 0.04, 0.14 and 0.15 for a reaction pressure of 10, 15 and 20 bar respectively. This indicates that most C9 alcohols were produced at a reaction pressure of 5 bar at the applied reduction conditions and reaction temperature. It was also difficult to compare the three reactions performed with a reaction pressure of 1.2, 15 and 20 bar with the reactions performed with reaction pressures of 5 and 10 bar, since the conversion was different. Due to this, the selectivity towards the different products were compared first for reaction pressures of 5 and 10 bar, and then for the three others.

At a reaction pressure of 5 bar, the selectivity towards ketones, aromatics and alkenes were higher than with a reaction pressure of 10 bar. When comparing the different pressures to the selectivity towards C6 alkenes and alkanes, it was higher selectivity towards C6 alkenes and alkanes when the reaction pressure was 10 bar. A reason for this may be that longer carbon chains produced, like C12 molecules, undergo cracking by the zeolite into smaller molecules, like C6. Another reason may be that the selectivity towards C6 alcohols was higher for 10 bar than 5 bar. This indicates that a higher pressure leads to more C6 hydrocarbons formed than C9 hydrocarbons at the applied reduction condition and reaction temperature. Aromatization of the products occur due to the zeolite.[1]

A reaction pressure of 1.2 bar leads to higher selectivity towards ketones than a reaction pressure of 15 and 20 bar. Only C6 alkenes and alkanes were produced which may be due to cracking of larger molecules due to the zeolite, or more C6 alcohols were produced at these pressures. Since only ketones were produced, it may be that the pressure was either too high or too low for hydrogenation of these ketones.

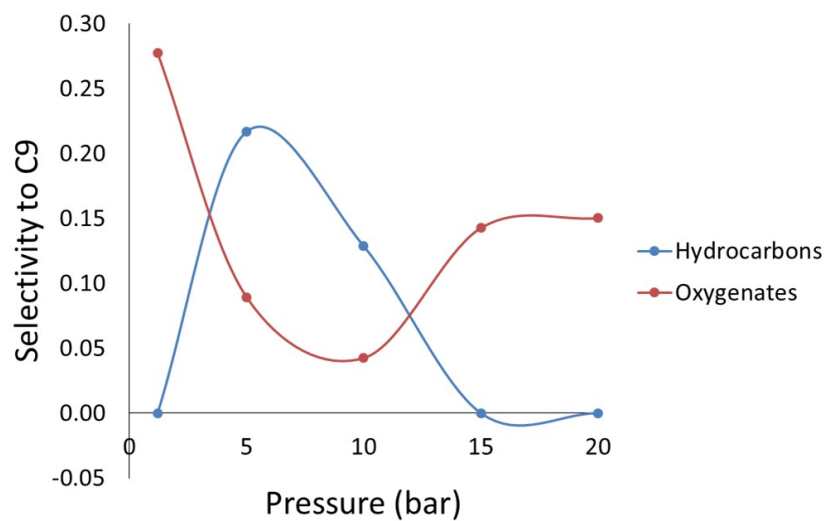


Figure 42: Selectivity for C9 hydrocarbons and oxygenates for reaction with  $TiO_2$  and zeolite at reduction conditions of 1.2 bar and 300°C and reaction conditions of 1.2, 5, 10, 15 and 20 bar and 300°C.

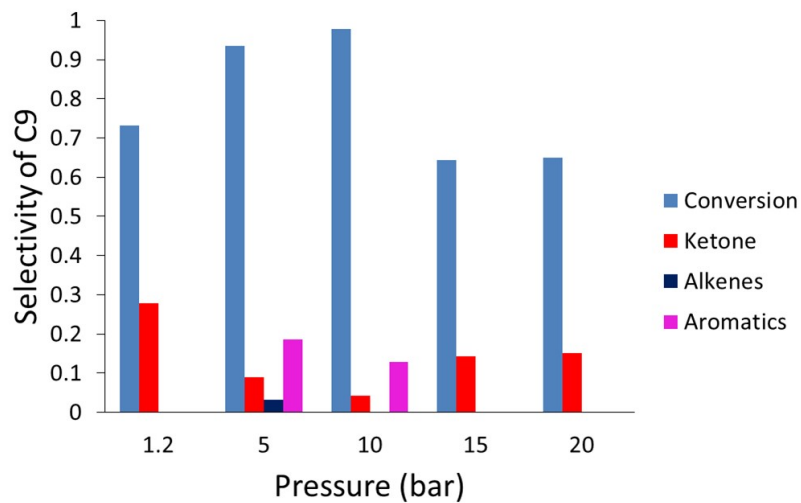


Figure 43: Selectivity for C9 ketones, alkanes and aromatics and conversion for reaction with  $TiO_2$  and zeolite at reduction conditions of 1.2 bar and 300°C and reaction conditions of 1.2, 5, 10, 15 and 20 bar and 300°C.

#### 4.3.4 Reaction with different catalysts

Four different reactions were performed with reduction conditions of 1.2 bar and 300°C and reaction conditions of 5 bar and 300°C, because these reduction and reaction conditions had highest selectivity towards C9 aromatics and alkenes. Catalysts used were  $TiO_2$  and 20 wt. %  $TiO_2/CNT$ . The last catalyst was used both under normal reaction conditions and at half of the partial pressure and flow of the reactant gases, as described in section 3.5. Values for conversion and selectivity towards all hydrocarbons and oxygenates are found in table E.3 in Appendix E.

The conversion was 100 % for reaction with  $TiO_2/CNT$  at normal partial pressure, and 99 % for reaction with  $TiO_2/CNT$  with half of the normal partial pressure as displayed in Figure 44. For  $TiO_2$  without zeolite, the conversion was around 50 %, while it was around 94 % when zeolite was used. This indicates that the zeolite was catalytic active in aldol condensation reaction and since the active sites of the zeolite was acid[1] it could be that acid sites of catalysts has an impact on aldol condensation reaction. This could be due to formation of intermediate in the zeolite pores, which helps during aldol condensation reaction. When carbon nanotubes, CNT, was used as support, the conversion was almost the same as for reaction with only  $TiO_2$ , even though a smaller amount of  $TiO_2$  was coated on CNT, since only 0.3 g of the total amount of the  $TiO_2/CNT$  catalyst contains  $TiO_2$ . This might be because CNT applied the catalyst with a higher surface area than for only  $TiO_2$  alone. [13, 17]

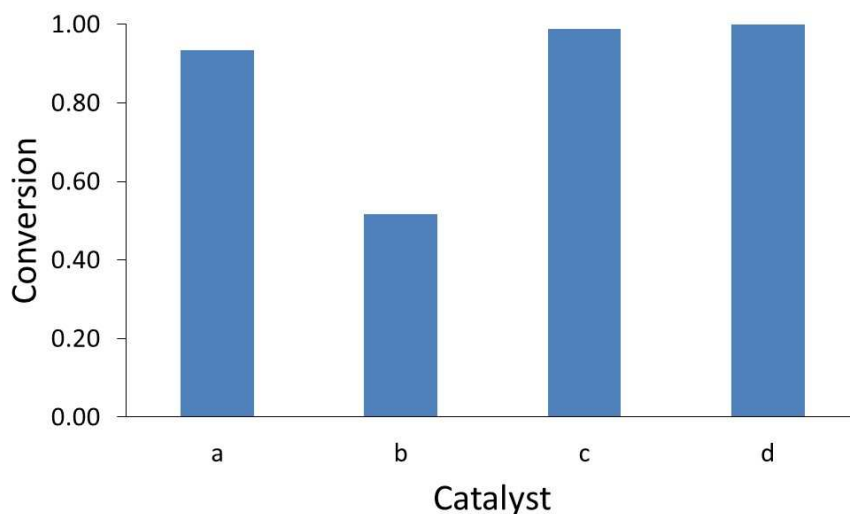


Figure 44: Conversion of products from reaction of  $TiO_2$  (a) without zeolite and (b) with zeolite. Reaction with 20 wt. %  $TiO_2/CNT$  with zeolite (c) at half of normal partial pressure and (b) at normal partial pressure. The conversion increases with addition of zeolite and CNT as support for the  $TiO_2$ .

Figure 45 illustrates that the selectivity towards hydrocarbons increased with addition of zeolite, from zero to 0.78, since the zeolite removed oxygen from the products.[1] Another reason may be that intermediates were formed in the pores of the zeolite which helps in transforming reactants to products. For reaction with 20 wt. %  $TiO_2/CNT$  at half of normal partial pressure and flow, the selectivity towards hydrocarbons was 0.90 while it was 0.92 for reaction with the same catalyst at normal partial pressure. Selectivity towards oxygenates decreased from one to 0.22 when zeolite was applied. For reaction with 20 wt. %  $TiO_2/CNT$  the selectivity towards oxygenates was 0.04 and zero when half of the normal partial pressure was applied and normal partial pressure was applied, respectively. The selectivity of oxygenates and hydrocarbons are higher than the combined selectivity of C6 and C9 oxygenates and hydrocarbons. This was because other products with C5, C7, C10 and C11 molecules were formed. These molecules are formed from cracking of higher molecules on the zeolite,[1] and were not included in these results.

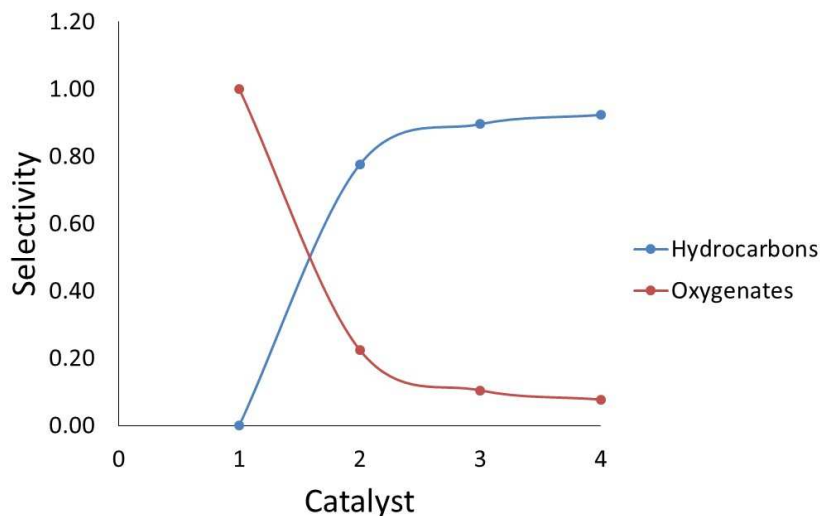


Figure 45: Selectivity for C6 hydrocarbons and oxygenates produced from reaction of  $TiO_2$  (1) without zeolite and (2) with and 20 wt. %  $TiO_2/CNT$  with zeolite at (3) half of normal partial pressure and flow and (4) at normal partial pressure and flow. The selectivity of hydrocarbons increased with addition of zeolite and CNT as support for  $TiO_2$ , while selectivity of oxygenates decreased.

When zeolite was added to the reaction, the amount of C6 hydrocarbons increased from zero to 0.06 and the amount of oxygenates decreased from 0.86 to 0.14 as illustrated in Figure 46. A reason for this may be that the zeolite removes oxygen from the products.[1] The selectivity towards C6 hydrocarbons slightly increased from 0.10 to 0.11 while the selectivity towards oxygenates decreased from 0.04 to zero when half of normal partial pressure and flow and normal partial pressure was applied, respectively. This indicates that the catalyst was slightly more active for converting C6 alcohols into hydrocarbons when CNT was used as support material for  $TiO_2$ .

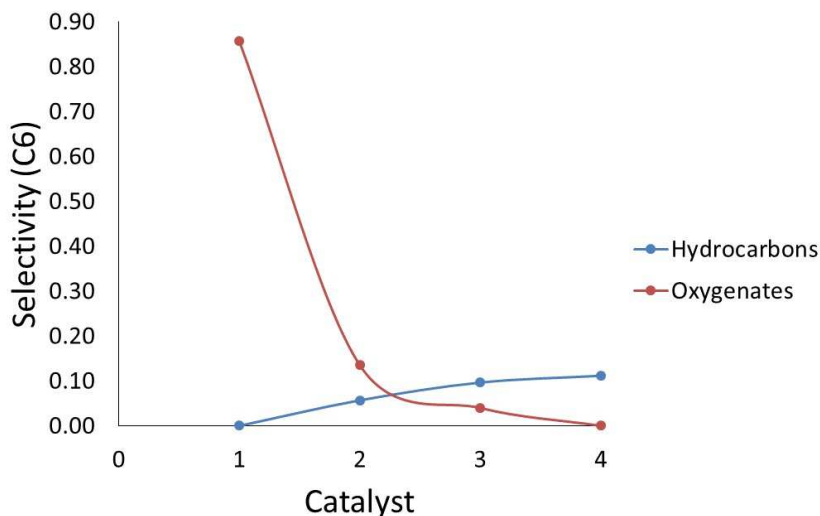


Figure 46: Selectivity for C6 hydrocarbons and oxygenates produced from reaction of (1)  $TiO_2$  without zeolite, (2)  $TiO_2$  with zeolite, (3) 20 wt. %  $TiO_2/CNT$  with zeolite at half of normal partial pressure and flow and (4) 20 wt. %  $TiO_2$  with zeolite at normal partial pressure and flow. The selectivity of hydrocarbons increased with addition of zeolite and CNT as support for  $TiO_2$ , while the selectivity of oxygenates decreased.

Figure 47 illustrates the conversion and selectivity towards ketones, aldehydes, alcohols, esters/ethers, alkanes and alkenes. Alcohols were produced with only  $TiO_2$  as a catalyst. When looking at the reaction mechanism in section 2.4.2, Figure 9,[12, 48] it is clear that alcohols are further dehydrogenated to alkenes or alkanes, and addition of zeolite was necessary for this step to occur at the applied reaction conditions. Only  $TiO_2$  as a catalyst gave a higher selectivity towards aldehydes than when  $TiO_2$  was coated on CNT. The amount of alkanes and alkenes were the same for reaction with  $TiO_2$  and reaction with  $TiO_2/CNT$ . This indicates that the ketones and aldehydes formed in the aldol condensation reaction, as shown in Figure 9, was further hydrogenated to alcohols and then dehydrogenated to alkenes and alkanes when both with and without CNT as support. A reason for this may be that  $TiO_2$  also is used as a catalyst support, due to its thermal stability and lower sintering, so addition of CNT may not give a better catalyst. [13, 19]

Esters and ethers are present when  $TiO_2/CNT$  was used, and not when only  $TiO_2$  was used. This may be because C-O coupling of molecules occur only when CNT is applied as a support. When half of the normal flow was applied, the selectivity towards C6 alkenes and alkanes was slightly higher than with a normal partial pressure. This may be due to an increased residence

time of the reactant gases in the reactor, which lead to creation of longer chained molecules. These molecules may have been cracked over zeolite into shorter molecules like C6.[1] Less selectivity towards esters/ethers was also found when half of the normal flow was applied. This indicated that the formation of esters/ethers where reduced when the residence time was longer. Since the hydrogen flow was kept constant, it may be that formation of esters/ethers decreases with increasing hydrogen flow when CNT was applied as support.

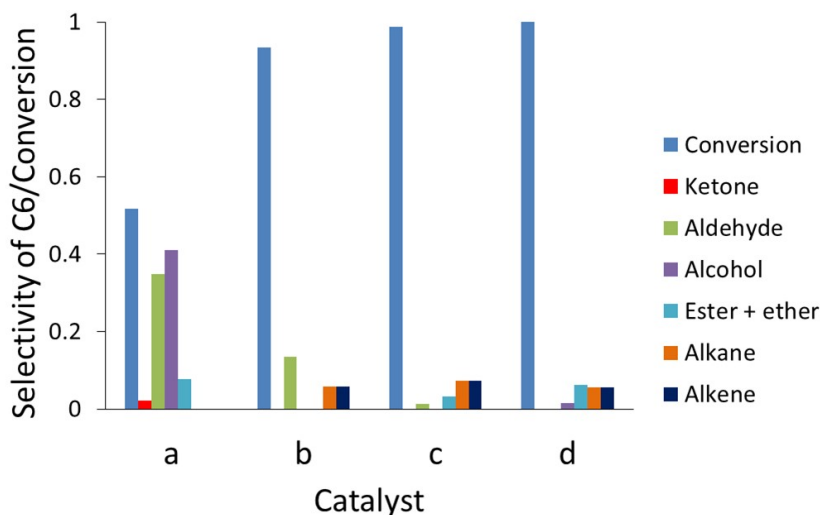


Figure 47: Selectivity for C6 ketones, aldehydes, alcohols, esters/ethers, alkanes and alkenes and the conversion produced. Reaction was performed with  $TiO_2$  (a) without zeolite and (b) with zeolite. Reaction was also performed with 20 wt. %  $TiO_2/CNT$  (c) with zeolite at half of normal partial pressure and flow and (d) normal partial pressure and flow. The selectivity of hydrocarbons increased with addition of zeolite.

The selectivity towards C9 hydrocarbons increased from zero to 0.22 with addition of zeolite, as illustrated in Figure 48. With addition of carbon nanotubes as support, the amount of hydrocarbons was at 0.22 and 0.19 when half of normal partial pressure and flow was applied and normal partial pressure was applied, respectively. The amount of C9 oxygenates was at 0.09 both with and without zeolite. This may have been due to cracking of higher molecules to C9 hydrogen when zeolite was added.[1] With addition of CNT as support, the selectivity for C9 oxygenates was 0.05 and 0.06 for reaction with half of normal partial pressure and flow and normal partial pressure and flow, respectively. This indicated that the removal of oxygen was due to the zeolite. [1] The selectivity towards C9 hydrocarbons did not change when CNT was applied as support material, and the reason may be that  $TiO_2$  usually is used as a support material as described above. [13]



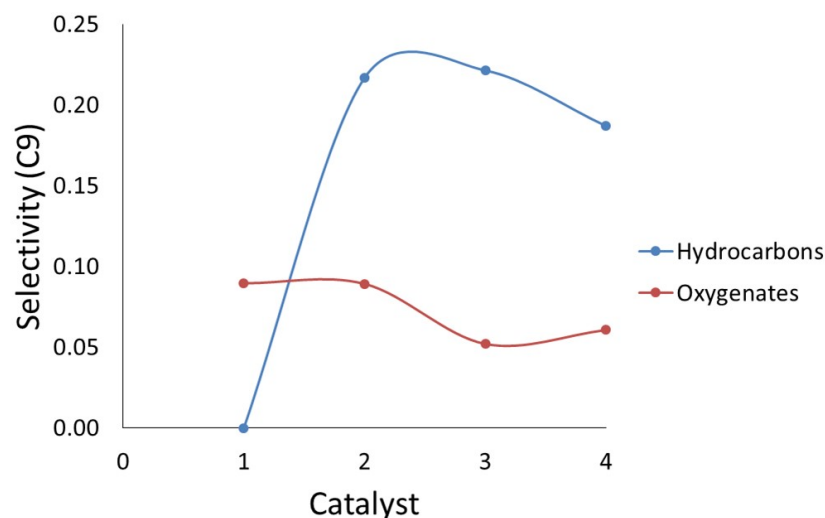


Figure 48: Selectivity for C9 hydrocarbons and oxygenates produced from reaction with  $TiO_2$  (1) with and (2) without zeolite and 20 wt. %  $TiO_2/CNT$  with zeolite at (3) half of normal partial pressure and flow and (4) at normal partial pressure and flow. The selectivity of hydrocarbons increased with addition of zeolite and CNT as support, while selectivity of oxygenates decreased.

C9 aromatics and alkenes were only produced when zeolite was added to the reaction, as illustrated in Figure 49. A reason for this was that dehydrogenation occurred due to the zeolite. When only  $TiO_2/CNT$  was used as catalyst with half of normal partial pressure and flow, there was only a small selectivity towards C9 ketones. This indicates that the zeolite may be reactive in the aldol condensation reaction, as explained above. When comparing the two different reactions with 20 wt. %  $TiO_2/CNT$ , it is indicated that when half of the partial pressure and flow was applied, a small amount of alkenes was produced along with aromatics. An explanation for this could be due to the increase of residence time for the reactant gases in the reactor, which may lead to formation of longer carbon molecules. The same selectivity towards alkenes was also observed for reaction with only  $TiO_2$ , and this may have been formed due to a higher amount of  $TiO_2$ , since  $TiO_2/CNT$  only contains 0.3 g of  $TiO_2$ .

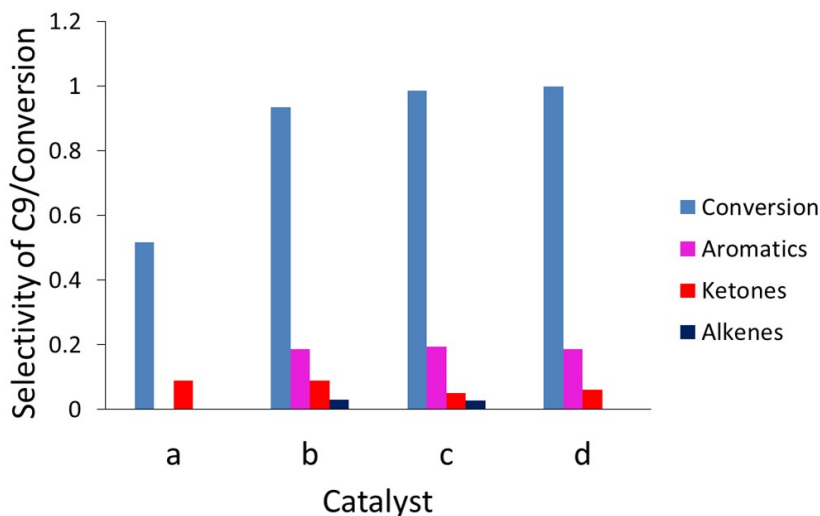


Figure 49: Selectivity for C9 aromatics, ketones and alkenes and the conversion produced. Reaction was performed with  $TiO_2$  (a) without zeolite and (b) with zeolite. Reaction was also performed with 20 wt. %  $TiO_2/CNT$  (c) with zeolite at half of normal partial pressure and flow and (d) at normal partial pressure and flow. The selectivity of hydrocarbons increased with addition of zeolite.

#### 4.3.5 Reaction with different zeolites

Two different zeolite types were tested, one with an Al/Si ratio of 30 and one with an Al/Si ratio of 80. The zeolite with an Al/Si ratio of 30 was calcinated both at 450°C, Z30(450), and 550°C, Z30(550), and the other was only calcinated at 550°C, Z80. The conversion is illustrated in Figure 50 and the values are found in Appendix E, table E.4 for both conversion and selectivity of all hydrocarbons and oxygenates. Both the reduction and reaction was performed with  $TiO_2$  powder and  $CuSiO_2$  at reduction and reaction conditions of 1.2 bar and 300°C. Products from Z30(450) was collected after four hours and 20 hours, and the products from Z30(550) was only collected after four hours, since the boiler shell broke when the products were gathered after four hours. Zeolite Z(80) was only collected after 20 hours, since the reaction setup had been changed for reaction with higher pressures.

The conversion was highest for the Z30(450) after reaction of time 20 hours at 0.95. Z80 had a conversion of 0.73, Z30(450) had a conversion of 0.56 after four hours and Z30(450) had a conversion of 0.24 after four hours. A reason for this may be that the reactants need more time for reaction, since the conversion was higher after 20 hours. Amount of hydrocarbons produced

where zero, which indicated that the zeolite was not working properly at the applied reaction conditions. Another reason may be that the zeolite only removes oxygen from alcohols, and no alcohols were produced. Since the conversion increased when the time of reaction increased, it may have been formed intermediates in the zeolite pores over time, which increased the amount of products in the aldol condensation reaction.

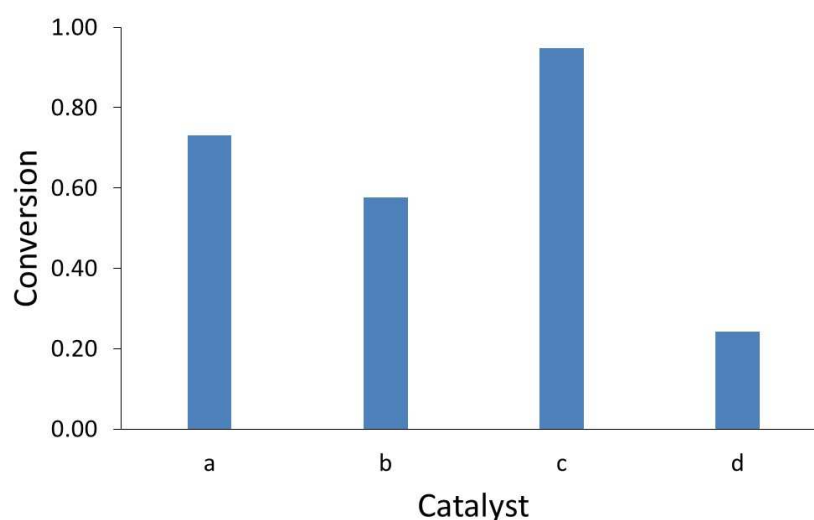


Figure 50: Conversion for (a) Z(80) after 20 hours, (b) Z30(450) after 4 hours, (c) Z30(450) after 20 hours and (d) Z30(550) after 4 hours

Selectivity towards hydrocarbons was 0.02 for Z80, while it was 0.09, 0.51 and 0.56 for reaction with Z30(450) after four hours and 20 hours and with Z(30)(550) after four hours, respectively as depicted in Figure 51. Selectivity towards oxygenates was 0.98 for Z80, 0.91 for Z30(450) after four hours, 0.49 for Z30(450) after 20 hours and 0.44 for Z30(550) after four hours. Z30(550) removed most oxygen and produced most hydrocarbons under the applied reaction conditions. This indicates that a calcination temperature of 550°C made the zeolite more reactive in removal of oxygen than a calcination temperature of 450°C. The zeolite with an Al/Si ratio of 30 removed more oxygen molecules than the zeolite with an Al/Si ratio of 80.

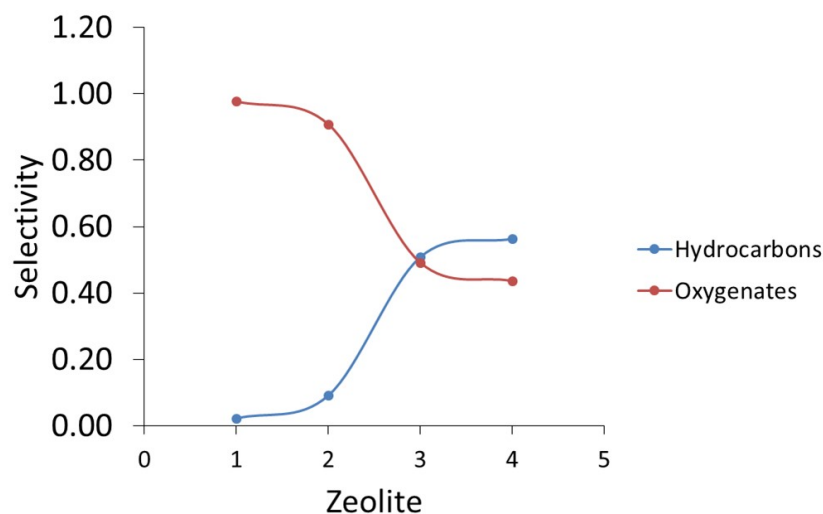


Figure 51: Selectivity for hydrocarbons and oxygenates for (1) Z(80) after 20 hours, (2) Z30(450) after 4 hours, (3) Z30(450) after 20 hours and (4) Z30(550) after 4 hours

Ketones, aldehydes and esters/ethers in the C6 molecule range was only found for Z80 after 20 hours and Z30(450) after four hours as illustrated in Figure 52. All the products were oxygenates, and the selectivity towards C6 oxygenates was higher when Z80 was applied. This indicates that a higher reaction pressure and/or higher/lower temperature has to be applied to convert C6 oxygenates to hydrocarbons.

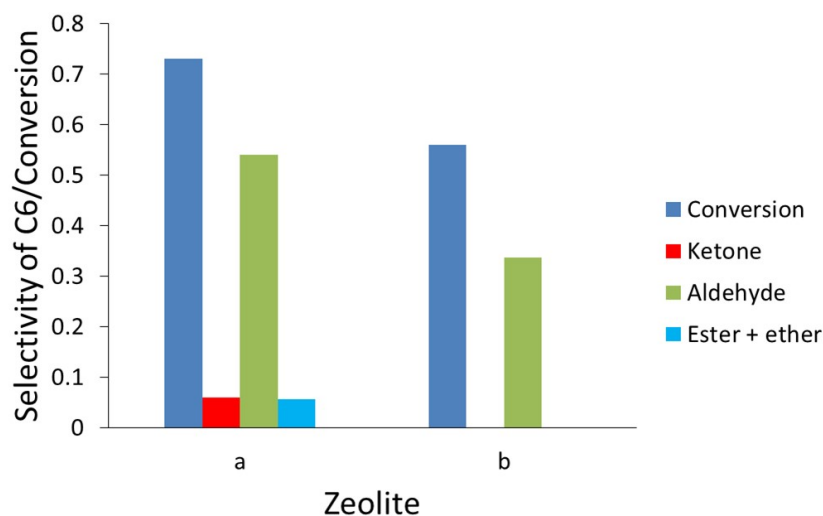


Figure 52: Selectivity for C6 ketones, aldehydes and esters/ethers and the conversion with (a) Z(80) after 20 hours and (b) Z30(450) after four hours.

Figure 53 illustrated the selectivity towards C9 hydrocarbon and oxygenates from reaction with different zeolite types and calcination temperature. Zeolite Z80 had zero selectivity towards C9 hydrocarbons after four hours, while Z30(450) had a selectivity of 0.09 and 0.41 after four and 20 hours, respectively. Z30(550) had a selectivity of 0.33 after four hours. The selectivity towards oxygenates was 0.28, 0.57, 0.31 and 0.44 for Z80 after four hours, Z30(450) after four hours, Z30(450) after 20 hours and Z30(550) after four hours.

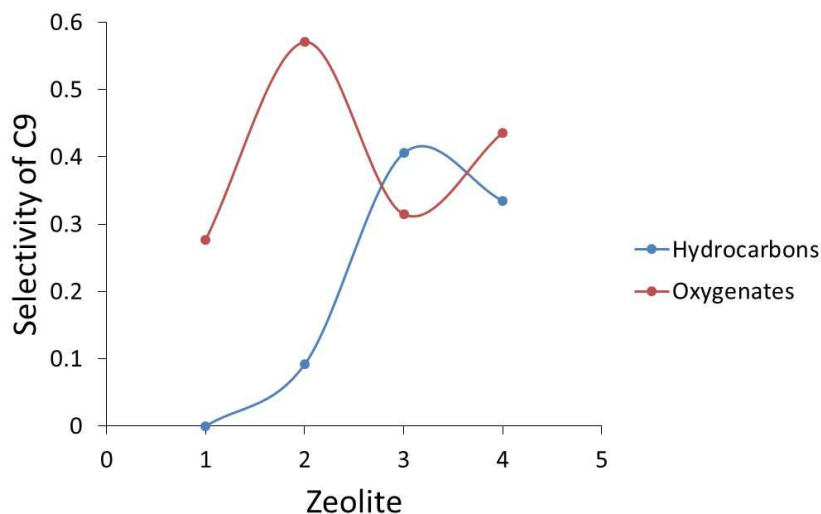


Figure 53: Selectivity for C9 hydrocarbons and oxygenates for reaction with different zeolites and different calcination temperature. (1) Z(80) after 20 hours, (2) Z30(450) after four hours, (3) Z30(450) after 20 hours and (4) Z30(550) after four hours

Figure 54 depicts the selectivity towards ketones, aromatics and the conversion for the different zeolites. This illustrated that the only hydrocarbons produced were aromatics, and the only oxygenates produced were ketones. Production of aromatics may be due to the zeolite. [1] With the Z30(450) zeolite it was produced more C9 ketones and aromatics after 20 hours than after four hours. This may be due to formation of intermediates in the pores as explained above.

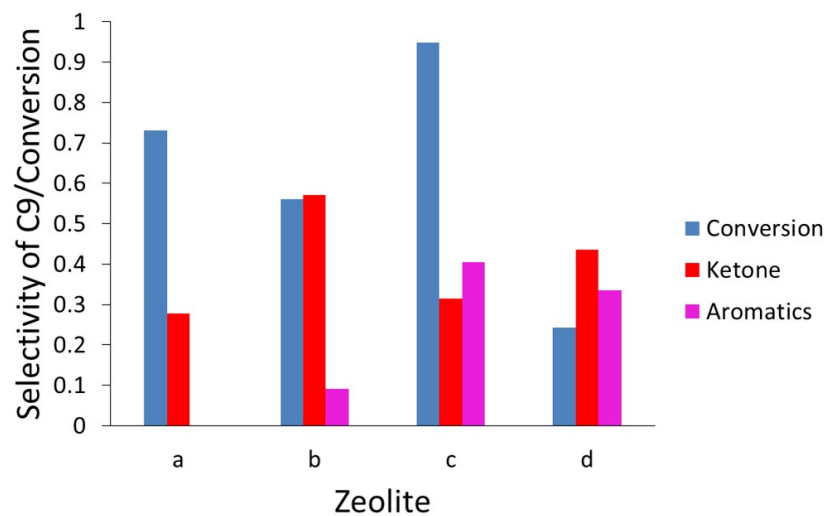


Figure 54: Selectivity for C9 ketones and aromatics and the conversion with (a) Z(80) after 20 hours, (b) Z30(450) after four hours, (c) Z30(450) after 20 hours and (d) Z30(550) after four hours





## 5 Further work

Optimal reduction temperature for the copper catalyst should be investigated by temperature programmed reduction. It was clear that a temperature of 300°C was better than 230°C, but there may be an even better reduction temperature. Reactions with different reduction temperatures should be performed to find the optimal reduction temperature. Reduction with different pressures, to find out if the reduction pressure does have an impact on the reduction of the copper catalyst needs to be performed.

Reaction with different reaction temperatures should also be applied, and due to time constraints and reactor problems there was not time to do this in this report. This is necessary to optimize the reaction to produce more C9 and higher hydrocarbons.

Most of the produced C9 hydrocarbons are aromatics, and is not desired when utilization of the products to fuel. Due to this, different approaches should be tested for converting aromatics into alkenes.

The only zeolite used was the HZSM 5 zeolite with different Si/Al ratios, so other types should be tested. There is many different zeolite types, like  $\beta$ - or  $\gamma$ -zeolites. These zeolite types may be more suitable for upgrading of the oxygen products, because of the larger pores.

Since most of the products contained both an oil phase and an aqueous phase, the aqueous phase should also be analysed. This was not done in this report, since different standard solutions has to be used.



## 6 Conclusion

X-ray diffraction spectra of titanium dioxide  $TiO_2$  before and after calcination showed that the peak was sharper after calcination, and the crystallite size was bigger. It was also found that the  $TiO_2$  was anatase  $TiO_2$ .

Results from temperature programmed desorption illustrated that both acid and basic sites were present for 10, 20, 30 and 40 wt. %  $TiO_2$  coated on CNT, for CNT and for  $TiO_2$ . When  $TiO_2$  is coated on CNT, the basic sites are stronger than for only  $TiO_2$  except for the 30 wt. %  $TiO_2/CNT$ . For the acid sites, the strength increased with decreasing loading, except for the 40 wt. %  $TiO_2/CNT$  catalyst.

Reaction was performed with different reduction temperatures and reaction pressures. A reduction temperature of 230°C is too low for fully reduction of the catalyst, since a higher conversion was achieved with a reduction pressure of 300°C. Most C9 hydrocarbons was produced when the reduction conditions was 1.2 bar and 300°C and the reaction conditions was 5 bar and 300°C. It is clear that the zeolite removes oxygen, since less oxygen is present with addition of zeolite. The same selectivity for C9 hydrocarbons was obtained both with  $TiO_2$  with and without CNT as support.



## References

- [1] George W Huber, Sara Iborra, and Avelino Corma. Synthesis of transportation fuels from biomass: chemistry, catalysts, and engineering. *Chemical reviews*, 106(9):4044–4098, 2006.
- [2] Michael Stöcker. Biofuels and biomass-to-liquid fuels in the biorefinery: Catalytic conversion of lignocellulosic biomass using porous materials. *Angewandte Chemie International Edition*, 47(48):9200–9211, 2008.
- [3] Joseph B Binder and Ronald T Raines. Simple chemical transformation of lignocellulosic biomass into furans for fuels and chemicals. *Journal of the American Chemical Society*, 131(5):1979–1985, 2009.
- [4] Mustafa Balat and Havva Balat. Recent trends in global production and utilization of bio-ethanol fuel. *Applied Energy*, 86(11):2273–2282, 2009.
- [5] Nurhan Turgut Dunford. 1 traditional and emerging feedstocks for food and industrial bioproduct manufacturing. *Food and Industrial Bioproducts and Bioprocessing*, page 1, 2012.
- [6] Arthur J Ragauskas, Charlotte K Williams, Brian H Davison, George Britovsek, John Cairney, Charles A Eckert, William J Frederick, Jason P Hallett, David J Leak, Charles L Liotta, et al. The path forward for biofuels and biomaterials. *science*, 311(5760):484–489, 2006.
- [7] David Tilman, Robert Socolow, Jonathan A Foley, Jason Hill, Eric Larson, Lee Lynd, Stephen Pacala, John Reilly, Tim Searchinger, Chris Somerville, et al. Beneficial biofuels the food, energy, and environment trilemma. *Science*, 325(5938):270, 2009.
- [8] Roger A Sheldon. Green and sustainable manufacture of chemicals from biomass: state of the art. *Green Chemistry*, 16(3):950–963, 2014.
- [9] David Martin Alonso, Jesse Q Bond, and James A Dumesic. Catalytic conversion of biomass to biofuels. *Green Chemistry*, 12(9):1493–1513, 2010.
- [10] David Martin Alonso, Stephanie G Wettstein, and James A Dumesic. Bimetallic catalysts for upgrading of biomass to fuels and chemicals. *Chemical Society Reviews*, 41(24):8075–8098, 2012.

- [11] J Haber, JH Block, and B Delmon. Manual of methods and procedures for catalyst characterization (technical report). *Pure and applied chemistry*, 67(8-9):1257–1306, 1995.
- [12] O. Cesak. Synthesis of fuels from biomass derived oxygenates. 2013.
- [13] Ib Chorkendorff and Johannes W Niemantsverdriet. *Concepts of modern catalysis and kinetics*. John Wiley & Sons, 2006.
- [14] Sumio Iijima et al. Helical microtubules of graphitic carbon. *nature*, 354(6348):56–58, 1991.
- [15] TW Ebbesen and PM Ajayan. Large-scale synthesis of carbon nanotubes. *Nature*, 358(6383):220–222, 1992.
- [16] Chin Li Cheung, Andrea Kurtz, Hongkun Park, and Charles M Lieber. Diameter-controlled synthesis of carbon nanotubes. *The Journal of Physical Chemistry B*, 106(10):2429–2433, 2002.
- [17] JM Planeix, N Coustel, B Coq, V Brotons, PS Kumbhar, R Dutartre, P Geneste, P Bernier, and PM Ajayan. Application of carbon nanotubes as supports in heterogeneous catalysis. *Journal of the American Chemical Society*, 116(17):7935–7936, 1994.
- [18] Jun Zhu, Anders Holmen, and De Chen. Carbon nanomaterials in catalysis: proton affinity, chemical and electronic properties, and their catalytic consequences. *ChemCatChem*, 5(2):378–401, 2013.
- [19] Gianmario Martra. Lewis acid and base sites at the surface of microcrystalline *tio*<sub>2</sub> anatase: relationships between surface morphology and chemical behaviour. *Applied Catalysis A: General*, 200(1):275–285, 2000.
- [20] M Gopal, WJ Moberly Chan, and LC De Jonghe. Room temperature synthesis of crystalline metal oxides. *Journal of Materials Science*, 32(22):6001–6008, 1997.
- [21] X Bokhimi, A Morales, M Aguilar, JA Toledo-Antonio, and F Pedraza. Local order in titania polymorphs. *International journal of hydrogen energy*, 26(12):1279–1287, 2001.
- [22] S Watson, D Beydoun, J Scott, and R Amal. Preparation of nanosized crystalline *tio*<sub>2</sub> particles at low temperature for photocatalysis. *Journal of Nanoparticle Research*, 6(2):193–207, 2004.
- [23] Mark A Barteau. Organic reactions at well-defined oxide surfaces. *Chemical reviews*, 96(4):1413–1430, 1996.

- [24] Beatriz Valle, Ana G Gayubo, Ainhoa Alonso, Andrés T Aguayo, and Javier Bilbao. Hydrothermally stable hzsm-5 zeolite catalysts for the transformation of crude bio-oil into hydrocarbons. *Applied Catalysis B: Environmental*, 100(1):318–327, 2010.
- [25] Pedro L Benito, Andrés T Aguayo, Ana G Gayubo, and Javier Bilbao. Catalyst equilibration for transformation of methanol into hydrocarbons by reaction-regeneration cycles. *Industrial & engineering chemistry research*, 35(7):2177–2182, 1996.
- [26] Toshio Okuhara. Water-tolerant solid acid catalysts. *Chemical Reviews*, 102(10):3641–3666, 2002.
- [27] Ana G Gayubo, Andrés T Aguayo, Alaitz Atutxa, Roberto Aguado, and Javier Bilbao. Transformation of oxygenate components of biomass pyrolysis oil on a hzsm-5 zeolite. i. alcohols and phenols. *Industrial & Engineering Chemistry Research*, 43(11):2610–2618, 2004.
- [28] Patrick Gamez, Isabel WCE Arends, Jan Reedijk, and Roger A Sheldon. Copper (ii)-catalysed aerobic oxidation of primary alcohols to aldehydes. *Chemical Communications*, (19):2414–2415, 2003.
- [29] Nan Jiang and Arthur J Ragauskas. Cu (ii)-catalyzed selective aerobic oxidation of alcohols under mild conditions. *The Journal of organic chemistry*, 71(18):7087–7090, 2006.
- [30] Hong-Yue Tang, Jason Greenwood, and Paul Erickson. Modeling of a fixed-bed copper-based catalyst for reforming methanol: Steam and autothermal reformation. *International Journal of Hydrogen Energy*, 2015.
- [31] Dominique Jean, Bendaoud Nohair, Jean-Yves Bergeron, and Serge Kaliaguine. Hydrogenolysis of glycerol over cu/zno-based catalysts: Influence of transport phenomena using the madon–boudart criterion. *Industrial & Engineering Chemistry Research*, 53(49):18740–18749, 2014.
- [32] ES Vasiliadou and AA Lemonidou. Investigating the performance and deactivation behaviour of silica-supported copper catalysts in glycerol hydrogenolysis. *Applied Catalysis A: General*, 396(1):177–185, 2011.
- [33] AW Coats and JP Redfern. Thermogravimetric analysis. a review. *Analyst*, 88(1053):906–924, 1963.

- [34] Jingly Fung and Ikai Wang. Determination of surface acidity and basicity of  $tio_2$   $zro_2$  by temperature programmed desorption of ammonia and acetic acid. *Applied Catalysis A: General*, 166(2):327–334, 1998.
- [35] Masaru Watanabe, Yuichi Aizawa, Toru Iida, Ryo Nishimura, and Hiroshi Inomata. Catalytic glucose and fructose conversions with  $tio_2$  and  $zro_2$  in water at 473k: Relationship between reactivity and acid–base property determined by tpd measurement. *Applied Catalysis A: General*, 295(2):150–156, 2005.
- [36] M Kruk, M Jaroniec, and A Sayari. Application of large pore mcm-41 molecular sieves to improve pore size analysis using nitrogen adsorption measurements. *Langmuir*, 13(23):6267–6273, 1997.
- [37] Tronstad O. *Overflate og porefordlingsmålinger*. Institutt for industriell kjemi, 1992.
- [38] K Byrappa, AS Dayananda, CP Sajan, B Basavalingu, MB Shayan, K Soga, and M Yoshimura. Hydrothermal preparation of zno: Cnt and  $tio_2$ : Cnt composites and their photocatalytic applications. *Journal of Materials Science*, 43(7):2348–2355, 2008.
- [39] Xiao-Hong Xia, Zhi-Jie Jia, Ying Yu, Ying Liang, Zhuo Wang, and Li-Li Ma. Preparation of multi-walled carbon nanotube supported  $tio_2$  and its photocatalytic activity in the reduction of  $co_2$  with  $h_2o$ . *Carbon*, 45(4):717–721, 2007.
- [40] Ahmad Monshi, Mohammad Reza Foroughi, and Mohammad Reza Monshi. Modified scherrer equation to estimate more accurately nano-crystallite size using xrd. *World Journal of Nano Science and Engineering*, 2(03):154, 2012.
- [41] Henrik Jensen, Joorgen H. Pedersen, JE Joorgensen, J Skov Pedersen, Karsten Dan Joensen, Steen B Iversen, and EG Soogaard. Determination of size distributions in nano-sized powders by tem, xrd, and saxs. *Journal of Experimental Nanoscience*, 1(3):355–373, 2006.
- [42] Douglas Skoog, Donald West, FL Holler, and Stanley Crouch. *Fundamentals of analytical chemistry*. Cengage Learning, 2013.
- [43] María E Sad, Matthew Neurock, and Enrique Iglesia. Formation of c–c and c–o bonds and oxygen removal in reactions of alkanediols, alkanols, and alkanals on copper catalysts. *Journal of the American Chemical Society*, 133(50):20384–20398, 2011.



- [44] Edward L Kunkes, Dante A Simonetti, Ryan M West, Juan Carlos Serrano-Ruiz, Christian A Gärtner, and James A Dumesic. Catalytic conversion of biomass to monofunctional hydrocarbons and targeted liquid-fuel classes. *Science*, 322(5900):417–421, 2008.
- [45] F. A. Carey. *Organic chemistry*. McGraw-Hill Higher Education, North America, 4th edition, 2000.
- [46] Juben N Chheda and James A Dumesic. An overview of dehydration, aldol-condensation and hydrogenation processes for production of liquid alkanes from biomass-derived carbohydrates. *Catalysis Today*, 123(1):59–70, 2007.
- [47] Deepa Sharma. *Advanced Organic Chemistry*. Kent, GBR: New Academic Science, 2012.
- [48] Carbon-carbon bond formation and oxygen removal in the reactions of oxygenates on au-based catalysts.
- [49] Juan Carlos Serrano-Ruiz and James A Dumesic. Catalytic production of liquid hydrocarbon transportation fuels. In *Catalysis for Alternative Energy Generation*, pages 29–56. Springer, 2012.
- [50] Gianfranco Pacchioni. Ketonization of carboxylic acids in biomass conversion over  $tio_2$  and  $zro_2$  surfaces: a dft perspective. *ACS Catalysis*, 4(9):2874–2888, 2014.
- [51] Ingvild Skeie Liland. One-pot conversion of cellulose to ethylene glycol and propylene glycol over nickel zinc oxide catalysts with cnt support. 2013.



# Appendices



## A Calculations

### Calculation example of 10 % $TiO_2$ -loading on CNT

Total mass:

$$m_{total} = 4 \text{ g}$$

The mass of the precursor and  $SiO_2$  was calculated by using equation 2.2, 2.3 and 2.4 in Section 2.2.1:

$$m_{CNT} = 4g \cdot 0.9 = 3.6 \text{ g}$$

$$m_{TiO_2} = 4g \cdot 0.1 = 0.4 \text{ g}$$

$$m_{precursor} = \frac{m_{TiO_2}}{M_{w,TiO_2}} \cdot M_{w,precursor} = \frac{0.3 \text{ g}}{79.87 \text{ g/mol}} \cdot 284.211 \text{ g} = 1.4234 \text{ g}$$

The ethanol volume was calculated by using equation 2.1 in Section 2.2.1:

$$V_{ethanol} = 3 \cdot 18.9 \text{ ml} = 56.7 \text{ ml}$$

$$V_{ethanol} = V_{CNT} - V_{precursor} = 56.7 \text{ ml} - 1.7 \text{ ml} = 55 \text{ ml}$$

Table A.1: Amount of CNT, precursor, ethanol and  $TiO_2$  used to make the four different catalysts

Catalyst	$m_{CNT}$ (g)	$m_{TiO_2}$ (g)	$m_{precursor}$ (g)	$V_{ethanol}$ (ml)
10% $TiO_2/CNT$	3.6	0.4	1.4258	55
20% $TiO_2/CNT$	3.2	0.8	2.8489	47
30% $TiO_2/CNT$	2.8	1.2	4.2733	39
40% $TiO_2/CNT$	2.4	1.6	5.6989	31

**Calculation example of n-propanol flow from gas flow to liquid flow**

$$F_{gas} = 7.49 \text{ ml/min}$$

$$n_{gas} = \frac{F_{gas}}{22.414 \text{ mol}} = \frac{7.49 \text{ ml/min}}{22.414 \text{ l/mol}} \cdot \frac{1 \text{ l}}{1000 \text{ ml}} = 0.000334 \text{ mol/min}$$

$$V_{liquid} = \frac{n_{gas} \cdot M_{w,n-propanol}}{\rho_{n-propanol}} = \frac{0.000334 \text{ mol/min} \cdot 60.1 \text{ g/mol}}{0.8 \text{ g/ml}} = 0.02278 \text{ ml/min}$$

Where:

$F_{gas}$  = the flow of the gas (ml)

$n_{gas}$  = mole of gas

$V_{liquid}$  = volume of the liquid flow

**Calculation example of the percent used in the flow controller**Example 2MFC:

Linear regression gives the equation:

$$y = 1.7846x - 0.2698$$

Where:

y = the desired flow

x = the percent

The desired flow for the 2 MFC controller is 22.27 ml/min.

$$22.27 = 1.7846x - 0.2698$$

$$x = 12.6$$

**Calculation example of conversion and selectivity**

Example pentanal 2-methyl:

Conversion and selectivity was calculated using equation 2.7, 2.8, 2.9, 2.10, 2.11 and 2.12 from Section 2.3.4.

$$\text{weight rate} = \frac{\text{peak area}}{\text{response factor}} = \frac{2500}{0.8} = 3125$$

$$\text{weight \%} = \frac{\text{weight rate}}{\sum \text{weight rates}} = \frac{3125}{111443} = 0.03$$

$$\text{mol rate} = \frac{\text{weight \%}}{\text{Molecular weight}} = \frac{0.03}{98} = 4.57 \cdot 10^{-4}$$

$$\text{mol \%} = \frac{\text{mol rate}}{\sum \text{mol rates}} = \frac{4.57 \cdot 10^{-4}}{0.014} = 0.02$$

$$\text{pentanal 2 - methyl} = \text{mol \%} \cdot \text{number of carbons in hydrocarbon structure} = 0.02 \cdot 6 = 0.06$$

$$\sum \text{number of } C_6(C_9, C_{12}) = 1.96$$

$$\text{Conversion} = \frac{\sum \text{number of } C_6(C_9, C_{12}) \text{ (rate)}}{\sum \text{number of } C_3 C_6 C_9 C_{12}} = \frac{0.02}{4.06} = 0.48$$

$$\text{Selectivity} = \frac{\sum \text{number of } C_6(C_9, C_{12}) \text{ (rate)}}{\sum \text{number of } C_{6+} \text{ (rate)}} = \frac{0.02 \cdot 6}{1.96} = 0.06$$

**Calculation example of partial pressure**Flow rate of reaction gases :

$$n_{\text{propanol}} = 7.49 \text{ ml/min}$$

$$H_2 = 7.42 \text{ ml/min}$$

$$N_2 = 44.54 \text{ ml/min}$$

Converting to moles :

$$n_{n\text{-propanol}} = \frac{F_{n\text{-propanol}}}{22.413996} = \frac{7.49 \text{ ml/min}}{22.413996 \text{ l/mol}} \cdot \frac{1 \text{ l}}{1000 \text{ ml}} = 3.34 \cdot 10^{-4} \text{ mol/min}$$

$$n_{H_2} = \frac{F_{H_2}}{22.413996} = \frac{7.42 \text{ ml/min}}{22.413996 \text{ l/mol}} \cdot \frac{1 \text{ l}}{1000 \text{ ml}} = 3.31 \cdot 10^{-4} \text{ mol/min}$$

$$n_{N_2} = \frac{F_{N_2}}{22.413996} = \frac{44.54 \text{ ml/min}}{22.413996 \text{ l/mol}} \cdot \frac{1 \text{ l}}{1000 \text{ ml}} = 1.987 \cdot 10^{-3} \text{ mol/min}$$

Molar fractions (y):

$$n_{\text{total}} = 2.652 \cdot 10^{-3} \text{ mol/min}$$

$$y_{n\text{-propanol}} = \frac{n_{n\text{-propanol}}}{n_{\text{total}}} = \frac{3.34 \cdot 10^{-4}}{2.652 \cdot 10^{-3}} = 0.126$$

$$y_{H_2} = \frac{n_{H_2}}{n_{\text{total}}} = \frac{3.31 \cdot 10^{-4}}{2.652 \cdot 10^{-3}} = 0.125$$

$$y_{N_2} = \frac{n_{N_2}}{n_{\text{total}}} = \frac{1.987 \cdot 10^{-3}}{2.652 \cdot 10^{-3}} = 0.749$$



Partial pressure (P):

$$P_{n-propanol} = P_{total} \cdot y_{n-propanol} = 5 \text{ bar} \cdot 0.126 = 0.63 \text{ bar}$$

$$P_{H_2} = p_{total} \cdot y_{N_2} = 5 \text{ bar} \cdot 0.125 = 0.625 \text{ bar}$$

$$P_{N_2} = p_{total} \cdot y_{N_2} = 5 \text{ bar} \cdot 0.749 = 3.745 \text{ bar}$$

**Calculation example of adsorbed CO<sub>2</sub> or NH<sub>3</sub>**

10 wt. % TiO<sub>2</sub>/CNT absorbed CO<sub>2</sub>

% difference = 0.16 %

$$mass = \frac{0.16\% \cdot 19.3 \text{ mg}}{100\%} = 3.18 \cdot 10^{-2} \text{ mg/mg}_{catalyst}$$

$$moles = \frac{3.18 \cdot 10^{-2} \text{ mg/mg}_{catalyst}}{44.01 \text{ mg/mmol}} = 7.22 \cdot 10^{-4}$$

## B Risk evaluation

A risk evaluation was performed before the work in the laboratory could be conducted. This risk evaluation is displayed in this appendix.

NTNU	Hazardous activity identification process			Prepared by	Number	Date
HSE				HSE section	HMSRV-26/01	09.01.2013
		Approved by	The Reactor	Replaces		
				01.12.2006		

**Date: 14.01.2015**

Unit: Department for Chemical engineering

Line manager: Eddi Anders Blekkan

Participants in the identification process: De Chen (responsible professor) and Astri Karin Torvik Jenssen (student)

Short description of the main activity/main process: Master project for student Astri Karin Torvik Jenssen.

Project title.: Catalytic conversion of oxygenates to fuels

Is the project work purely theoretical? NO

requiring risk assessment are involved in the work. If YES, briefly describe the activities below. The risk assessment form need not be filled out.

Signatures: Responsible supervisor:



Student: Astri Karin Torvik Jenssen

ID nr.	Activity/process	Responsible person	Existing documentation	Existing safety measures	Laws, regulations etc.	Comment
1	Synthesis of catalyst	Astri Karin Torvik Jenssen	No	Safety datasheet	No	
2	Reactor setup	Astri Karin Torvik Jenssen	No	No	No	The rig is under construction
3	N2-adsorption	Astri Karin Torvik Jenssen	Apparatus card	Proper training, safety gloves, goggles, insulated gloves (liquid N <sub>2</sub> ) and laboratory coat	No	
4	Temperature gravity analysis	Astri Karin Torvik Jenssen	Apparatus card	Gas detector when using CO and H <sub>2</sub> , protective goggles	No	Flush with inert before opening the furnace after suing CO and H <sub>2</sub> .
5	X-ray diffraction	Astri Karin Torvik Jenssen	Apparatus card	Be sure to close the apparatus card properly	No	
6	S(T)EM	Astri Karin Torvik Jenssen	Apparatus card	Protective gloves and coat to enter the nanolab	No	

NTNU		Prepared by		Date	
HSE/KS		HSE section		04.02.2011	
Risk assessment		Number		Replaces	
		HMSRV2603E		01.12.2006	
		Approved by		The Rector	

**Date: 14.01.2015**

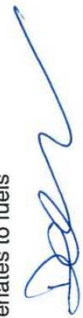
**Unit:** Department of chemical engineering

**Line manager:** Edd Anders Blekkan

**Participants in the identification process** (including their function):

**Short description of the main activity/main process:** Master project for Astri Karin Torvik Jenssen.

**Project title:** Catalytic conversion of oxygenates to fuels

**Signatures:** *Responsible supervisor:* 

*Student:* Astri Karin Torvik Jenssen

Activity from the identification process form	Potential undesirable incident/strain	Likelihood (1-5)	Consequence:		Risk Value (human)	Comments/status Suggested measures
			Human (A-E)	Environment (A-E)		
1.1 Use of nitric acid	Spill	2	A	B	B2	Use of gloves, goggles and laboratory coat
1.2 Use of CNT	Spill	3	B	B	B3 (uncertain)	Use of double gloves, mask, goggles and laboratory coat
1.3 Use of C <sub>12</sub> H <sub>28</sub> TiO <sub>4</sub>	Spill	2	B	A	B2	Use of gloves, goggles and laboratory coat
1.4 Use of acetone for cleaning	Spill, fire	2	A	A	A2	Use of gloves, goggles and laboratory coat
1.5 Use of Ethanol	Spill	2	A	B	A2	Use of gloves goggles and laboratory coat
1.6 Use of silicone dioxide	Spill	3	A	B	A3	Use of gloves, goggles and lab coat
1.7 Use of Copper(II) nitrate hemi(pentahydrate)	Spill, toxic	2	B	C	B2	Use of gloves, goggles and lab coat
1.8 Use of Zeolite (HZSM 5)	Spill, inhalation of small particles	2	A	A	A2	Use of gloves, goggles and lab coat
1.9 Use of Titanium	Spill, inhalation of	2	A	A	A2	Use of gloves, goggles

NTNU		Prepared by		Number	Date
		HSE section		HMSRV2603E	04.02.2011
HSE/KS		Approved by			Replaces
		The Reactor			01.12.2006

Risk assessment

dioxide	small particles					and lab coat
2.1 Use of Hydrogen for reaction	Gas leak, explosive gas	2	B	A	B	Use hydrogen in a room with proper ventilation. Leak test the pipe line before use. Turn off hydrogen supply if leak is detected.
2.2 Exposure to evaporator	May cause skin burn	1	B	A	A	Do not touch the hot surface
3.1 Liquid nitrogen	Spill	2	B	A	A	Use of isolating gloves, goggles and lab coat
4.1 Hot furnace	May cause skin burn	1	A	A	A	Do not touch the hot surface
4.2 Ammonia gas	Gas leak, toxic gas	2	B	B	A	Leak test the pipeline before use
5.1 Radiation	Cell destruction	1	C	A	A	Turn off radiation before opening doors
6.1 High voltage	May in worst case lead to death	1	D	A	A	Turn off high voltage before opening doors

**Likelihood, e.g.:**

1. Minimal
2. Low
3. Medium
4. High
5. Very high

**Consequence, e.g.:**

- A. Safe
- B. Relatively safe
- C. Dangerous
- D. Critical
- E. Very critical

**Risk value (each one to be estimated separately):**

- Human = Likelihood x Human Consequence
- Environmental = Likelihood x Environmental consequence
- Financial/material = Likelihood x Consequence for Economy/material

**Potential undesirable incident/strain**

Identify possible incidents and conditions that may lead to situations that pose a hazard to people, the environment and any materiel/equipment involved.

**Criteria for the assessment of likelihood and consequence in relation to fieldwork**

Each activity is assessed according to a worst-case scenario. Likelihood and consequence are to be assessed separately for each potential undesirable incident. Before starting on the quantification, the participants should agree what they understand by the assessment criteria:

NTNU		Prepared by		Number		Date	
HSE/KS		HSE section		HMSRV2603E		04.02.2011	
		Approved by				Replaces	
		The Rector				01.12.2006	

**Risk assessment**

<b>Likelihood</b>	<b>Minimal</b> 1	<b>Low</b> 2	<b>Medium</b> 3	<b>High</b> 4	<b>Very high</b> 5
	Once every 50 years or less	Once every 10 years or less	Once a year or less	Once a month or less	Once a week

<b>Consequence Grading</b>	<b>Human</b>	<b>Environment</b>	<b>Financial/material</b>
<b>E</b> Very critical	May produce fatality/ies	Very prolonged, non-reversible damage	Shutdown of work >1 year.
<b>D</b> Critical	Permanent injury, may produce serious serious health damage/sickness	Prolonged damage. Long recovery time.	Shutdown of work 0.5-1 year.
<b>C</b> Dangerous	Serious personal injury	Minor damage. Long recovery time	Shutdown of work < 1 month
<b>B</b> Relatively safe	Injury that requires medical treatment	Minor damage. Short recovery time	Shutdown of work < 1 week
<b>A</b> Safe	Injury that requires first aid	Insignificant damage. Short recovery time	Shutdown of work < 1 day

The unit makes its own decision as to whether opting to fill in or not consequences for economy/materiel, for example if the unit is going to use particularly valuable equipment. It is up to the individual unit to choose the assessment criteria for this column.

**Risk = Likelihood x Consequence**

Please calculate the risk value for "Human", "Environment" and, if chosen, "Economy/materiel", separately.

**About the column "Comments/status, suggested preventative and corrective measures":**

Measures can impact on both likelihood and consequences. Prioritise measures that can prevent the incident from occurring; in other words, likelihood-reducing measures are to be prioritised above greater emergency preparedness, i.e. consequence-reducing measures.

NTNU		Risk matrix		Date	
				8 March 2010	
HSE/KS				Prepares	
		prepared by		Number	
		HSE Section		HMSRY/2604	
		approved by		Page	
		Rector		4 of 4	
				Date	
				9 February 2010	

MATRIX FOR RISK ASSESSMENTS at NTNU

		E1	E2	E3	E4	E5
Extremely serious		D1	D2	D3	D4	D5
Serious		C1	C2	C3	C4	C5
Moderate		B1	B2	B3	B4	B5
Minor		A1	A2	A3	A4	A5
Not significant		Very low	Low	Medium	High	Very high
		<b>LIKELIHOOD</b>				
<b>CONSEQUENCE</b>						

Principle for acceptance criteria. Explanation of the colours used in the risk matrix.

Colour	Description
Red	Unacceptable risk. Measures must be taken to reduce the risk.
Yellow	Assessment range. Measures must be considered.
Green	Acceptable risk. Measures can be considered based on other considerations.

## C Calibration of mass flow controllers

Table C.1 and Figure C.1 shows the calibration values and standard curve for the mass flow controller for nitrogen (100 ml) and table C.2 and Figure C.2 shows the calibration values and standard curve for the mass flow controller for nitrogen (250 ml). The calibration values and standard curve for the hydrogen mass flow controller are shown in table C.3 and Figure C.3. Two different standard curves were made for the n-propanol mass flow controller, since two different gas flows had to be used. The values for the standard curves are shown in table C.4 and C.5, while the standard curves are shown in Figure C.4 and C.5.

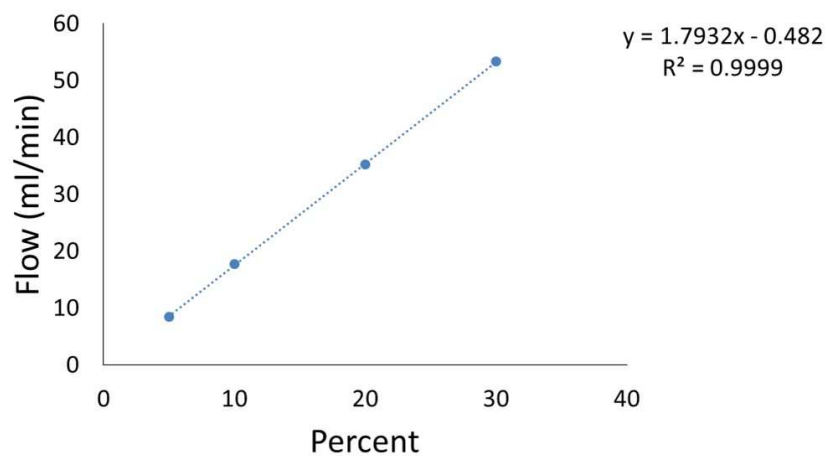


Figure C.1: Calibration curve for the mass flow controller for nitrogen (100 ml),  $NH_2$ .

Table C.1: Values obtained during calibration of the mass flow controller for nitrogen (100 ml),  $N_2$ .

	Time (s)	Percent	Time (s)	Percent	Time (s)	Percent	Time (s)	Percent
	64.25	5	30.63	10	15.37	20	10.13	30
	64.57	5	31.03	10	15.25	20	10.12	30
	64.31	5	30.59	10	15.19	20	10.16	30
	64.69	5	30.56	10	15.40	20	10.09	30
	64.75	5	30.28	10	-	20	-	30
	64.60	5	30.56	10	-	20	-	30
	64.60	5	30.56	10	-	20	-	30
Average (ml/min)	64.53	5	30.61	10	15.30	20	10.13	30
Flow (ml/min)	8.37		17.64		35.29		53.33	



Table C.2: Values obtained during calibration of the mass flow controller for nitrogen (250 ml),  $N_2$ .

	Time (s)	Percent	Time (s)	Percent	Time (s)	Percent	Time (s)	Percent	Time (s)	Percent
	63.68	4.0	57.00	4.5	29.84	10	10.34	25	7.20	36
	63.75	4.0	57.16	4.5	26.38	10	10.31	25	7.28	36
	63.65	4.0	57.25	4.5	25.09	10	10.25	25	7.25	36
	63.60	4.0	57.19	4.5	25.09	10	10.47	25	7.19	36
	63.71	4.0	57.22	4.5	25.12	10	10.41	25	-	36
	63.34	4.0	57.22	4.5	24.97	10	10.38	25	-	36
	63.34	4.0	57.35	4.5	27.31	10	10.19	25	-	36
	-	4.0	-	4.5	-	10	10.34	25	-	36
	-	4.0	-	4.5	-	10	10.35	25	-	36
	-	4.0	-	4.5	-	10	10.35	25	-	36
Average (ml/min)	63.58	4.0	57.20	4.5	26.26	5	10.34	25	7.23	36
Flow (ml/min)					20.57		52.23		74.69	

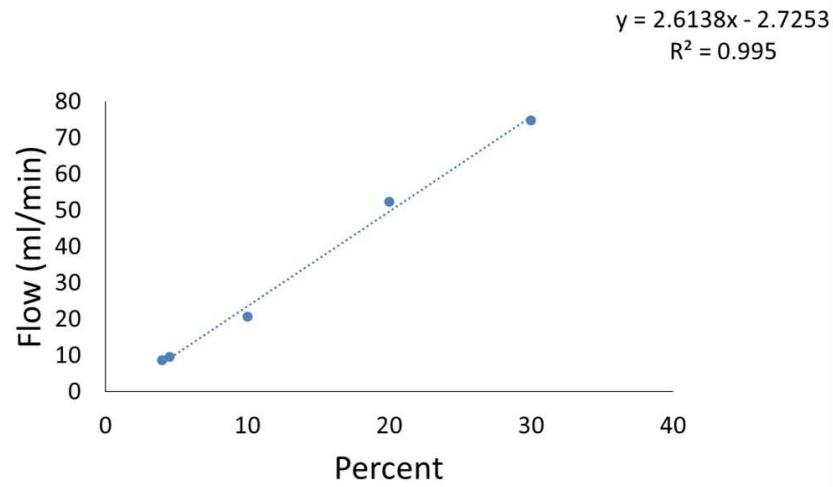


Figure C.2: Calibration curve for the mass flow controller for nitrogen (250 ml),  $N_2$ .

Table C.3: Values obtained during calibration of the mass flow controller for hydrogen,  $H_2$ .

	Time (s)	Percent	Time (s)	Percent	Time (s)	Percent
	8.84	2	4.78	4	3.28	6
	8.03	2	4.53	4	3.44	6
	8.03	2	4.91	4	3.29	6
	8.03	2	4.75	4	3.31	6
	7.91	2	4.60	4	3.44	6
	7.97	2	4.91	4	3.65	6
	-	2	4.78	4	3.38	6
	-	2	4.38	4	3.47	6
	-	2	4.84	4	-	6
Average	8.16	2	4.72	4	3.41	6
(ml/min)						
Flow	7.36		12.71		17.61	
(ml/min)						

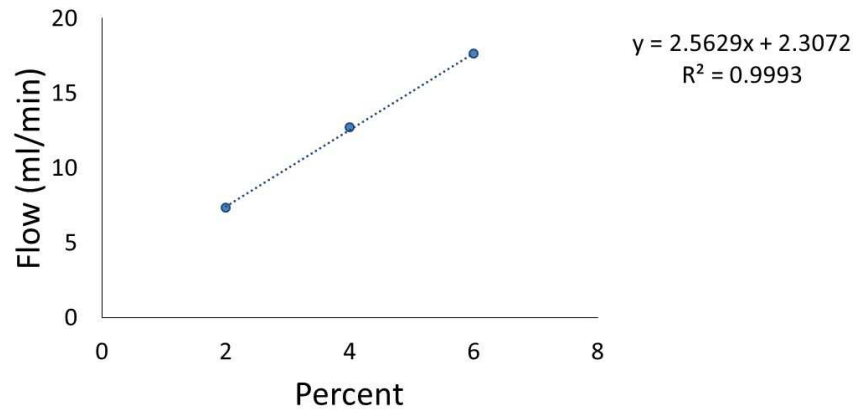


Figure C.3: Calibration curve for the mass flow controller for hydrogen,  $H_2$ .

Table C.4: Values obtained during calibration of the mass flow controller for n-propanol, to get 7.42 ml/min (gas flow).

	Flow (g/h)	Percent	Flow (g/h)	Percent	Flow (g/h)	Percent
	1.11	56	1.25	59	1.09	61
	1.00	56	1.15	59	1.14	61
	1.05	56	0.97	59	1.15	61
Average	8.16	2	4.72	4	3.41	6
(ml/min)						
Flow	7.36		12.71		17.61	
(ml/min)						

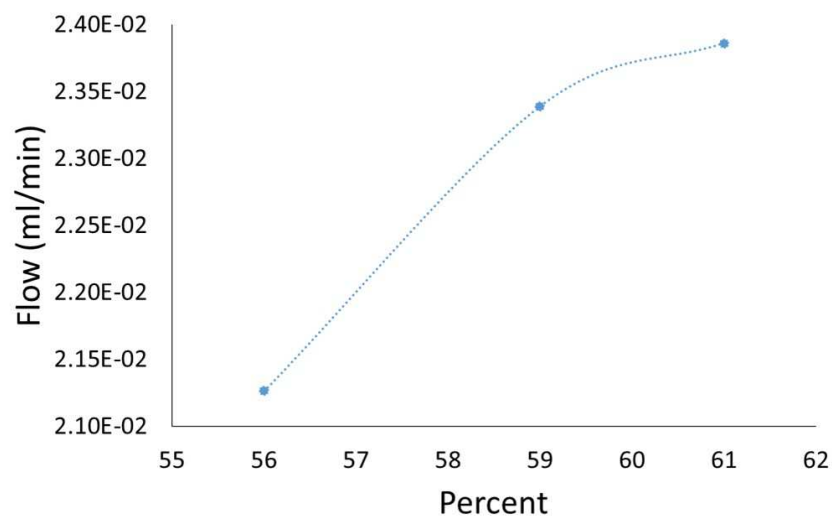


Figure C.4: Calibration curve for the mass flow controller for n-propanol (7.42 ml/min, gas flow).

Table C.5: Values obtained during calibration of mass flow controller for n-propanol, to get 3.71 ml/min (gas flow).

	Flow (g/h)	Percent	Flow (g/h)	Percent	Flow (g/h)	Percent
	0.50	25	0.50	27	0.59	29
	0.46	25	0.58	27	0.62	29
	0.54	25	0.54	27	0.59	29
Average (ml/min)	8.16	2	4.72	4	3.41	6
Flow (ml/min)	7.36		12.71		17.61	

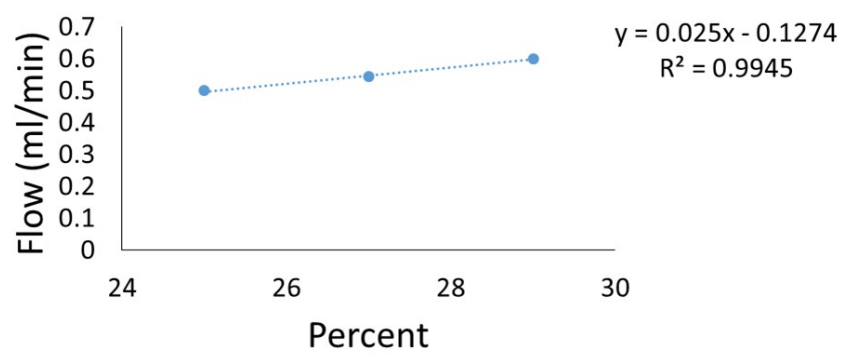


Figure C.5: Calibration curve for the mass flow controller for n-propanol (3.71 ml/min, gas flow).

## D Percents and mass for basic and acid sites

The percents and masses used to calculate the  $CO_2$  adsorbed is found in table D.1 and the percents and masses used to calculate the  $NH_3$  desorbed is found in table D.2.

Table D.1: Mass and percent for the basic sites.

Catalyst	Mass (mg)	Percent $CO_2$ adsorbed
10 wt. % $TiO_2/CNT$	19.04	0.16
20 wt. % $TiO_2/CNT$	18.36	0.24
30 wt. % $TiO_2/CNT$	17.87	0.07
40 wt. % $TiO_2/CNT$	17.68	0.15
CNT	16.23	0.014
$TiO_2$	18.84	0.07

Table D.2: Mass and percent for the acid sites.

Catalyst	Mass (mg)	Percent $NH_3$ desorbed
10 wt. % $TiO_2/CNT$	19.4	0.73
20 wt. % $TiO_2/CNT$	16.82	0.50
30 wt. % $TiO_2/CNT$	18.26	0.29
40 wt. % $TiO_2/CNT$	17.43	0.85
CNT	16.36	0.95
$TiO_2$	-	-

Figure D.1, D.2, D.3, D.4, D.5 and D.6 illustrates the adsorption of  $CO_2$  for the different catalysts and CNT.

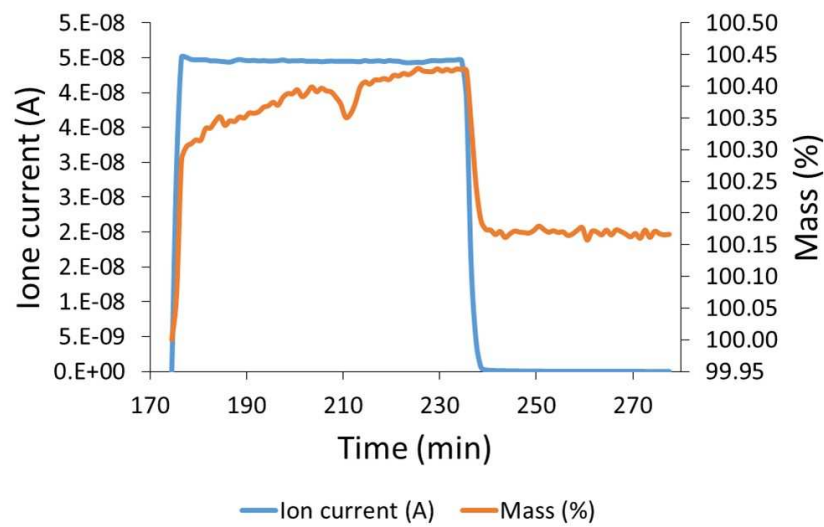


Figure D.1: Ion current (A) and mass (%) for the adsorption of  $CO_2$  on the 10 wt. %  $TiO_2/CNT$ .

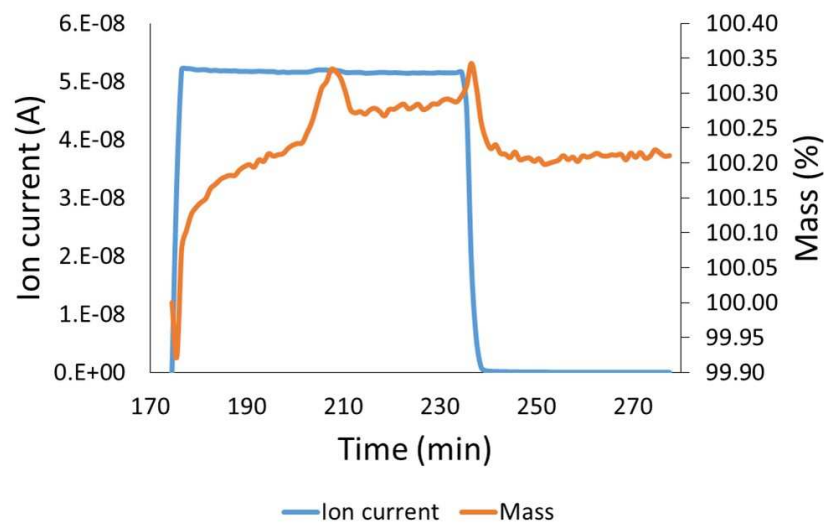


Figure D.2: Ion current (A) and mass (%) for the adsorption of  $CO_2$  on the 20 wt. %  $TiO_2/CNT$ .

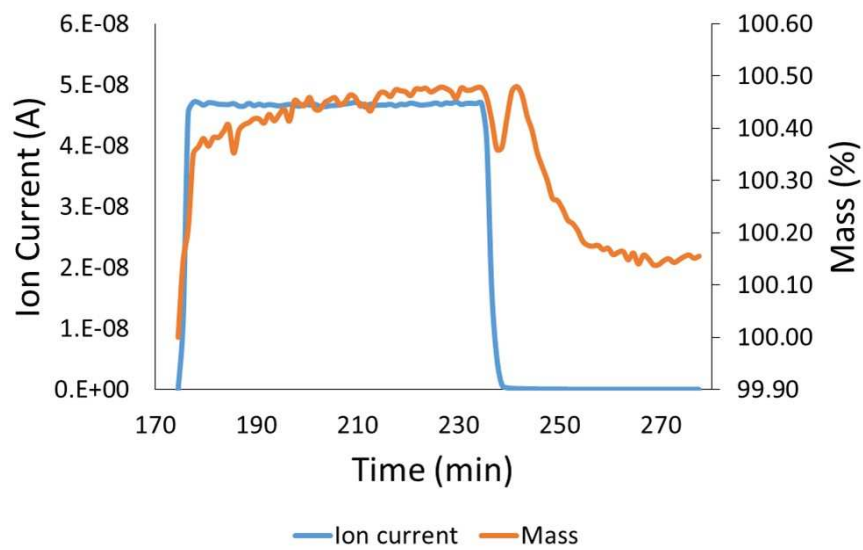


Figure D.4: Ion current (A) and mass (%) for the adsorption of  $CO_2$  on the 40 wt. %  $TiO_2/CNT$ .

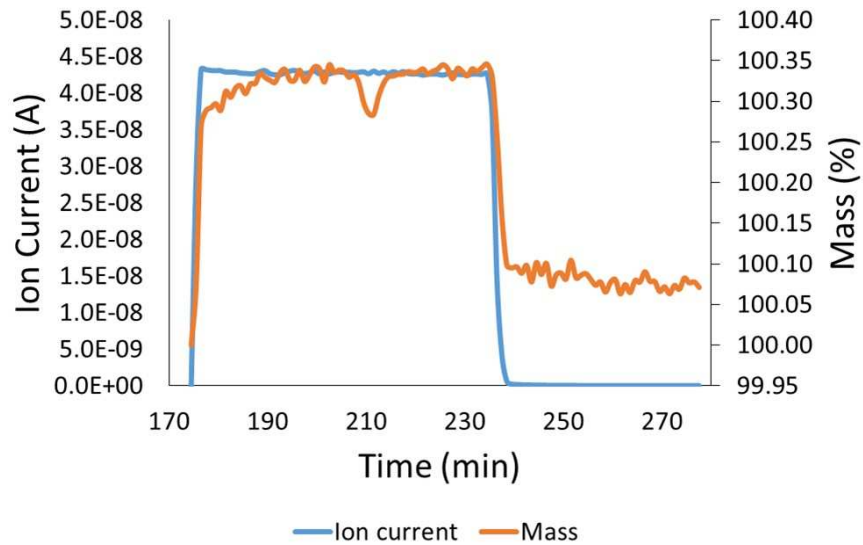


Figure D.3: Ion current (A) and mass (%) for the adsorption of  $CO_2$  on the 30 wt. %  $TiO_2/CNT$ .



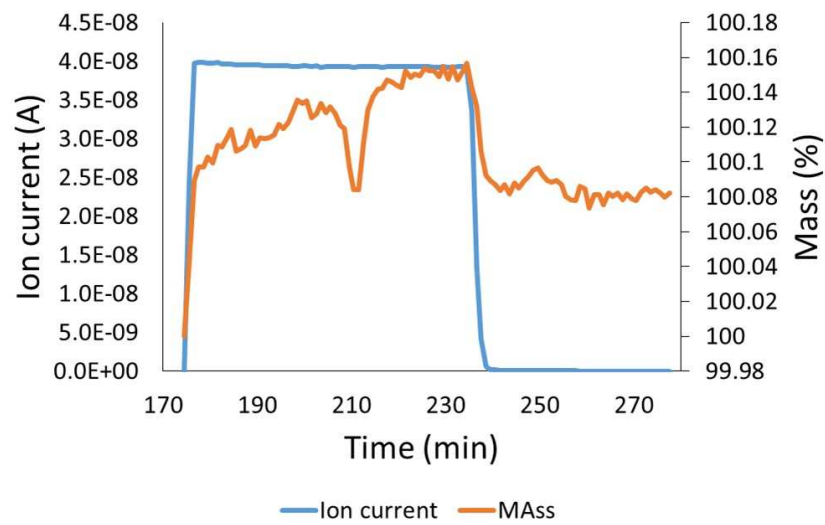


Figure D.5: Ion current (A) and mass (%) for the adsorption of  $CO_2$  on the  $TiO_2$ .

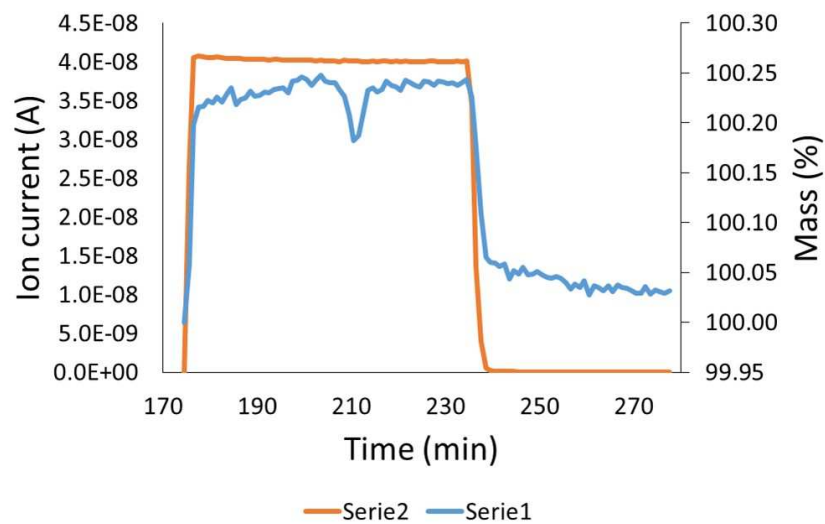


Figure D.6: Ion current (A) and mass (%) for the adsorption of  $CO_2$  on the CNT.

## E Tables for product conversion and selectivity for oxygenates and hydrocarbons

Table E.1 displays the conversion and selectivity for reduction at 1.2 bar and 300°C. The conversion and selectivity for reduction at 1.2 bar and 230°C is displayed in table E.2. Conversion and selectivity for different catalysts is displayed in table E.3 and the conversion and selectivity for different zeolite types is displayed in table E.4

Table E.1: Conversion and selectivity of all the oxygenates and hydrocarbons in the products from experiments with  $TiO_2$ , Zeolite and  $CuSiO_2$  at reduction conditions of 1.2 bar and 300°C and reaction conditions of 1.2, 5, 10, 15 and 20 bar and 300°C.

Reduction at 300°C and 1.2 bar			
Pressure (bar)	Conversion	Hydrocarbons	Oxygenates
1.2	0.73	0.02	0.98
5	0.93	0.78	0.22
10	0.98	0.84	0.16
15	0.64	0.36	0.64
20	0.65	0.44	0.56

Table E.2: Conversion and selectivity of all the oxygenates and hydrocarbons in the products from experiments with  $TiO_2$ , Zeolite and  $CuSiO_2$  at reduction conditions of 1.2 bar and 230°C and reaction conditions of 5, 10, 15 and 20 bar and 300°C.

Reduction at 230°C and 1.2 bar			
Pressure (bar)	Conversion	Hydrocarbons	Oxygenates (g)
5	0.57	0.46	0.54
10	0.44	0.24	0.76
15	0.44	0.41	0.59
20	0.40	0.30	0.70

E TABLES FOR PRODUCT CONVERSION AND SELECTIVITY FOR OXYGENATES  
 E.2 AND HYDROCARBONS

Table E.3: Conversion and selectivity with different catalysts.

Catalysts	Conversion	Hydrocarbons	Oxygenates
$TiO_2$	0.93	0.00	1.00
$TiO_2$ and Z80	0.52	0.78	0.22
$TiO_2/CNT$ and Z80 at half of normal partial pressure	0.99	0.90	0.10
$TiO_2/CNT$ and Z80 at normal partial pressure	1.00	0.92	0.08

Table E.4: Conversion and selectivity with different zeolite types

Zeolite	Time (h)	Conversion	Hydrocarbons	Oxygenates
R80	20	0.73	0.02	0.98
R30(450)	4	0.58	0.09	0.91
R30(450)	20	0.95	0.51	0.49
R30(550)	4	0.24	0.56	0.44

## **F Response factors for the products**

The response factors for the different products are displayed in table F.1.

Table F.1: Response factors for the different products.

Product	Formula	Functional group	Molecular weight	Response factor, F
Propanal	$C_3H_5O$	Aldehyde	57.07	0.60
1-propanol	$C_3H_7O$	Alcohol	59.09	0.60
Acetic acid	$C_2H_4O_2$	Carboxylic acid	60.05	0.60
Propene	$C_3H_6$	Alken	42.08	1.14
Propanoic acid	$C_3H_6O_2$	Carboxylic acid	42.08	0.60
1-Propene, 2-methyl	$C_4H_8$	Alken	56.10	1.14
Pentane	$C_5H_{12}$	Alken	84.16	1.11
2-Pentene (E)	$C_5H_{10}$	Alken	70.13	1.14
Cyclopropane, 1,1-dimethyl	$C_5H_{10}$	Alkan	70.13	1.14
Cyclopropane, 1,2-dimethyl-, trans	$C_5H_{10}$	Alkan	70.13	1.14
Butane, 2-methyl	$C_5H_{12}$	Alkan	72.15	1.11
1-pentene, 4-methyl	$C_6H_{12}$	Alken	84.16	1.14
n-Hexane	$C_6H_{14}$	Alkane	86.17	1.12
1-pentene, 2-methyl	$C_6H_{12}$	Alken	84.16	1.14
2-pentene, 4-methyl-, (Z)	$C_6H_{12}$	Alken	84.16	1.14
2-hexene	$C_6H_{12}$	Alken	84.16	1.14
2-pentene, 3-methyl (Z)	$C_6H_{12}$	Alken	84.16	1.14
2-Pentene, 2-methyl-	$C_6H_{12}$	Alken	84.16	1.14
2,4-Hexadien	$C_6H_{10}$	Alken	82.14	1.17
2-butenal, 2-ethyl	$C_6H_{10}O$	Aldehyde	98.14	0.80
4-penten-2-one, 3-methyl	$C_6H_{10}O$	Keton	98.14	0.80
3-hexen-2-one	$C_6H_{10}O$	Keton	98.14	0.80
pentanal-2-methyl	$C_6H_{10}O$	Aldehyde	98.14	0.80
2-Butenal, 2-ethyl-	$C_6H_{10}O$	Aldehyde	98.14	0.80
3-Pentanone, 2-methyl	$C_6H_{12}O$	Keton	100.16	0.80
Pentanal, 2-methyl	$C_6H_{12}O$	Aldehyde	100.16	0.80
Propanoic acid propyl ester	$C_6H_{12}O_2$	Esther	116.12	0.80
Pentane 2-methyl	$C_6H_{16}$	Alkane	86.17	1.12
Pentane, 3-methyl	$C_6H_{16}$	Alkane	86.17	1.12
1-Butanol, 2-ethyl	$C_6H_{14}O$	Alcohol	102.17	0.80
Di-n-propyl ether	$C_6H_{14}O$	Ether	102.17	0.80
1-pentanol, 2-methyl	$C_6H_{14}O$	Alcohol	102.17	0.80
Cyclopentene, 1-methyl-	$C_6H_{10}$	Alkene	82.14	1.17
2,4-Hexadiene, 3-methyl-	$C_7H_{11}$	Alkene	95.16	1.18
2,4-Hexadiene, 4-methyl-	$C_7H_{10}$	Alkene	94.15	1.19
Hexane, 2-methyl-	$C_7H_{16}$	Alkane	100.20	1.12

Table F.2: Response factors for the different products.

Product	Formula	Functional group	Molecular weight	Response factor, F
Hexane, 3-methyl-	$C_7H_{16}$	Alkane	100.20	1.12
Pentane, 2,4-dimethyl	$C_7H_{16}$	Alkane	100.20	1.12
2-Heptene	$C_7H_{14}$	Alkene	98.18	1.14
2-Hexene, 3-methyl-, (Z)-	$C_7H_{14}$	Alkene	98.18	1.14
1,4-Hexadiene, 2-methyl	$C_7H_{12}$	Alken	96.17	1.17
2-Hexyne, 4-methyl	$C_7H_{12}$	Alken	96.17	1.17
1,3-Pentadiene, 2,3-dimethyl-	$C_7H_{12}$	Alken	96.17	1.17
1,4-Hexadiene, 5-methyl-	$C_7H_{12}$	Alken	96.17	1.17
Cyclobutane, (1-methylethylidene)-	$C_7H_{12}$	Alken	96.17	1.17
Toluene	$C_7H_8$	Alken	92.13	1.22
Ethylbenzene	$C_8H_{10}$	Alken	106.16	1.21
Benzene, 1,3-dimethyl-	$C_8H_{10}$	Alken	106.16	1.21
Cyclopentene, 4,4-dimethyl	$C_8H_{12}$	Alken	108.18	1.19
Heptane, 4-methyl-	$C_8H_{18}$	Alkane	114.22	1.12
p-Xylene	$C_8H_{10}$	Alken	106.16	1.21
1,3-Benzenediol, 4,5-dimethyl	$C_8H_{10}O_2$	Alcohol	138.16	1.00
Cyclopentene, 1,2,3-trimethyl	$C_8H_{14}$	Alken	110.19	1.17
4-Methyl, 1,3-heptadiene	$C_8H_{14}$	Alken	110.19	1.17
5,5-Dimethyl-1,3-hexadiene	$C_8H_{14}$	Alken	110.19	1.17

Table F.3: Response factors for the different products.

Product	Formula	Functional group	Molecular weight	Response factor, F
1,4-Benzenediol, 2,5-dimethyl-	$C_8H_{10}O_2$	Alcohol	138.16	1.00
2-Tolyloxirane	$C_9H_{10}O$	Alkene	134.17	1.00
Benzene, 1-ethyl-2-methyl	$C_9H_{12}$	Alken	120.19	1.20
Benzene, 1-ethyl-3 methyl	$C_9H_{12}$	Alken	120.19	1.20
Benzene, 1-ethyl-4-methyl-	$C_9H_{12}$	Alken	120.19	1.20
Benzene, 1,2,3-trimethyl	$C_9H_{12}$	Alken	120.19	1.20
cis-1,4-Dimethyl-2-methylenecyclohexane	$C_9H_{16}$	Alkyl	124.22	1.16
3-octyne, 2-methyl	$C_9H_{16}$	Alkyl	124.22	1.16
Benzene, 1-methyl-3-propyl	$C_{10}H_{14}$	Alken	134.21	1.20
Benzene, 1,2-diethyl	$C_{10}H_{14}$	Alken	134.21	1.20
Benzene, 2-ethyl-1,4-dimethyl	$C_{10}H_{14}$	Alken	134.21	1.20
Cyclohexane, 1-methyl-4-(1-methylethyl)-cis	$C_{10}H_{20}$	Alkane	140.26	1.14
2-cyclopenten-1-one, 2,3,4,5-tetramethyl	$C_9H_{14}O$	Keton	138.20	1.00
Benzene, 1-methyl-4-(1-methylpropyl)	$C_{11}H_{16}$	Alken	148.24	1.19
3-acetyl, 2,4,4-trimethylcyclohex-2-en-1-one	$C_{11}H_{16}O_2$	Keton	162.16	1.00
2 (3H)-Naphthaleone, 4,4a,5,6,7,8-hexahydro-1-methoxy	$C_{11}H_{16}O_2$	keton	180.24	1.00
Naphthalene, 2,6 dimethyl	$C_{12}H_{12}$	Alkene	156.22	1.23

## G Areas obtained for the different products on the GC-FID

The areas obtained from the GC-FID for the 10 wt. %  $TiO_2/CNT$  from the specialization project in fall 2014 is shown in table G.1.

Table G.1: Areas obtained for the different products on the GC-FID from reaction of 10 wt. %  $TiO_2/CNT$  from the specialization project fall 2014. The reduction conditions where 230°C and 1.2 bar and 300°C and 1.2 bar and the reaction conditions where 230°C and 300°C and 1.2 bar.

Product	10 wt. % $TiO_2/CNT$			
	Area at 230°C and 4 hours	Area at 230°C and 20 hours	Area at 300°C and 4 hours	Area at 300°C and 20 hours
Propanal	6155	1963	96	3774
1-propanol	52269	31891	37193	50238
1-pentanol-2-methyl	13539	8818	23045	13649
2-pentanal,2-methyl	0	0	2500	3557
Pentanal-2-methyl	5861	2318	4082	4287
Pentanoic acid 2-methyl	1500	0	1063	0
Propane-1,1-dipropoxy	0	0	4642	3880
Propyl-2-mthylvalerate	0	0	1153	11665
2-cyclopenten-1-one,2,3,4,5-tetramethyl	0	0	5136	0
2,3-dimethyl-3-heptene	0	0	0	1738



The different areas used in calculation of conversion and selectivity of the products from the different reactions are shown in table G.2, G.3, G.4 and G.

Table G.2: Areas obtained for the different products on the GC-FID. The reduction conditions where 230°C and 1.2 bar and the reaction conditions where 300°C and 5, 10, 15 and 20 bar.

Product	Reduction at 230°C and 1.2 bar			
	Reaction at 300°C			
	5 bar Area	10 bar Area	15 bar Area	20 bar Area
Propanal	2177	2304	1724	2091
1-propanol	4770	5563	6043	8747
Propene	58	151	197	0
1-pentene, 2-methyl	409	678	492	531
2-pentene, 4-methyl-, (Z)	2444	327	0	0
2-hexene	0	0	412	0
2-pentene, 3-methyl (Z)	0	947	2254	2459
3-Pentanone, 2-methyl	0	379	252	673
Pentanal, 2-methyl	3209	0	0	1936
Propanoic acid propyl ester	1131	914	600	1058
1-Butanol, 2-ethyl	0	2439	1869	470
Di-n-propyl ether	279	0	0	1857
1-pentanol, 2-methyl	1381	0	0	0
p-Xylene	1153	0	0	0
Benzene, 1-ethyl-3 methyl	1210	0	0	0
Benzene, 1,2,3-trimethyl	575	0	0	0
2-cyclopenten-1-one, 2,3,4,5-tetramethyl	0	1377	1125	0
3-acetyl, 2,4,4-trimethylcyclohex-2-en-1-one	0	746	518	0

Table G.3: Areas obtained for the different products on the GC-FID. The reduction conditions where 300°C and 1.2 bar and the reaction conditions where 300°C and 1.2, 5, 10, 15 and 20 bar.

Product	Reduction at 300°C and 1.2 bar				
	Reaction at 300°C				
	1.2 bar	5 bar	10 bar	15 bar	20 bar
Propanal	1687	2777	0	2143	4683
1-propanol	2903	5406	1968	7450	19984
Propene	0	475	0	0	1689
1-Propene, 2-methyl	0	276	0	0	0
Cyclopropane, 1,1-dimethyl	0	1437	3689	0	0
Cyclopropane, 1,2-dimethyl-, trans	0	0	3967	0	0
Butane, 2-methyl	0	2777	1417	0	0
1-pentene, 4-methyl	0	1516	5682	0	0
1-pentene, 2-methyl	0	1150	6820	1556	3727
2-pentene, 4-methyl-, (Z)	0	6516	21294	6937	17768
2-pentene, 3-methyl (Z)	0	0	5912	0	4490
2-butenal, 2-ethyl	0	6034	0	0	0
4-penten-2-one, 3-methyl	289	0	0	0	0
pentanal-2-methyl	0	5704	6724	0	0
2-Butenal, 2-ethyl-	0	6034	0	0	0
3-Pentanone, 2-methyl	0	0	1456	673	2325
Pentanal, 2-methyl	7700	0	0	3739	6936
Propanoic acid propyl ester	938	0	2134	1049	2064
Di-n-propyl ether	0	0	0	692	2149
1-pentanol, 2-methyl	0	0	0	2916	5822
Hexane, 2-methyl-	0	2375	0	0	0

Hexane, 3-methyl-	0	0	1278	0	0
Pentane, 2,4-dimethyl	0	0	2163	0	0
2-Hexene, 3-methyl-, (Z)-	0	4296	0	0	0
1,4-Hexadiene, 5-methyl-	0	2530	2815	0	0
Cyclobutane, (1-methylethylidene)-	0	2940	1655	0	0
Toluene	0	4487	3521	0	0
Ethylbenzene	0	6516	4712	0	0
p-Xylene	385	18489	11380	0	0
5,5-Dimethyl-1,3-hexadiene	0	9658	2075	0	0
1,4-Benzenediol, 2,5-dimethyl-	0	0	2083	0	2893
Benzene, 1-ethyl-2-methyl	0	20894	0	0	0
Benzene, 1-ethyl-4-methyl-	0	0	10995	0	0
Benzene, 1,2,3-trimethyl	0	9048	4985	0	0
cis-1,4-Dimethyl-2-methylenecyclohexane	0	0	0	0	0
3-octyne, 2-methyl	0	5066	0	0	0
Benzene, 1-methyl-3-propyl	0	7332	7008	0	0
Benzene, 1,2-diethyl	0	7097	0	0	0
Benzene, 2-ethyl-1,4-dimethyl	0	6975	3468	0	0
2-cyclopenten-1-one, 2,3,4,5-tetramethyl	4551	13785	5047	3241	8962
Benzene, 1-methyl-4-(1-methylpropyl)	0 3380	0	0	0	
2 (3H)-Naphthaleone, 4,4a,5,6,7,8-hexahydro-1-methoxy	776	0	0	1261	0

Table G.4: Areas obtained for the different products on the GC-FID from reaction with  $TiO_2$  and  $CuSiO_2$  without zeolite and 20 wt. %  $TiO_2/CNT$ ,  $CuSiO_2$  with zeolite at normal partial pressure and half of the normal partial pressure. The reduction conditions where 300°C and 1.2 bar and the reaction conditions where 300°C and 5 bar.

Product	Reduction at 300°C and 1.2 bar		
	Catalyst: $TiO_2$ and $CuSiO_2$	Catalyst: 20 wt. % $TiO_2/CNT$ , $CuSiO_2$ and zeolite	Catalyst: 20 wt. % $TiO_2/CNT$ , $CuSiO_2$ and zeolite (half of normal partial pressure)
Propanal	7183	0	0
1-propanol	24582	0	2304
1-Propene, 2-methyl	0	2364	0
Pentane	0	4318	0
2-Pentene (E)	0	4519	0
Cyclopropane, 1,1-dimethyl	0	0	3879
Cyclopropane, 1,2-dimethyl-, trans	0	0	4196
Butane, 2-methyl	0	1860	0
n-Hexane	0	2258	0
2-pentene, 4-methyl-, (Z)	0	5280	9309
2-pentene, 3-methyl (Z)	0	1935	6184
2,4-Hexadien	0	0	2504
pentanal-2-methyl	0	0	7928
3-Pentanone, 2-methyl	822	0	0
Pentanal, 2-methyl	13441	0	0
Propanoic acid propyl ester	1501	0	0
Pentane 2-methyl	0	4971	5592
Pentane, 3-methyl	0	1881	0
Di-n-propyl ether	1687	0	0
1-pentanol, 2-methyl	16213	0	0
Cyclopentene, 1-methyl-	0	1677	0
2,4-Hexadiene, 3-methyl-	0	3919	0

Product	Reduction at 300°C and 1.2 bar		
	Reaction at 300°C and 5 bar		
	Catalyst: $TiO_2$ and $CuSiO_2$	Catalyst: 20 wt. % $TiO_2/CNT$ , $CuSiO_2$ and zeolite	Catalyst: 20 wt. % $TiO_2/CNT$ , $CuSiO_2$ and zeolite (half of normal partial pressure)
2,4-Hexadiene, 4-methyl-	0	1440	0
Hexane, 2-methyl-	0	3254	4736
Hexane, 3-methyl-	0	2309	3051
Pentane, 2,4-dimethyl	0	0	0
2-Heptene	0	0	3709
1,4-Hexadiene, 2-methyl	0	0	4735
2-Hexyne, 4-methyl	0	0	6358
1,3-Pentadiene, 2,3-dimethyl-	0	0	2663
1,4-Hexadiene, 5-methyl-	0	3610	7209
Toluene	0	7869	12471
Ethyl benzene	0	6332	0
Benzene, 1,3-dimethyl-	0	22647	0
Cyclopentene, 4,4-dimethyl	0	3816	0
Heptane, 4-methyl-	0	7189	0
p-Xylene	0	5527	7368
1,3-Benzenediol, 4,5-dimethyl	0	0	3268
Cyclopentene, 1,2,3-trimethyl	0	3998	0
4-Methyl, 1,3-heptadiene	0	0	44603
5,5-Dimethyl-1,3-hexadiene	0	5400	0
1,4-Benzenediol, 2,5-dimethyl-	0	2845	0
2-Tolyloxirane	0	5138	0
Benzene, 1-ethyl-2-methyl	0	21024	0
Benzene, 1-ethyl-4-methyl-	0	0	30595
Benzene, 1,2,3-trimethyl	0	9144	16626
cis-1,4-Dimethyl-2-methylenecyclohexane	0	0	6904
Benzene, 1-methyl-3-propyl	0	5610	9483
Benzene, 1,2-diethyl	0	0	8507
Benzene, 2-ethyl-1,4-dimethyl	0	5397	10089
Cyclohexane, 1-methyl-4-(1-methylethyl)-cis	0	0	3317
2-cyclopenten-1-one, 2,3,4,5-tetramethyl	3984	4081	12174
Benzene, 1-methyl-4-(1-methylpropyl)	0	0	3019
2 (3H)-Naphthaleone, 4,4a,5,6,7,8-hexahydro-1-methoxy	2553	0	0
Naphthalene, 2,6 dimethyl	0	0	1906

Table G.5: Areas obtained for the different products on the GC-FID from reaction with different zeolite types.

Product	R30(550)	R30(450)	R30(450)
	4h	4h	20h
Propanal	2022	0	351
1-propanol	10516	3903	390311475
pentanal-2-methyl	0	15051	6882
Ethyl benzene	448	0	0
Benzene, 1,3-dimethyl-	602	0	0
Benzene, 1-ethyl-3 methyl 0	22661	2295	
Benzene, 1-ethyl-4-methyl-	1035	0	0
Benzene, 1,2,3-trimethyl	500	19712	0
Benzene, 1-methyl-3-propyl 6817.647949 Benzene, 2-ethyl-1,4-dimethyl	0	3940	0
2-cyclopenten-1-one, 2,3,4,5-tetramethyl	1914	31472	13650